Workshop on Megathrust Earthquakes and Tsunami

Prof. Thorne Lay

CONCEPTS:

Earthquake Magnitude
Surface Waves
Earthquake Numbers

Supplementary Reading (Optional, for more details/rigor)
Lay and Wallace, *Modern Global Seismology*, Ch. 2
Stein and Wysession, *An Introduction to Seismology, Earthquakes and Earth Structure*, Ch. 2

Wavefronts and travel time curves for P and S waves in the Earth depend only on the medium properties (seismic velocity structure), not on the source type (explosion, faulting, landslide, etc.). We can use the travel time curves and observed arrival times of phases to LOCATE the source in space and time without needing to know what type of source it was.

The motions on the wavefronts do depend on the source – so, we analyze amplitude and directions of shaking in the seismograms to tell us information about the source other than where and when it occurred. Amplitudes are used to define *seismic magnitudes*, indicating amount of wave energy generated by the source, and P and S wave displacement directions are used to identify symmetry patterns of forces at the source that We can relate to the nature of the source (explosions produce outward P wave motions in all directions and no S waves; earthquakes produce alternating patterns of P wave motions toward and away from the source.

General form of Magnitude scales:

$$M = \log(A/T) + F(h, \Delta) + C$$

A is the amplitude of the signal

T is its dominant period

F is a correction for the variation of amplitude with the earthquake's depth h and distance Δ from the seismometer

C is a regional scale factor

Table 2.2-1 Relationships Between Wave Variables

QUANTITY	UNITS	
Velocity	distance/time	$v = \omega/k = f\lambda = \lambda/T$
Period	time	$T = 2\pi/\omega = 1/f = \lambda/v$
Angular Frequency	time^{-1}	$\omega = 2\pi/T = 2\pi f = kv$
Frequency	time^{-1}	$f = \omega/(2\pi) = 1/T = v/\lambda$
Wavelength	distance	$\lambda = 2\pi/k = v/f = vT$
Wavenumber	distance^{-1}	$k = 2\pi/\lambda = \omega/v = 2\pi f/v$

Figure 2.2-4: Harmonic wave, *$u = A \cos(\omega t - kx)$*.

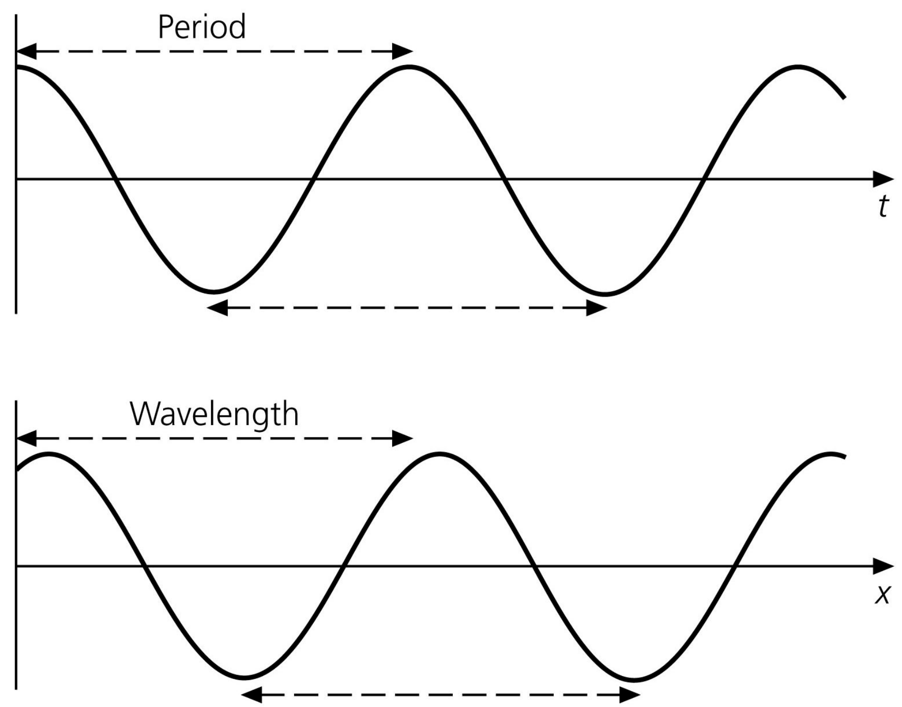

Magnitude scales are logarithmic, so an increase in one unit, as from magnitude "5" to a "6", indicates a ten-fold increase in seismic wave amplitude.

Measured magnitudes range more than 10 units because the displacements measured by seismometers span more than a factor of 10^{10}.

"Richter scale" (local magnitude) was introduced by Charles Richter in 1935 for Southern California earthquakes measured on a *Wood-Anderson* seismograph.

$$M_L = \log A + 2.76 \log \Delta - 2.48$$

The instrument period (0.8 s) and nearly constant (shallow) depth are incorporated in the constants, and the distance is in km.

We call P and S waves, which travel throughout the 'body' of a medium, Body waves. Richter magnitudes usually are based on S waves, as the S wave shaking from an earthquake faulting event are about 5 times Stronger than the P wave shaking.

We can measure seismic magnitudes for any particular phase, as long As we have appropriate propagation corrections. For P waves, we use:

Body wave magnitude:

$$m_b = \log(A/T) + Q(h, \Delta)$$

A is the ground motion amplitude in microns after the effects of the seismometer are removed

T is the wave period in seconds

Q is an empirical term depending on the distance and focal depth.

Surface wave magnitude (measured using the largest amplitude

Figure 4.6-2: Example of a Q factor map as a function of distance and earthquake depth.

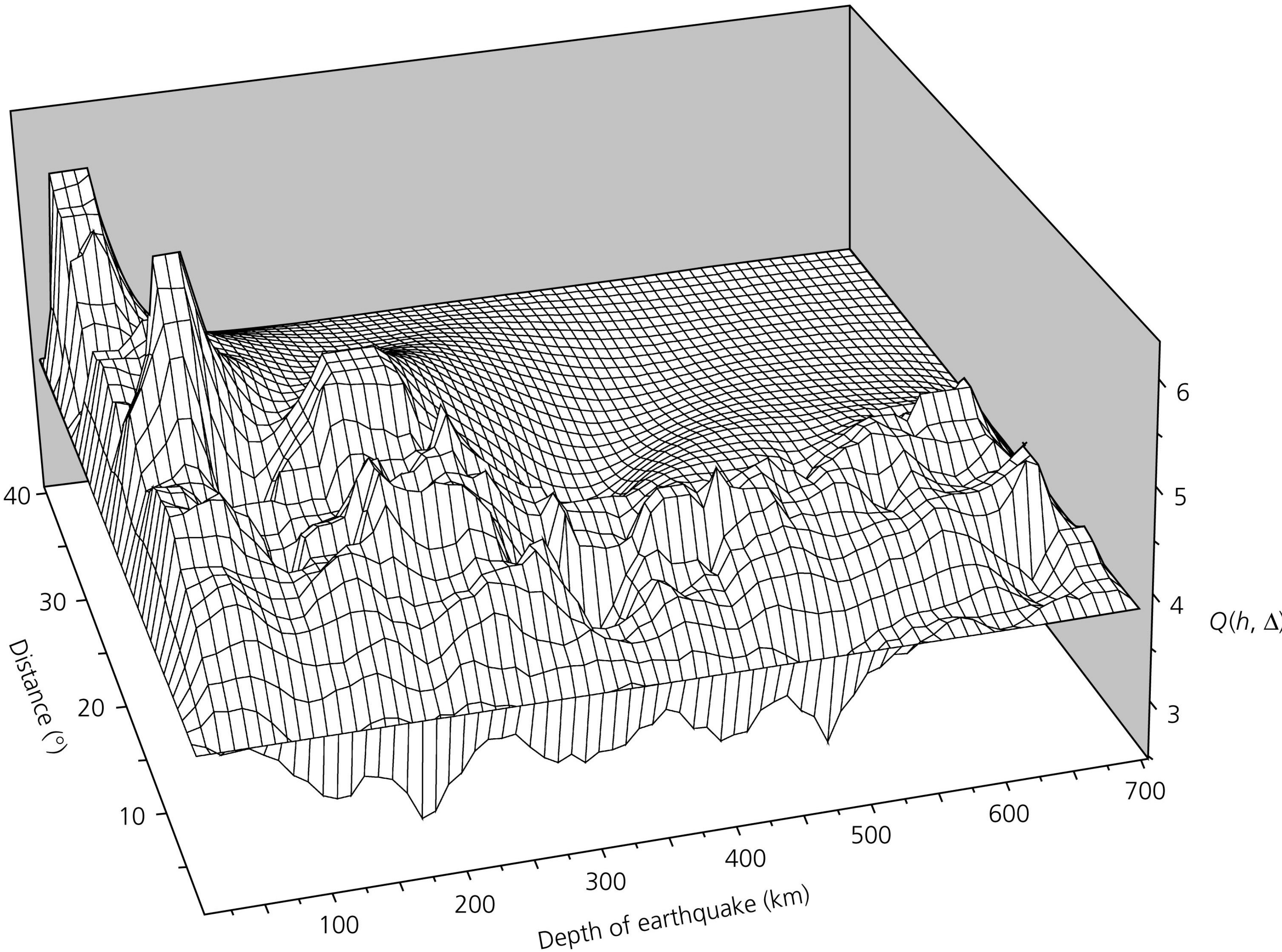

P and S waves are the complete set of motions generated in the elastic medium, but, as we have seen the P and S wave fields get very complex due to reflection, transmission, and conversion of energy in the layered spherical Earth structure.

The wave interactions with the surface of the Earth are particularly complex as stresses acting on the surface vanish, and near-surface rocks have low seismic velocities in the crust. This produces interference of P and S waves at the surface that develop collective motions that we visualize as “surface waves”, essentially traveling along the surface with wave velocities that are lower than Vp and Vs.

Reverberating horizontal ground shearing of S waves interfere to make *Love waves*.

Interference of P and S waves moving along the surface produces *Rayleigh waves*.

The velocity of these waves depends on the period of the ground motion, so they are *dispersive* – they pull apart with longer periods traveling faster (usually), and resulting motions going on for a long time.

Love Wave (L-Wave) Animation

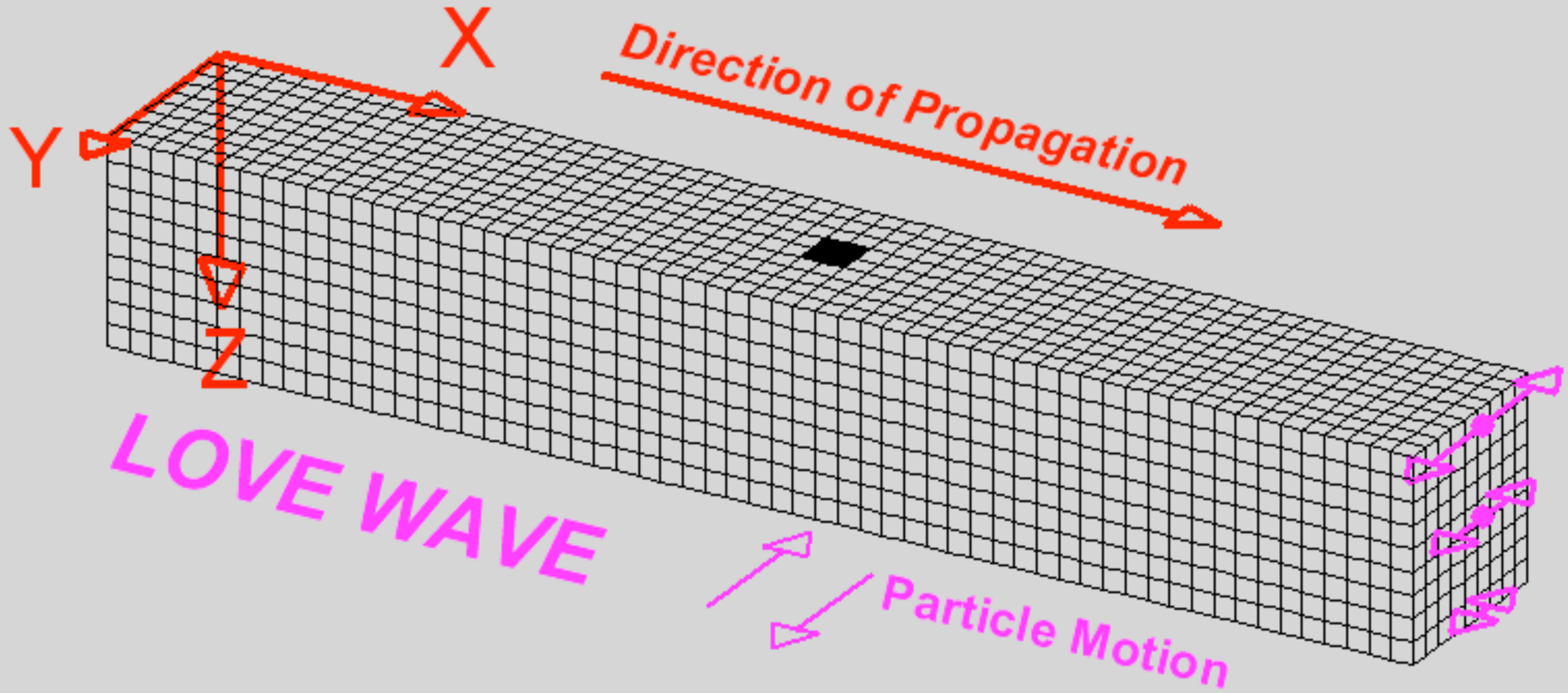

Deformation propagates. Particle motion consists of alternating transverse motions. Particle motion is horizontal and perpendicular to the direction of propagation (transverse). To aid in seeing that the particle motion is purely horizontal, focus on the Y axis (red line) as the wave propagates through it. Amplitude decreases with depth. Material returns to its original shape after wave passes.

Rayleigh Wave (R-Wave) Animation

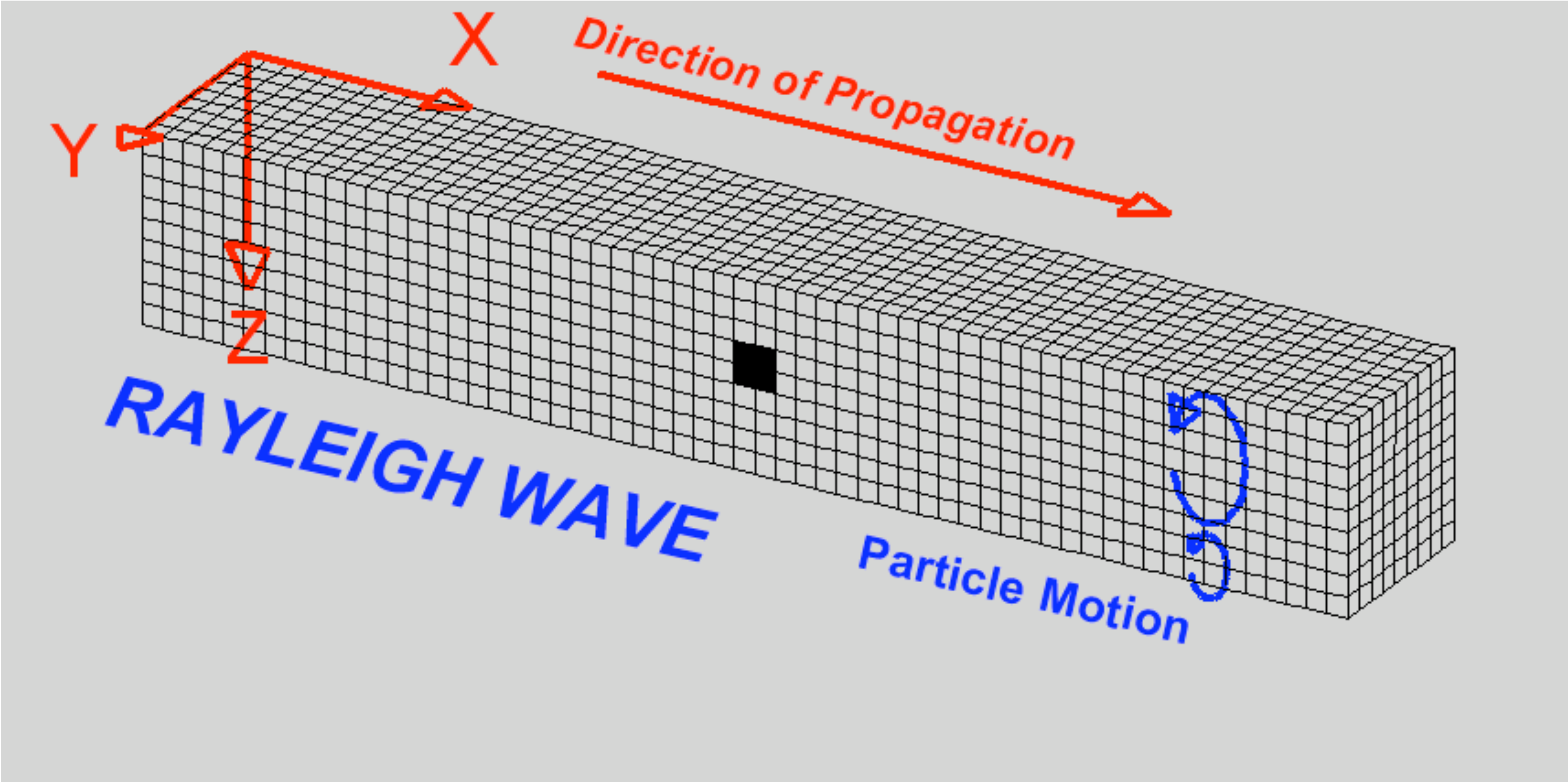

Deformation propagates. Particle motion consists of elliptical motions (generally retrograde elliptical) in the vertical plane and parallel to the direction of propagation. Amplitude decreases with depth. Material returns to its original shape after wave passes.

Seismic Surface Waves

Wave Type (and names)	Particle Motion	Other Characteristics
L, **Love**, Surface waves, Long waves	Transverse horizontal motion, perpendicular to the direction of propagation and generally parallel to the Earth's surface.	Love waves exist because of the Earth's surface. They are largest at the surface and decrease in amplitude with depth. Love waves are dispersive, that is, the wave velocity is dependent on frequency, generally with low frequencies propagating at higher velocity. Depth of penetration of the Love waves is also dependent on frequency, with lower frequencies penetrating to greater depth.
R, **Rayleigh**, Surface waves, Long waves, Ground roll	Motion is both in the direction of propagation and perpendicular (in a vertical plane), and "phased" so that the motion is generally elliptical – either prograde or retrograde.	Rayleigh waves are also dispersive and the amplitudes generally decrease with depth in the Earth. Appearance and particle motion are similar to water waves. Depth of penetration of the Rayleigh waves is also dependent on frequency, with lower frequencies penetrating to greater depth. Generally, Rayleigh waves travel slightly slower than Love waves.

Figure 2.7-1: Seismograms recorded at a distance of 110°, showing surface waves.

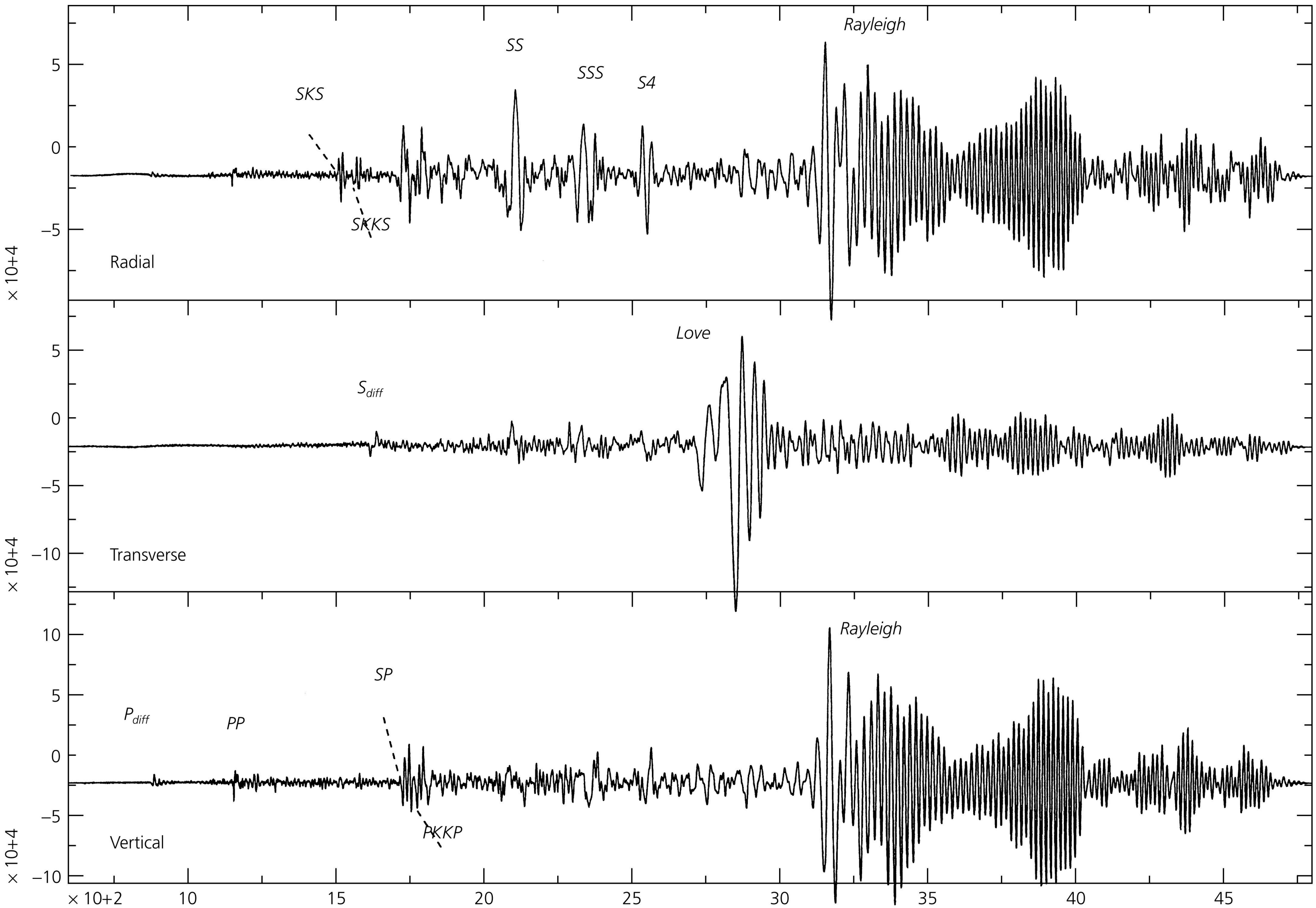

Three-component seismograms for the M6.5 west coast of Chile earthquake recorded at NNA

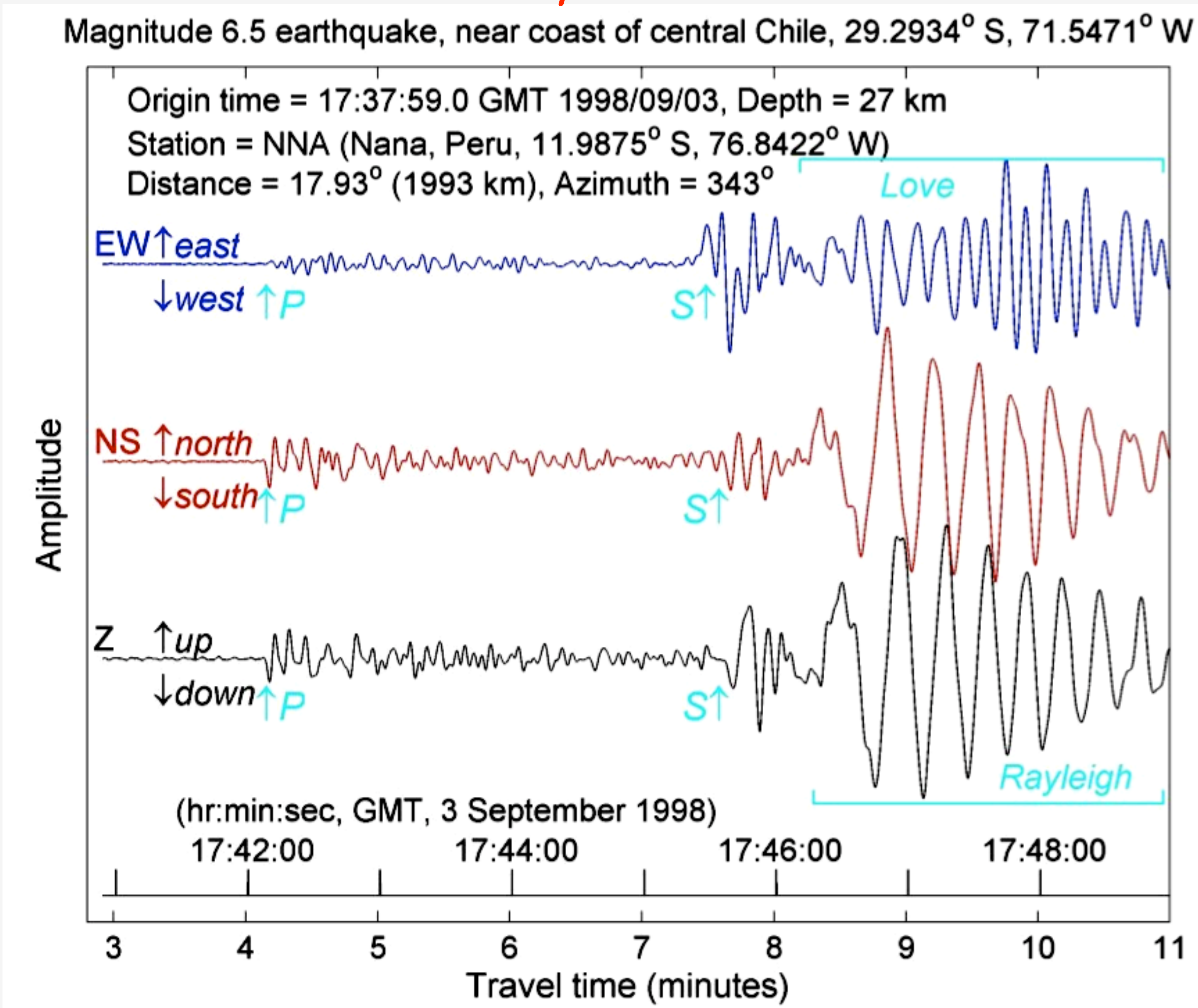

Seismic magnitudes are also defined for surface waves. We do this for specific periods, as the wave dispersion must be allowed for. The most Common measurement is called Ms.

Surface wave magnitude (measured using the largest amplitude, zero to peak, of the surface waves):

$$M_s = \log(A/T) + 1.66 \log \Delta + 3.3 \qquad \text{(general form)}$$

$$M_s = \log A_{20} + 1.66 \log \Delta + 2.0 \qquad \text{(for 20 second period Rayleigh waves)}$$

(Δ is in degrees)

Seismic Moment, a physical measure of the overall faulting process:

$Mo = \mu A D$ (N-m; or dyne-cm) [1 N-m = 10^7 dyne-cm]

A – area of rupture (m^2); D – average fault slip (m); μ – rigidity (N/m^2)

Every earthquake produced by fault slip has a corresponding seismic moment. These are the 'static' final values of the faulting energy release. This corresponds to zero frequency, or infinite period motion. The Mo value captures the total elastic strain energy change that goes into seismic elastic deformation.

We can define another seismic magnitude, called the *Moment magnitude*, M_w, which is now the preferred measure for relative overall earthquake size:

$$M_w = [\log10(Mo)-16.1]/1.5 \qquad \text{Mo in units dyne-cm}$$

Figure 4.6-3: Comparison of the magnitudes of four earthquakes.

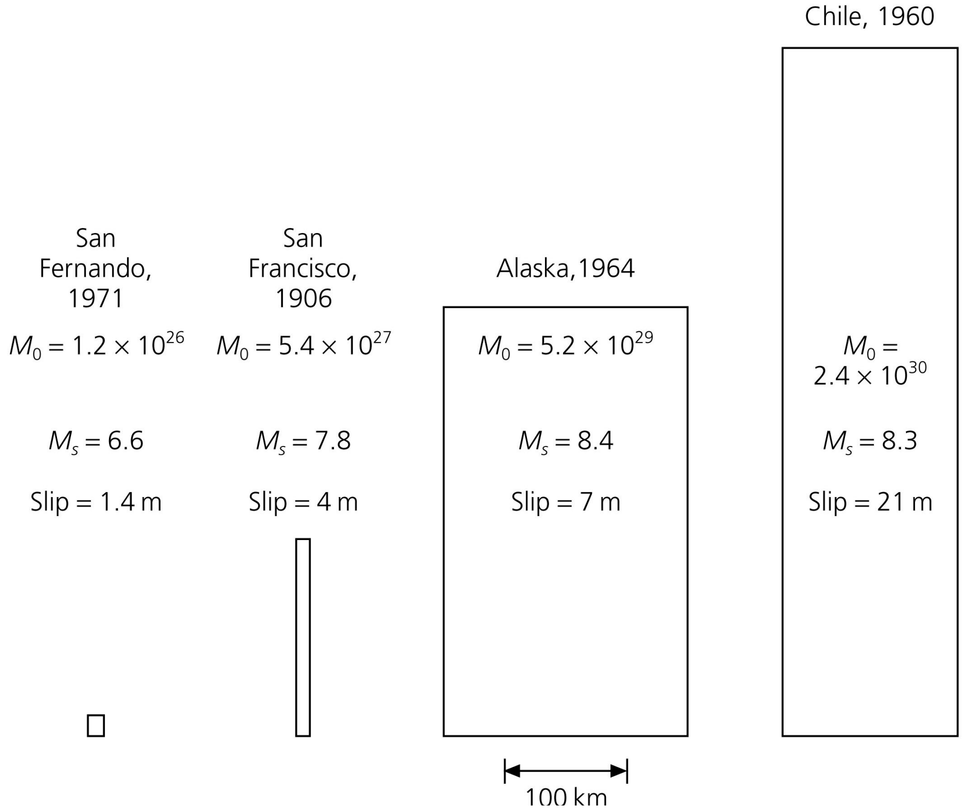

Moment magnitude:

$$M_w = \frac{\log M_0}{1.5} - 10.73$$

(with M_0 in dyn-cm)

Earthquake	Body wave magnitude m_b	Surface wave magnitude M_s	Fault area (km^2) length × width	Average dislocation (m)	Moment (dyn-cm) M_0	Moment magnitude M_w
Truckee, 1966	5.4	5.9	10 × 10	0.3	8.3×10^{24}	5.8
San Fernando, 1971	6.2	6.6	20 × 14	1.4	1.2×10^{26}	6.7
Loma Prieta, 1989	6.2	7.1	40 × 15	1.7	3.0×10^{26}	6.9
San Francisco, 1906		8.2	320 × 15	4	6.0×10^{27}	7.8
Alaska, 1964	6.2	8.4	500 × 300	7	5.2×10^{29}	9.1
Chile, 1960		8.3	800 × 200	21	2.4×10^{30}	9.5

Why can an earthquake have different magnitudes for different periods?

The shape of the earthquake seismic wave radiation as a function of wave frequency, is called the source function is controlled by two time scales active during faulting motion.

One time scale is how long it take the fault to rupture, approximated by fault length, L, divided by rupture velocity, V_R: $T_R = L/V_R$. Rupture velocities are on the order of 3 km/s. So, a 100-km long rupture will have sliding for about 33 s, And that would give a magnitude ~7.3 size event.

The second time scale is how long it takes for any point on the fault to slide to the final offset. The typical sliding velocity is ~1 m/s. For a magnitude 7.3 size event, the average slip can be ~2.5 m, so the sliding at each point lasts for about T_D = 2-3 s. T_D is usually less than T_R.

The source spectrum is shaped by interference of wave motions coming off the fault for wave periods lower than these time scales; the spectrum reduces due to destructive interference. It falls off proportional to frequency, *f* (1/period) raised to the power of -2. With angular frequency, $\omega = 2 \pi f$, this is called the ω-squared source model (flat at low frequency, falling off at high frequency).

Fourier’ s Theorem

For a totally general function, F(t), we can exactly represent F(t) by an infinite sum (integral) of harmonic (cos and/or sin) functions with suitable amplitudes and phase alignments (e.g., for a set of cosines):

$$F(t) = \int_0^{\infty} A(\omega) \cos (kx - \Phi(\omega))\, d\omega$$

$A(\omega)$: Amplitude Spectrum (amplitude of each harmonic cosine)

$\Phi(\omega)$: Phase spectrum (time alignment of each harmonic component)

Time domain:

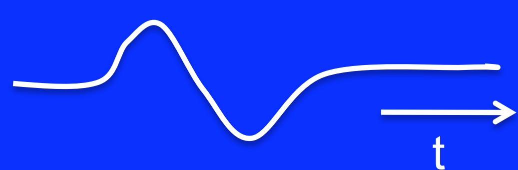

Frequency domain:

$A(\omega)$

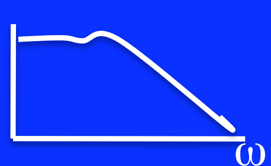

$\Phi(\omega)$

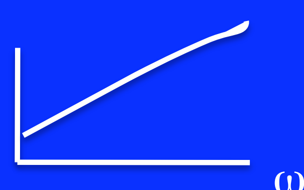

Figure 2.2-8: Waves on a string as a summation of modes.

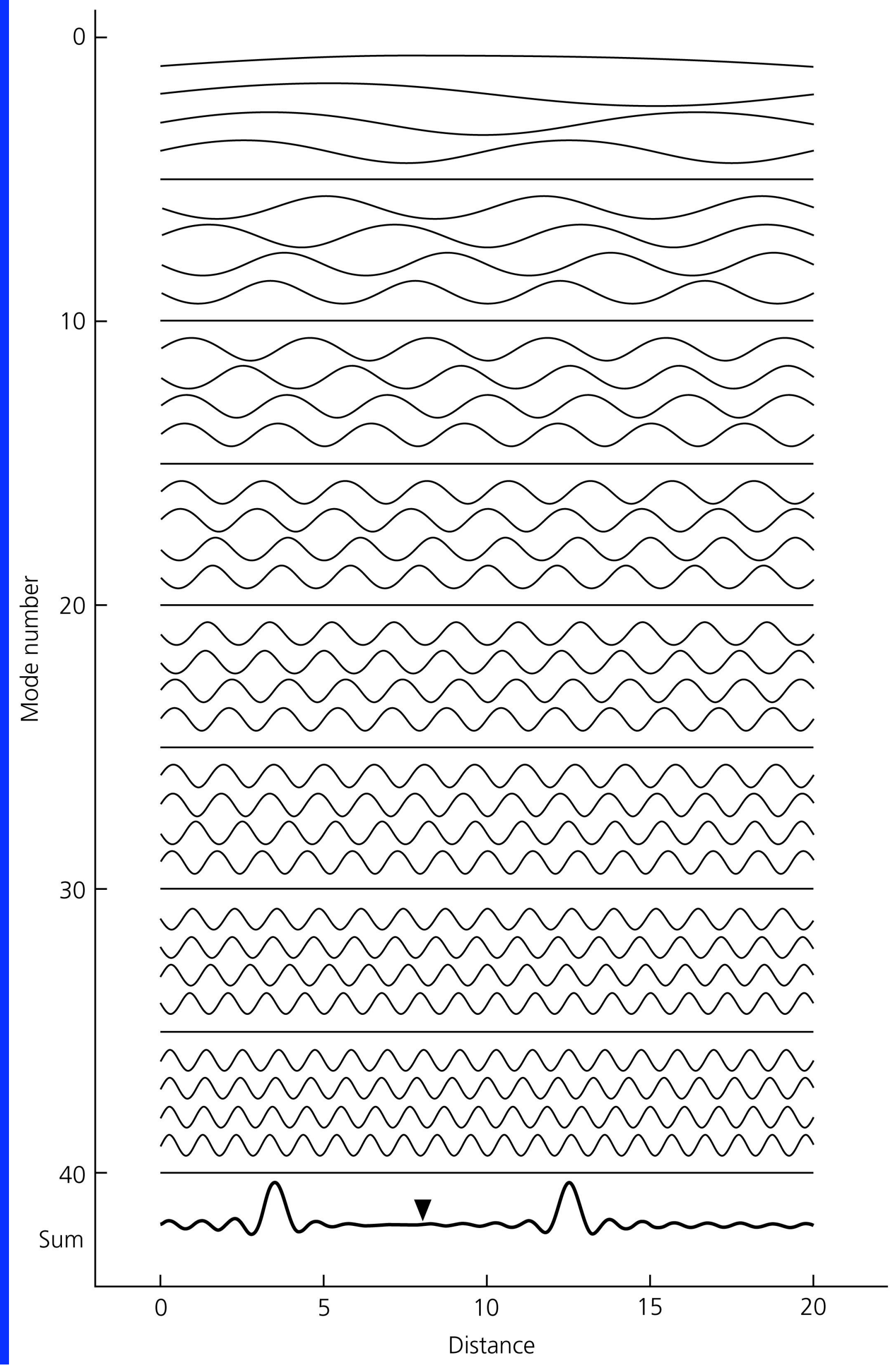

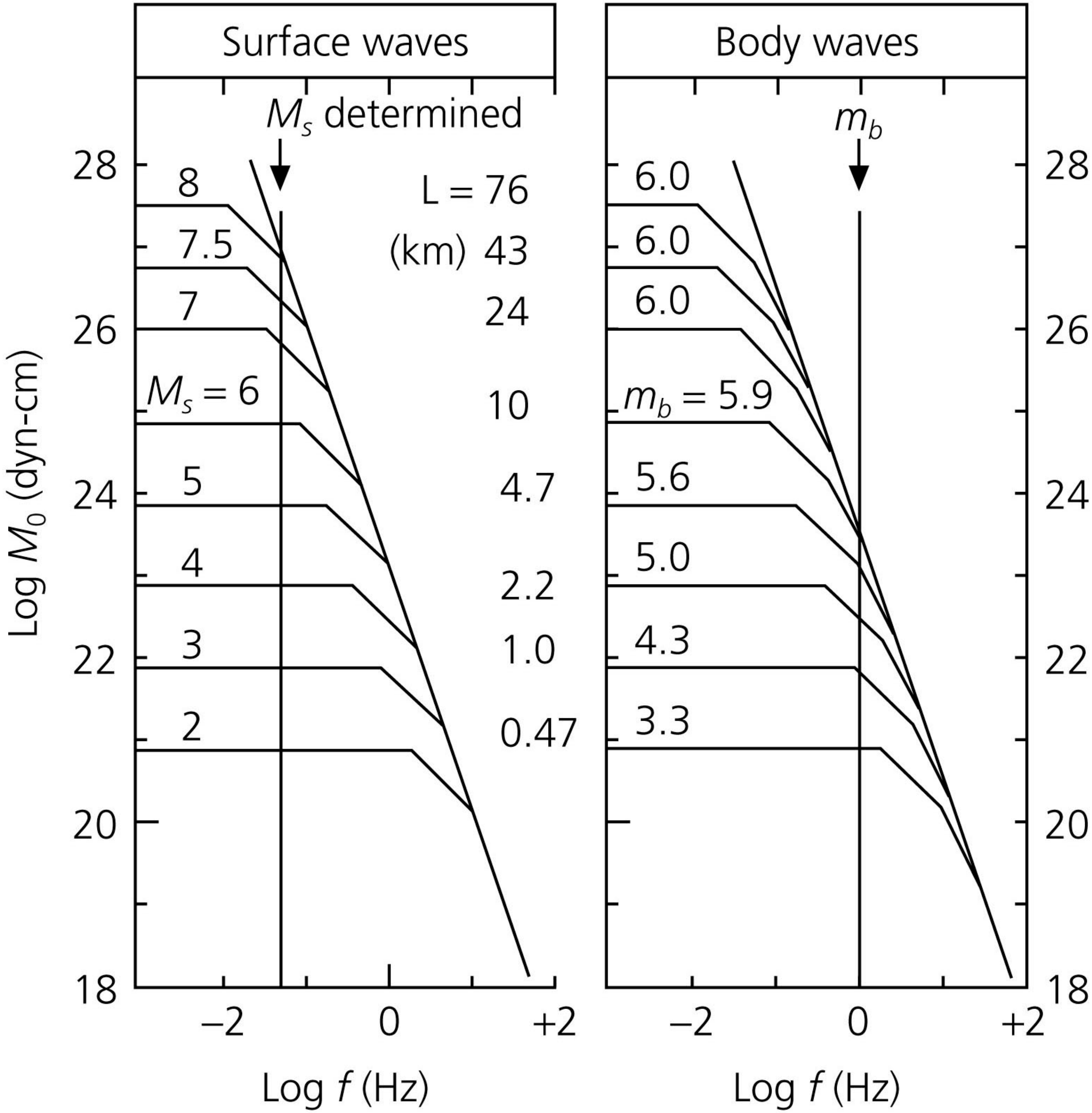

The ‘strength’ of the source depends on the period. At zero frequency we get the seismic moment. At higher frequency, we may get a lower source strength.

Figure 4.6-6: Demonstration of the saturation of body and surface wave magnitudes.

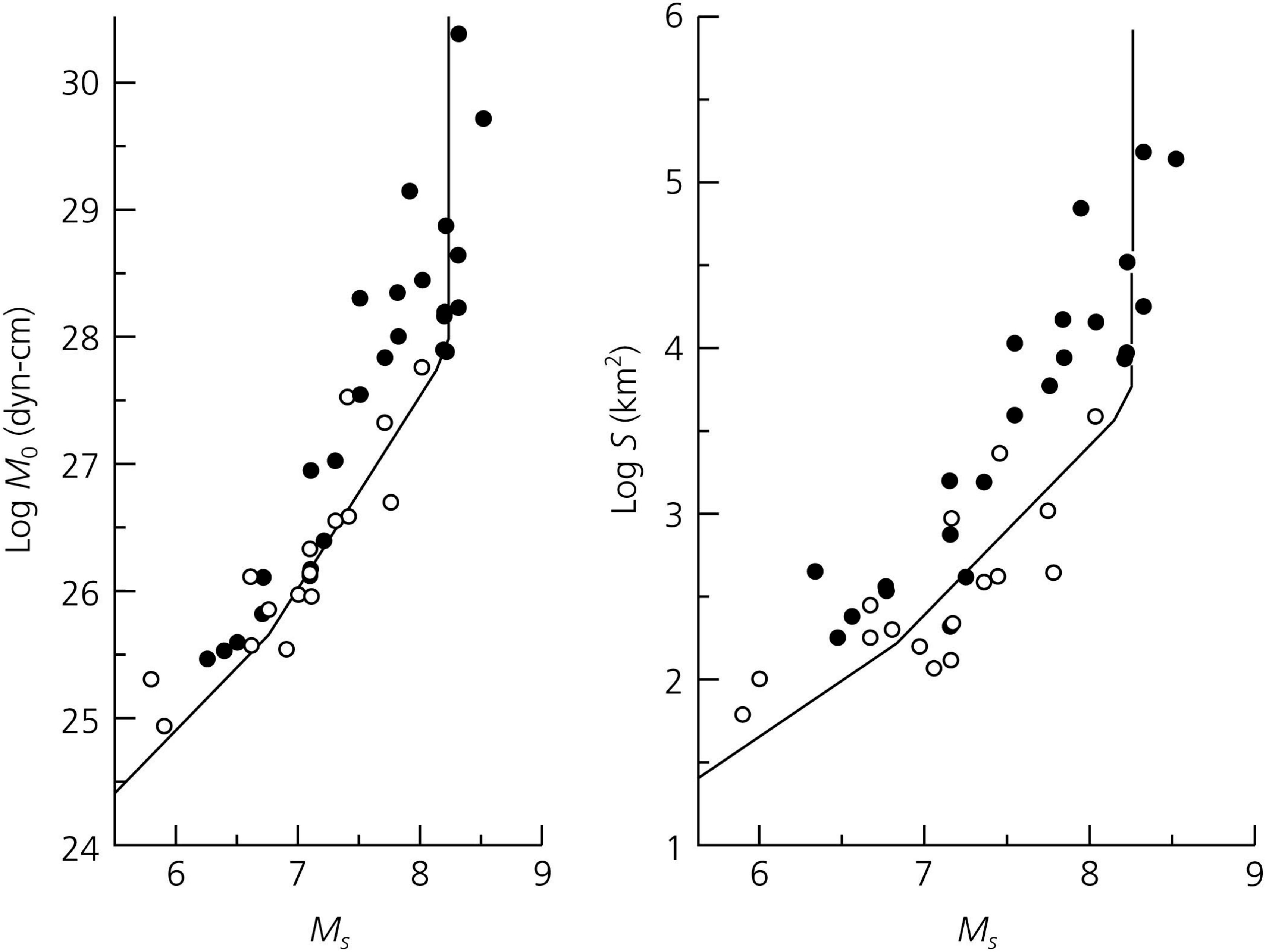

Earthquake Scaling Relations

m_b and M_s are related by

$$
\begin{array}{ll}
m_b = M_s + 1.33 & M_s < 2.86 \\
m_b = 0.67\ M_s + 2.28 & 2.86 < M_s < 4.90 \\
m_b = 0.33\ M_s + 3.91 & 4.90 < M_s < 6.27 \\
m_b = 6.00 & 6.27 < M_s.
\end{array}
$$

Assuming $L = 2W$, M_s and fault area (in km^2) are related by

$$
\begin{array}{ll}
\log S = 0.67\ M_s - 2.28 & M_s < 6.76 \\
\log S = M_s - 4.53 & 6.76 < M_s < 8.12 \\
\log S = 2M_s - 12.65 & 8.12 < M_s < 8.22 \\
M_s = 8.22 & S > 6080 \text{ km}^2
\end{array}
$$

Assuming a stress drop of 50 bars, $\log M_0$ (in dyn-cm) and M_s are related by

$$
\begin{array}{ll}
\log M_0 = M_s + 18.89 & M_s < 6.76 \\
\log M_0 = 1.5\ M_s + 15.51 & 6.76 < M_s < 8.12 \\
\log M_0 = 3M_s + 3.33 & 8.12 < M_s < 8.22 \\
M_s = 8.22 & \log M_0 > 28.
\end{array}
$$

The 'Greatest' 1960 Chile, M_w= 9.5

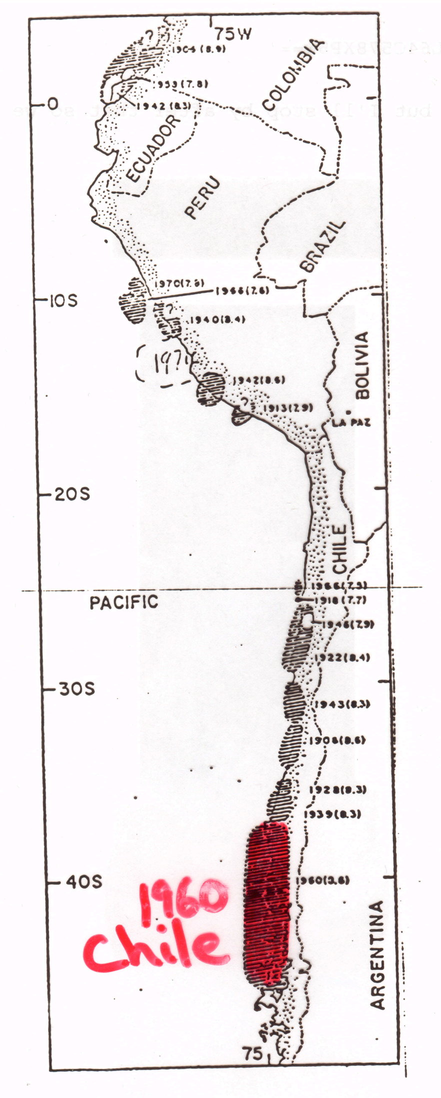

Other huge events of the past 120 years of seismological history (for which we have a seismic recording to measure):

1964 Alaska M_w 9.2
2004 Sumatra M_w 9.15
2011 Tohoku M_w 9.0
1952 Kamchatka M_w 9.0
2010 Chile M_w 8.8

Copyright © The McGraw-Hill Companies, Inc. Permission required for reproduction or display.

Table 4.3
Earthquakes in the World Each Year

Magnitude	Number of Quakes Per Year	Description
8.5 and up	0.3	
8–8.4	1	Great
7.5–7.9	3	
7–7.4	1 5	Major
6.6–6.9	56	
6–6.5	210	Strong (destructive)
5–5.9	800	Moderate (damaging)
4–4.9	6,200	Light
3–3.9	49,000	Minor
2–2.9	350,000	Very minor
0–1.9	3,000,000	

Japan (past 1300 years):
190 earthquakes with M > 7
20 with M > 8

Southern California (since 1816):
about 180 earthquakes with M > 6
24 with M > 7
1 with M > 8

New Madrid (since 1816):
about 16 earthquakes with M > 5
2 with M > 6

Why is there a downturn for
large and small events?

- Detection limits
- Fault width saturates

Figure 4.7-1: Frequency-magnitude plot for earthquakes during 1968-1997.

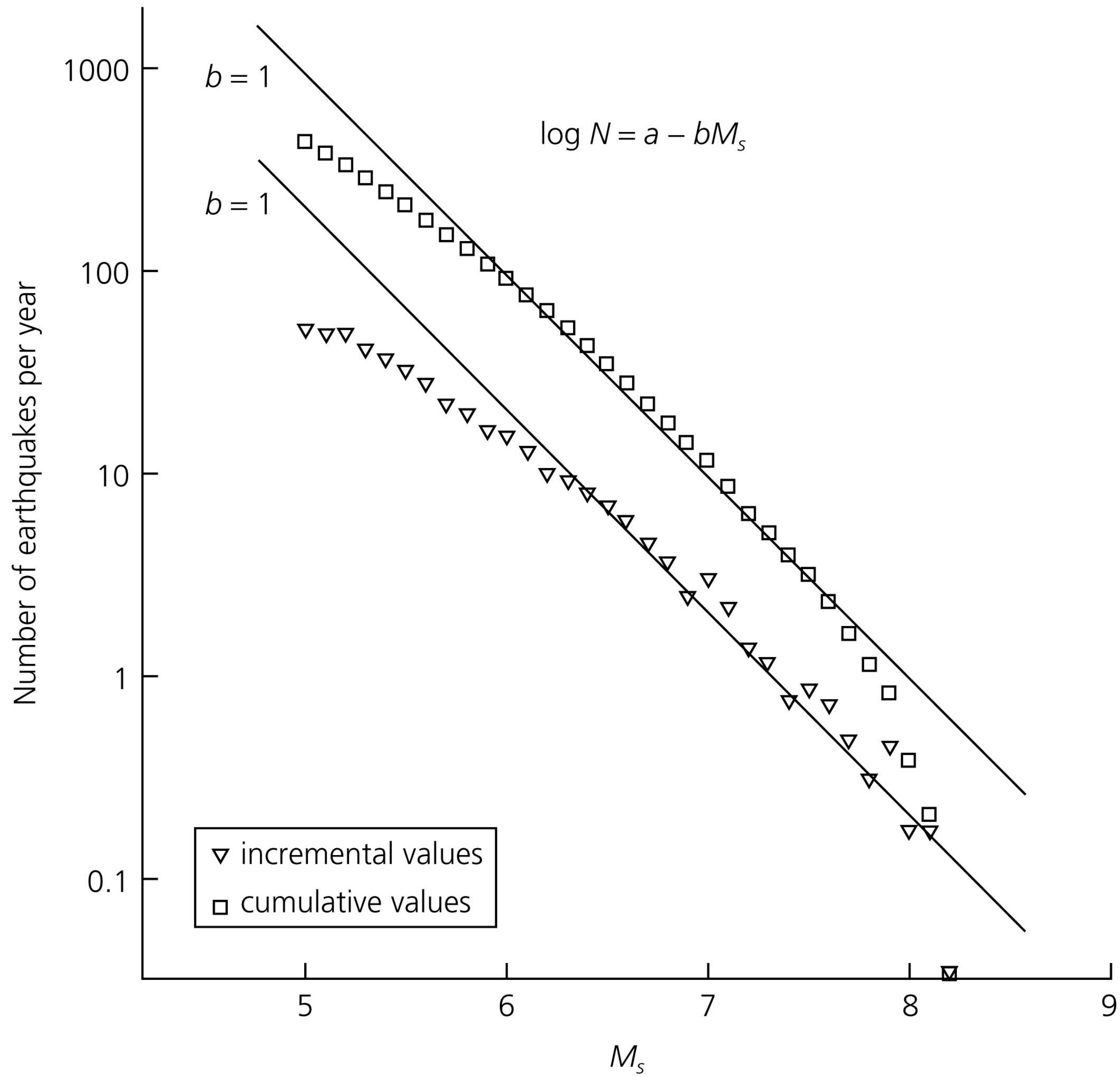

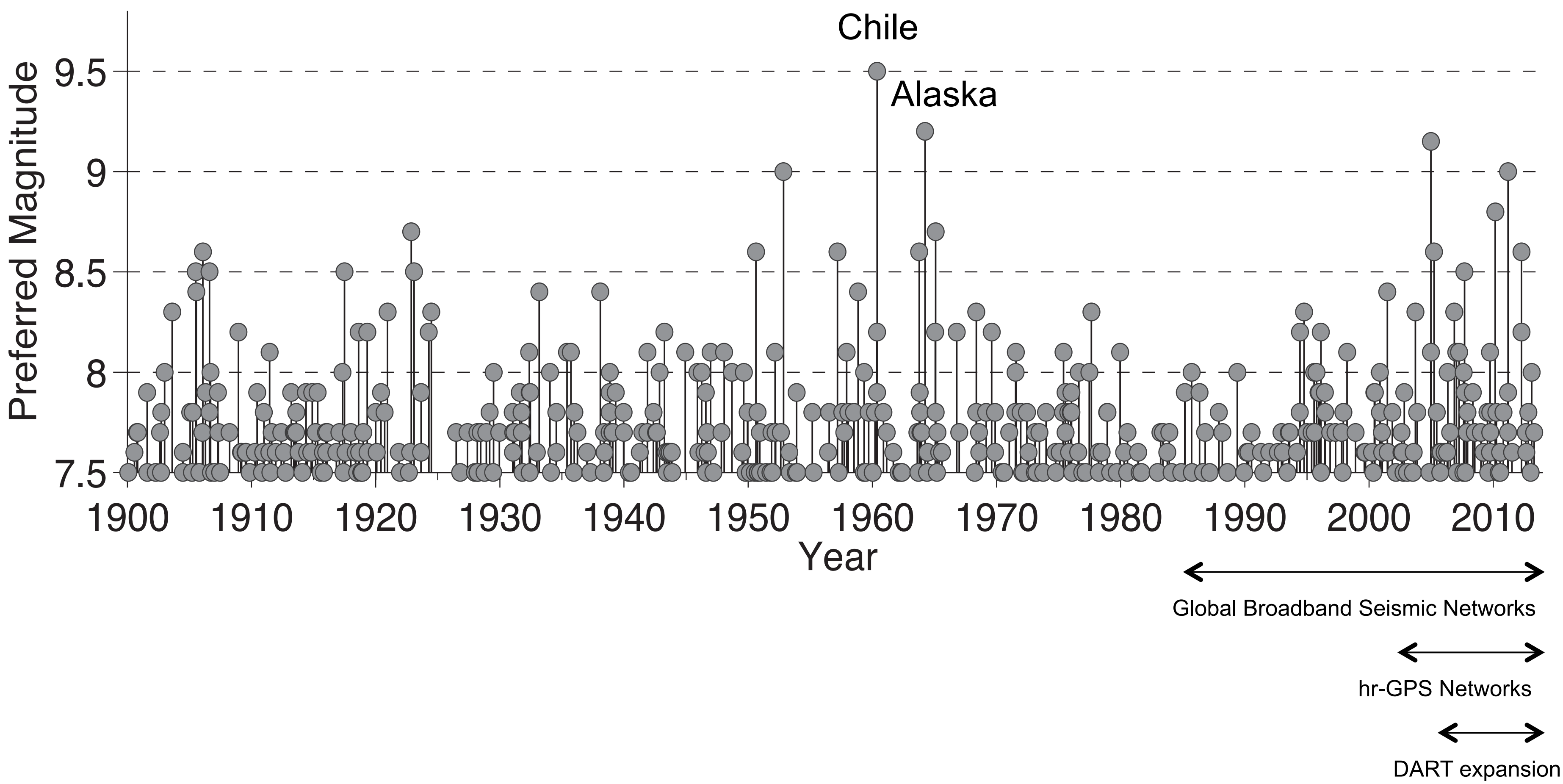

after, Ammon et al., SRL, 2010

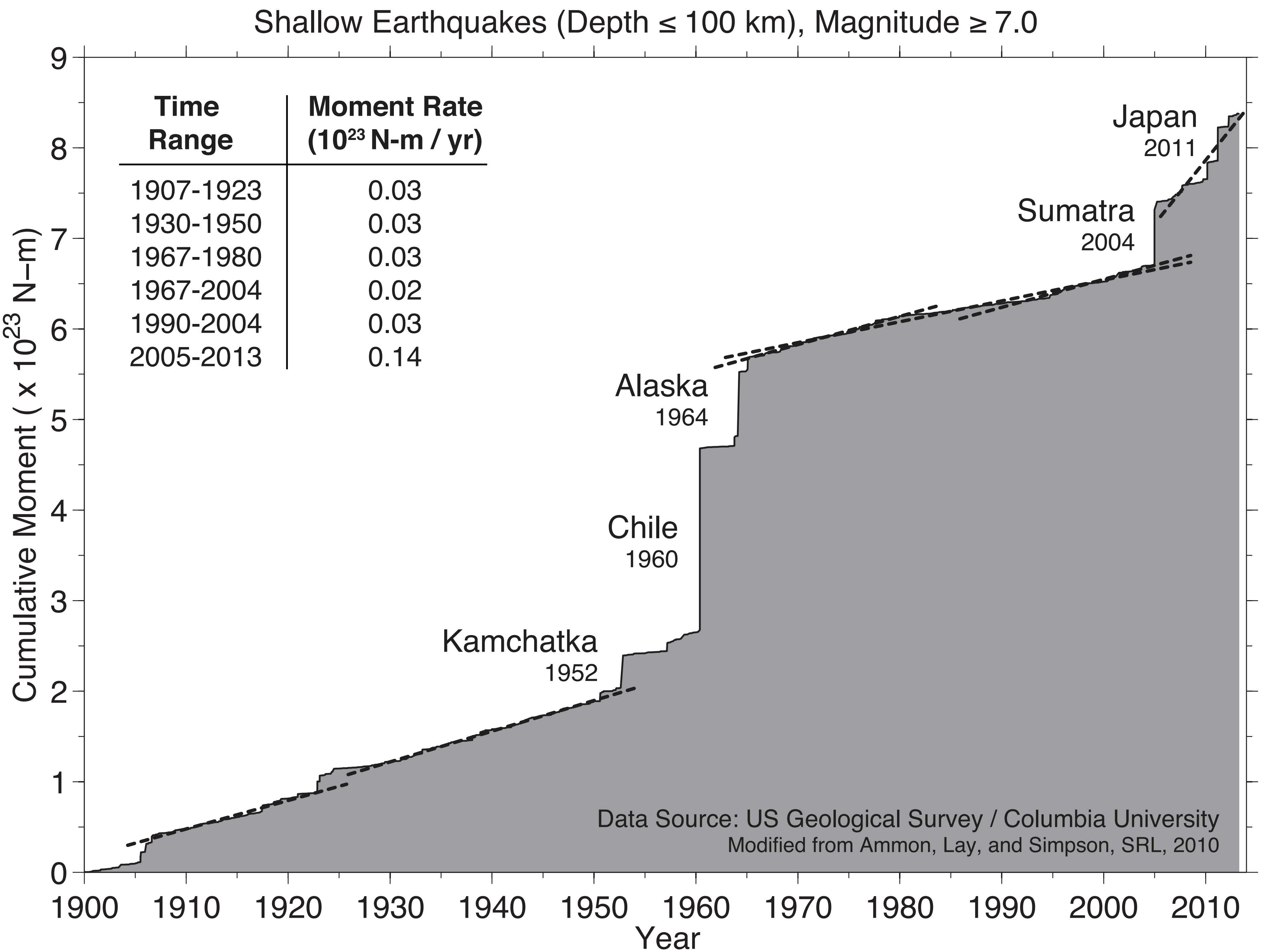
Shallow Earthquakes (Depth ≤ 100 km), Magnitude ≥ 7.0
Time Range
Moment Rate (10^{23} N-m / yr)
1907-1923 0.03
1930-1950 0.03
1967-1980 0.03
1967-2004 0.02
1990-2004 0.03
2005-2013 0.14
Cumulative Moment (x 10^{23} N–m)
Year
Kamchatka 1952
Chile 1960
Alaska 1964
Sumatra 2004
Japan 2011
Data Source: US Geological Survey / Columbia University
Modified from Ammon, Lay, and Simpson, SRL, 2010
0
1
2
3
4
5
6
7
8
9
1900
1910
1920
1930
1940
1950
1960
1970
1980
1990
2000
2010

Figure 4.7-4: Cumulative seismic moment for earthquakes 1976-1998.

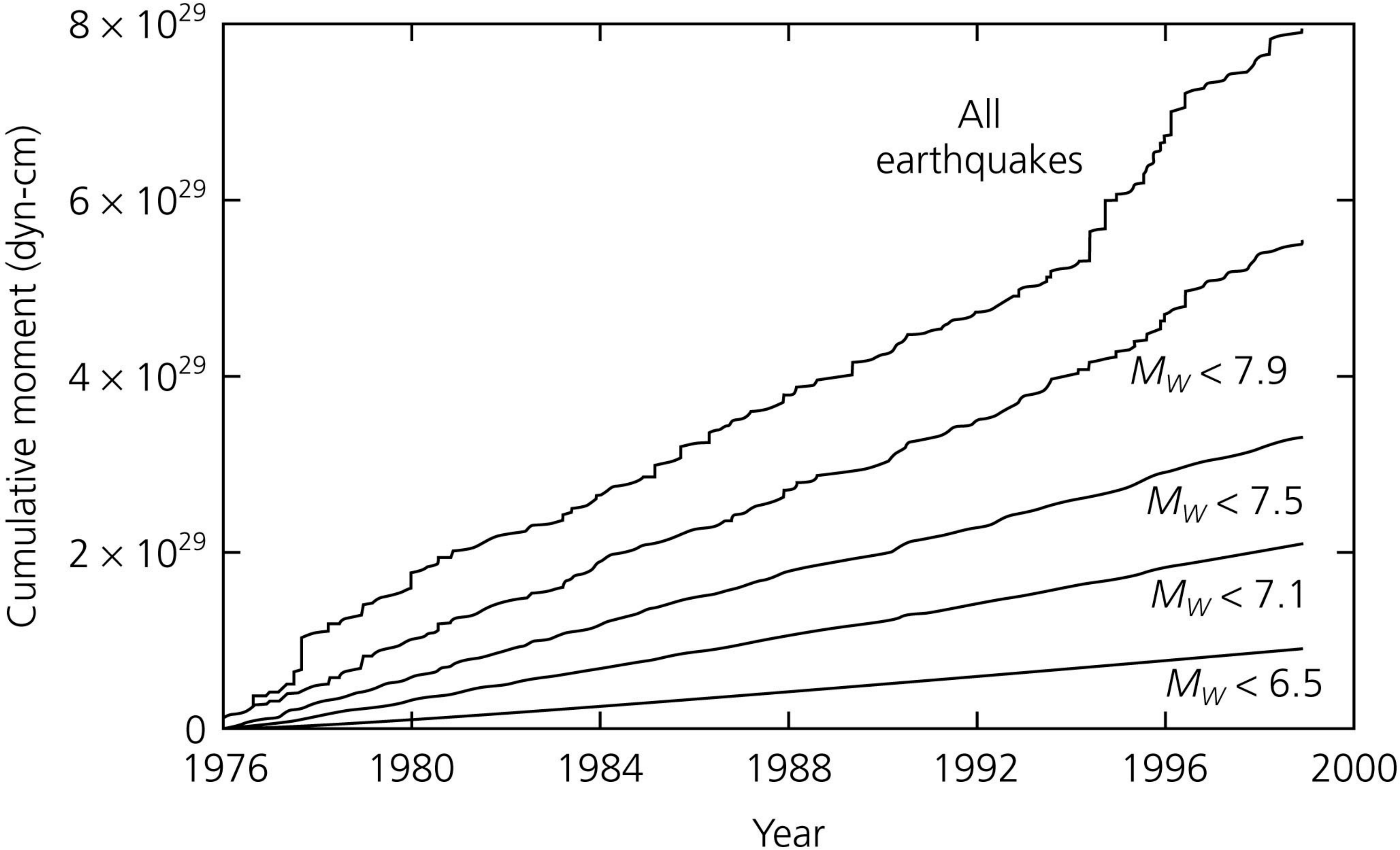

Last 9.0 yrs - 16 great shallow earthquakes: rate 1.8/yr; rate over preceding century 0.7/yr

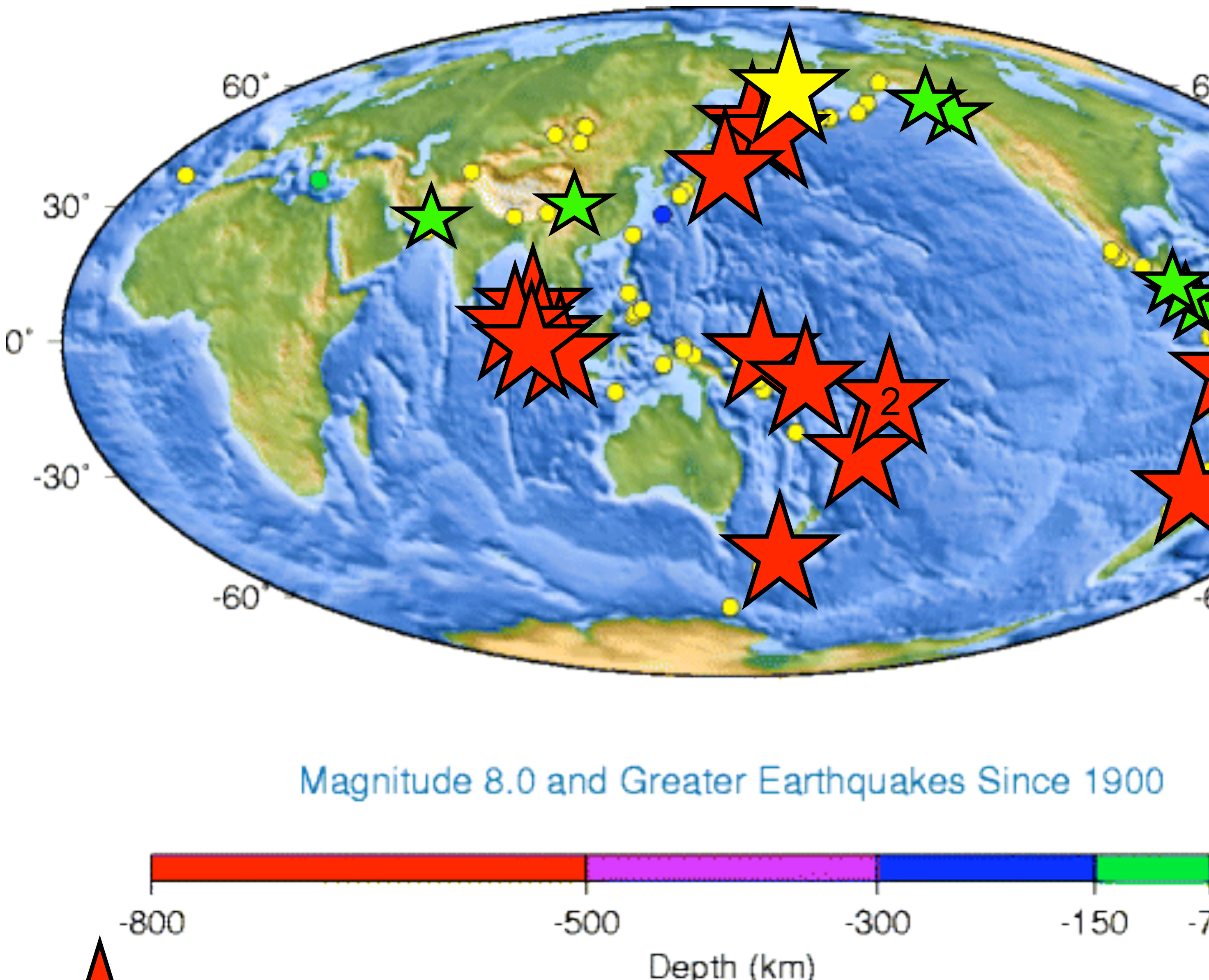

1.8/yr !

Great (M_w > 8) shallow events from Dec. 2004-Nov. 2013

STUDYING EARTHQUAKE FAULTING FROM THE SEISMIC WAVES IT GENERATES IS AN INVERSE PROBLEM

Arrival time of seismic waves at seismometers at different sites is first used to find the location and depth of earthquake

Amplitudes and motions of radiated seismic waves used to study

- size of the earthquake
- geometry of the fault on which it occurred
- direction and amount of slip

Seismic waves give an excellent picture of the kinematics of faulting, needed to understand regional tectonics

"Rheological" Layering

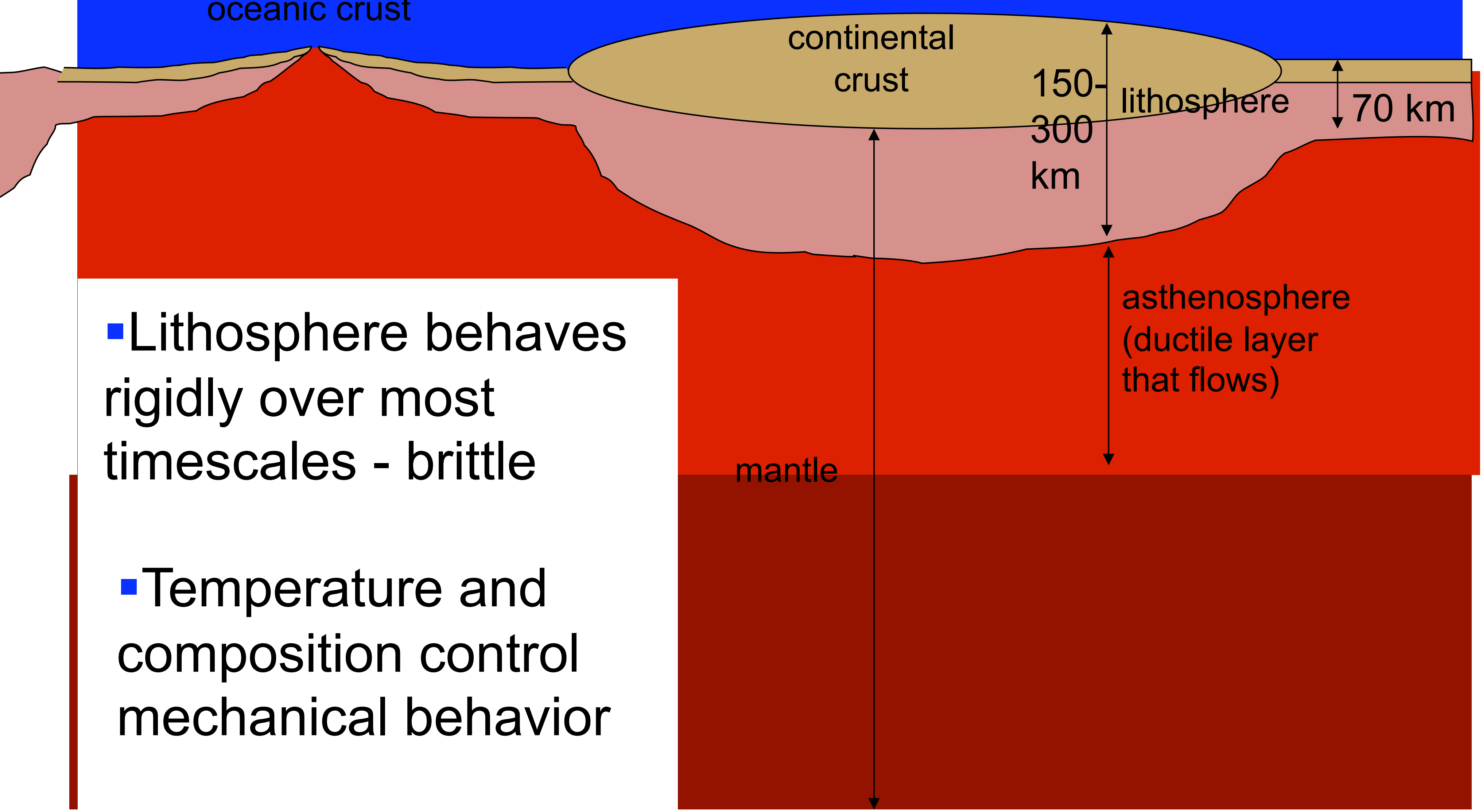

- Lithosphere behaves rigidly over most timescales - brittle

- Temperature and composition control mechanical behavior

1906 San Francisco Rupture

This earthquake was associated with lateral displacements of about 5 m along ~300 km
$M_w = 7.9$

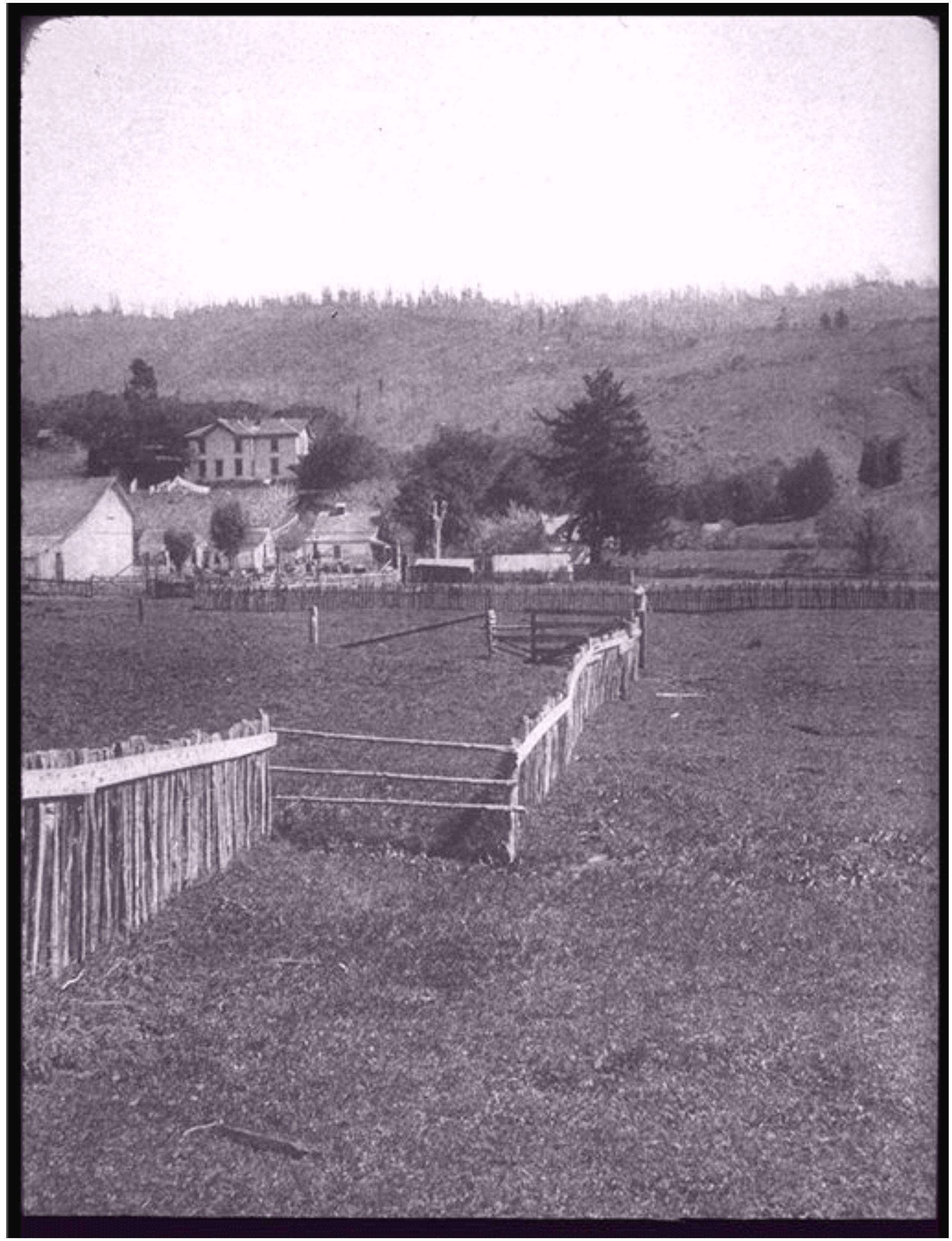

How do we describe faults? It started with miners….

Copyright © The McGraw-Hill Companies, Inc. Permission required for reproduction or display.

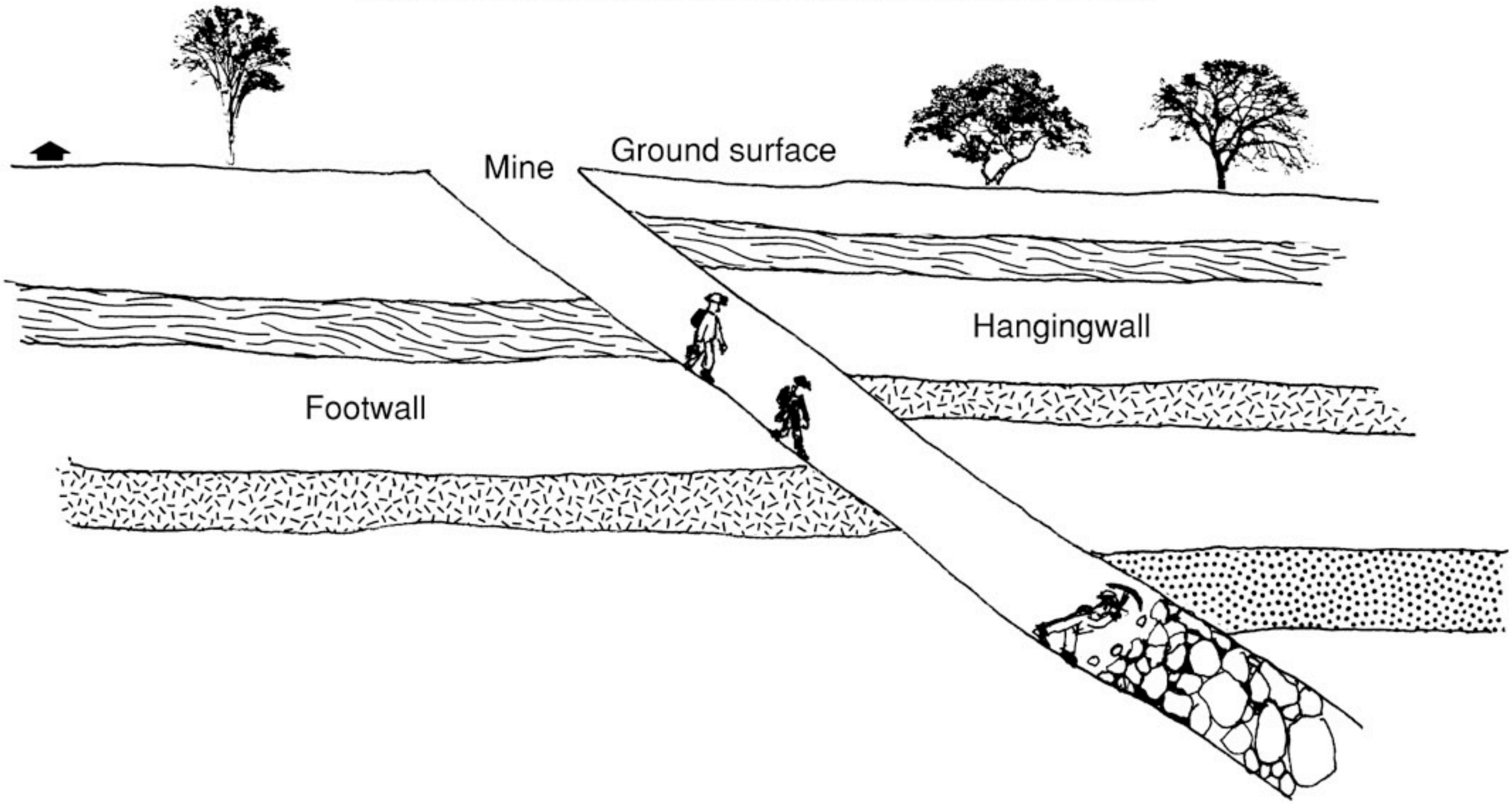

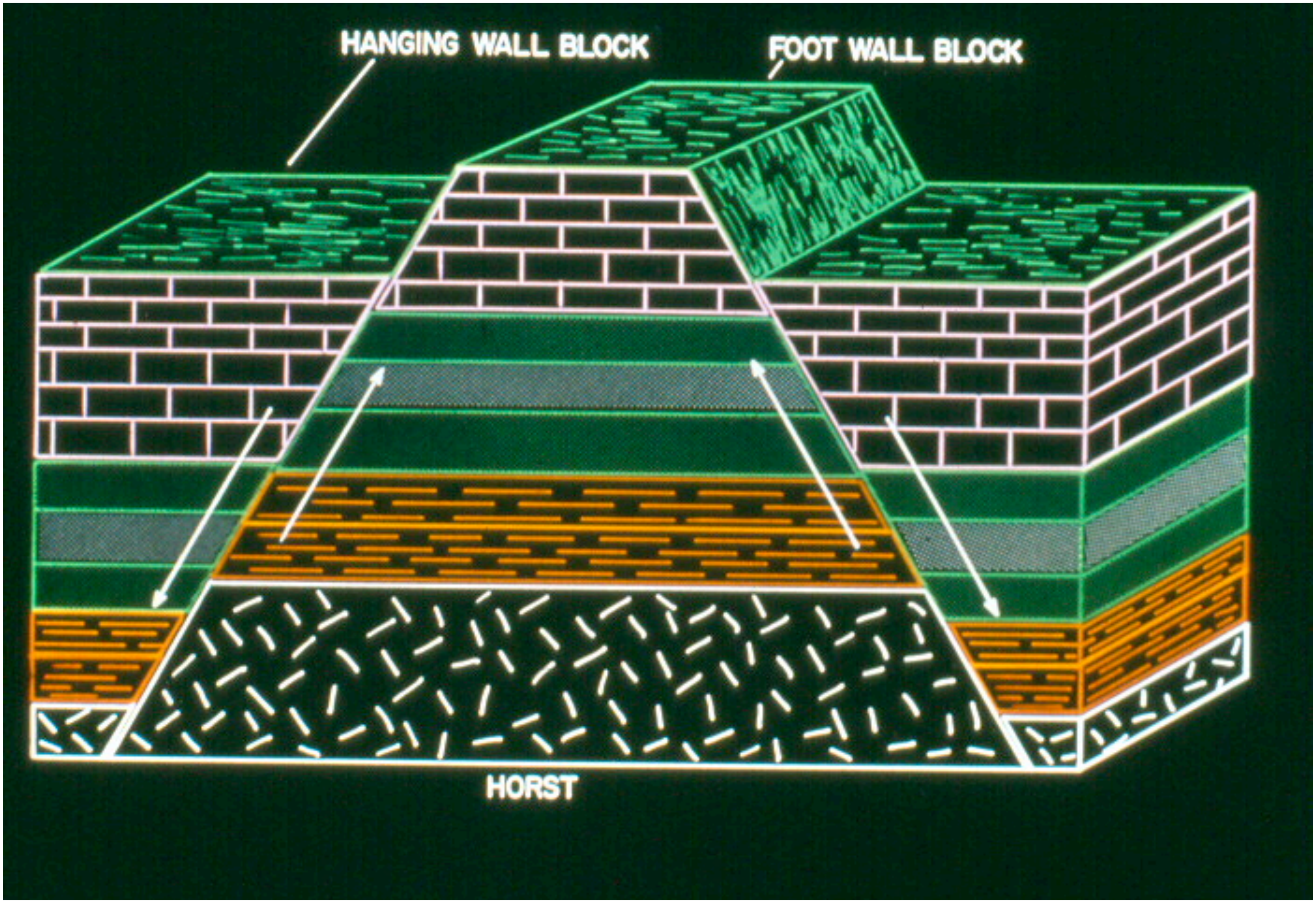
HANGING WALL BLOCK
FOOT WALL BLOCK
HORST

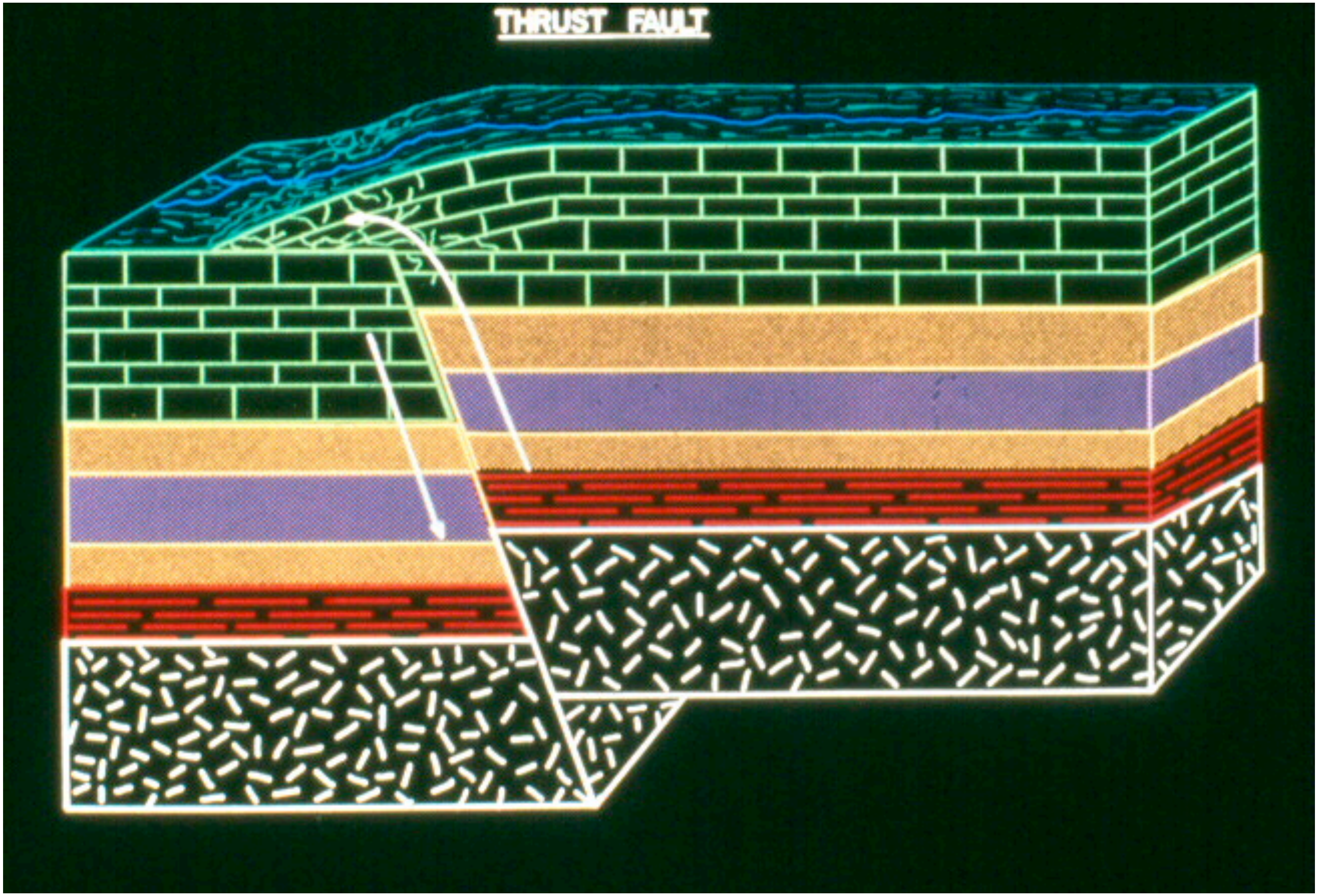
THRUST FAULT

Subduction zones have huge thrust faults where plates rub

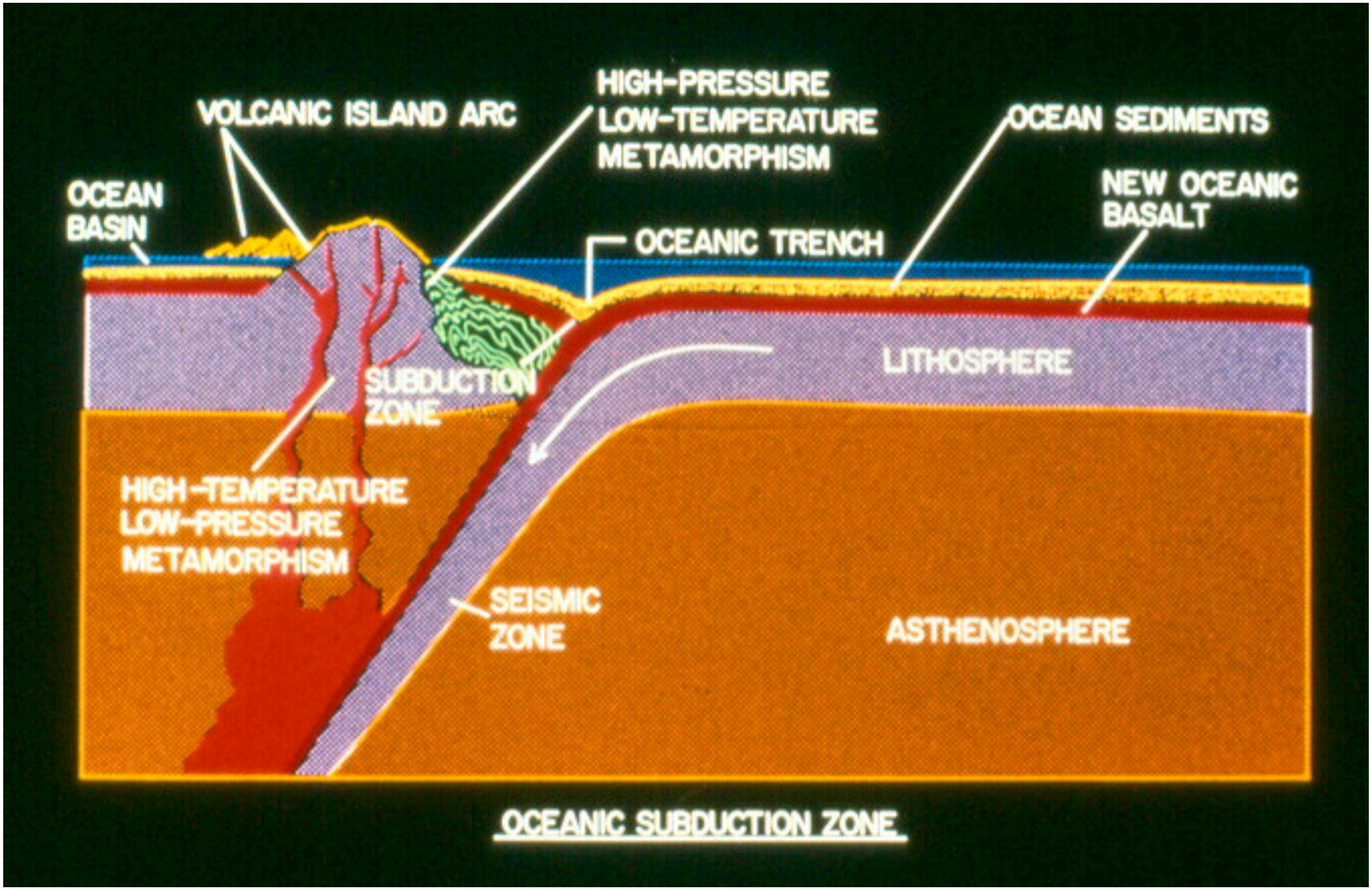

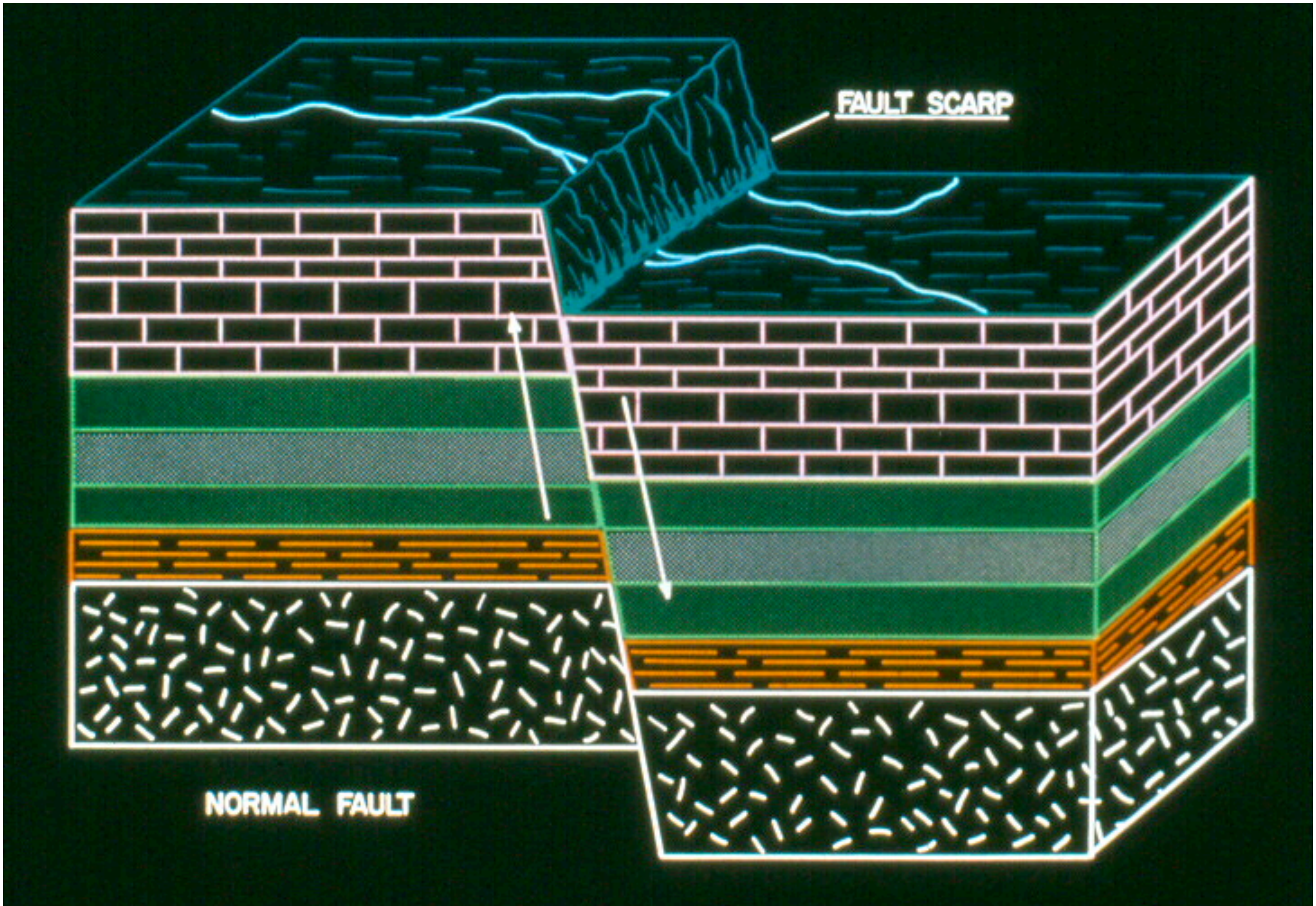

Normal faults exist in regions of extension/rifting

Figure 4.2-1: Fault scarp near Crowley Lake, California.

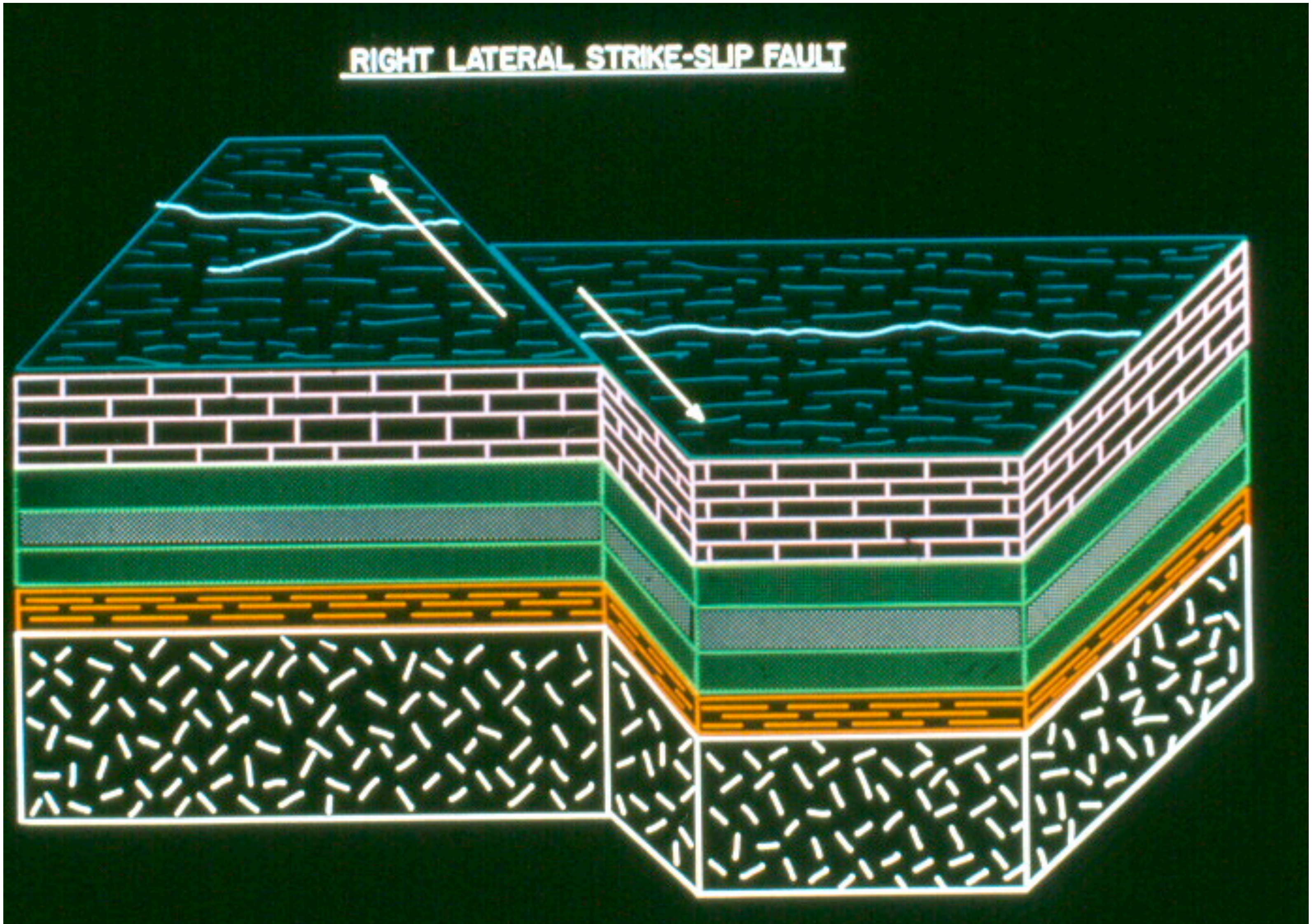

Strike-slip faults occur where crust is shearing horizontally

Strike-Slip Fault

Figure 4.1-4: Displacement of crops rows during the 1979 Imperial fault earthquake.

APPROXIMATE FAULT AS PLANAR WITH GEOMETRY REPRESENTED BY

Three angles: strike ϕ_f, dip δ, slip λ

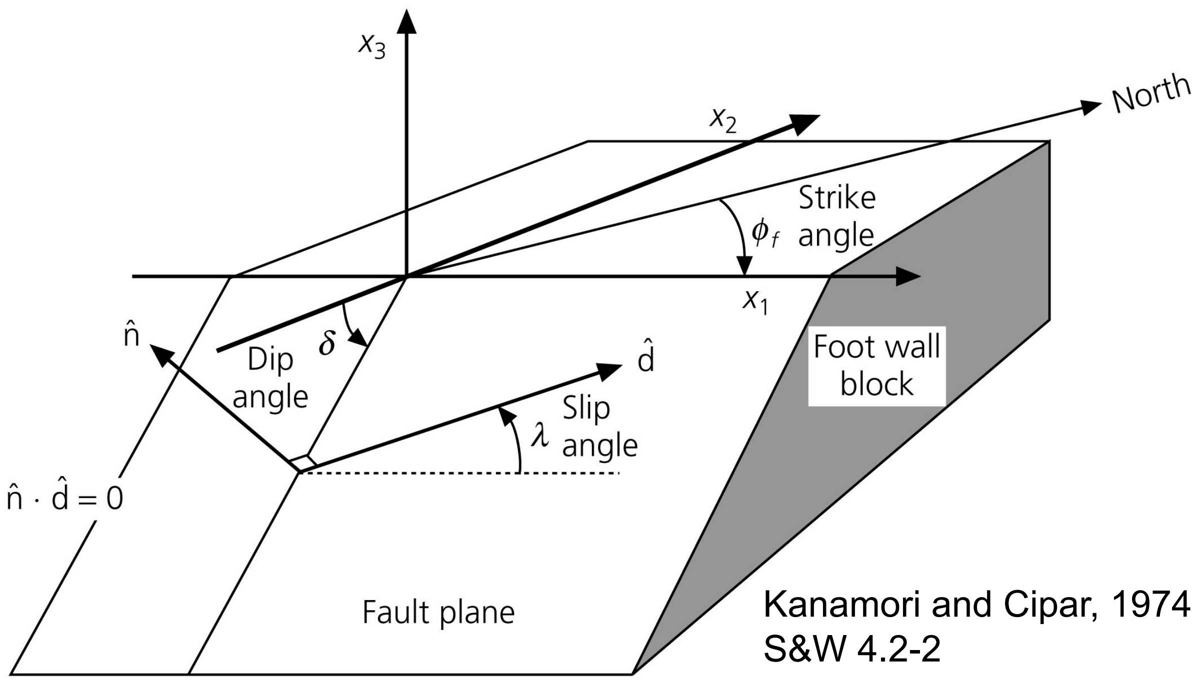

Kanamori and Cipar, 1974
S&W 4.2-2

Coordinate axes chosen with x_3 vertical and x_1 oriented along the fault in the plane of the earth's surface, such that the fault dip angle, δ measured from the $-x_2$ axis, is < 90°.

Slip angle λ is measured between the x_1 axis and d in the fault plane.

ϕ_f is the strike of the fault measured clockwise from north.

Strike, Dip and Rake

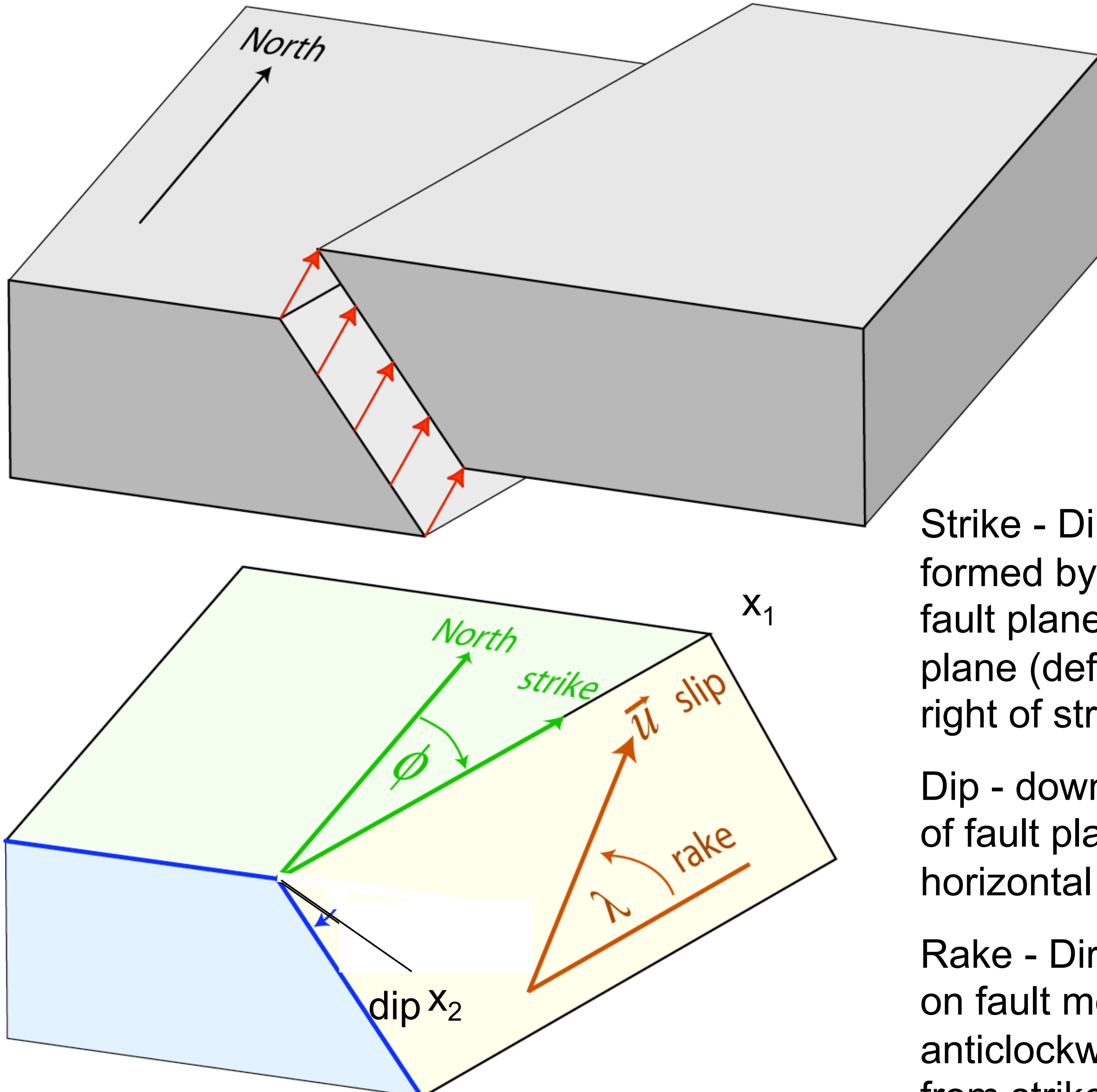

Strike - Direction of line formed by intersection of fault plane and horizontal plane (defined so dip is to right of strike)

Dip - downward inclination of fault plane relative to horizontal

Rake - Direction of motion on fault measured anticlockwise on fault plane from strike direction

SLIP ANGLE λ CHARACTERIZES FAULT TYPE

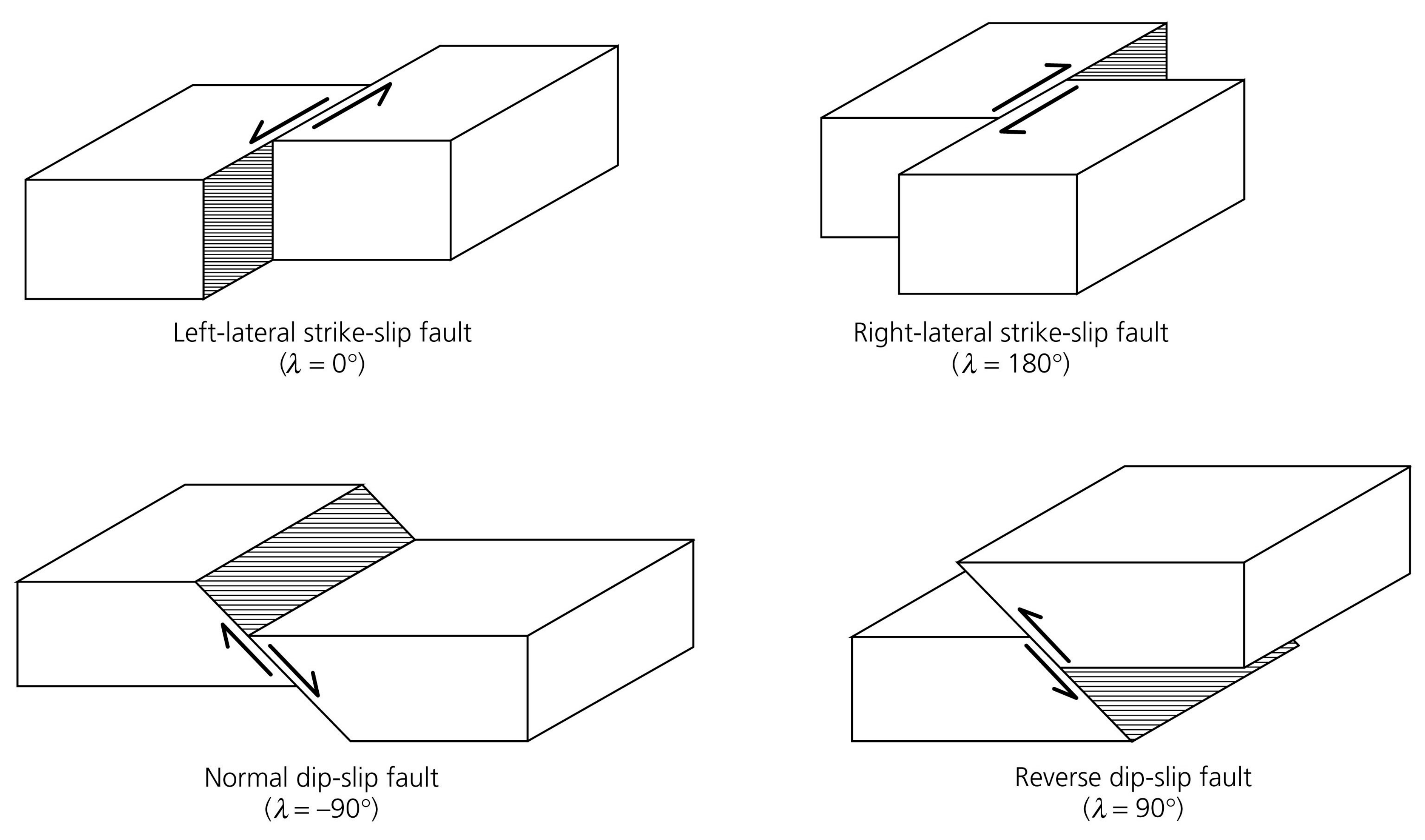

Most earthquakes consist of some combination of these motions, and have slip angles between these values

Earthquake Explanation

- An Earthquake is the process of sudden, shearing slip on a fault (or creation of a new crack) combined with resultant vibrations

- Earthquakes are Frictional Sliding instabilities. Repeated stick-slip behavior is observed. Friction depends on pressure, temperature, fluids, slip velocity, fault history, and material properties in the fault zone.

Strain accumulates in the volume of rock around the fault called the fault zone.

Sliding between the two rock masses is resisted by friction (static friction)

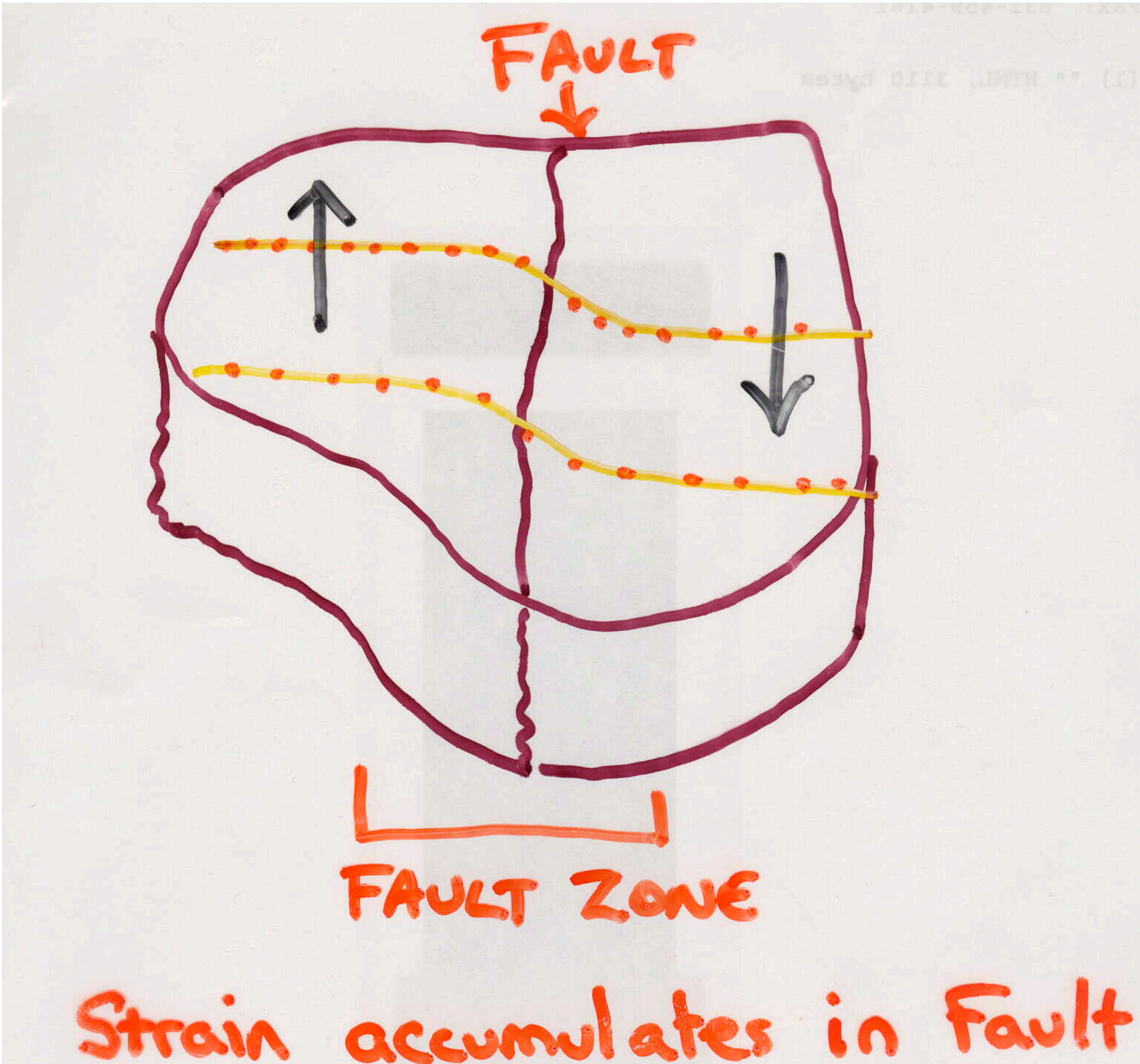

When the strain in the rock approaches the limiting value of about 1.0×10^{-4}, you will either break the rock (form a new fault), or overcome frictional resistance of the fault, abruptly releasing stored strain energy.

The sudden change in stress/strain in the source volume generates P and S waves that expand outward from the source volume. Much of the energy is consumed in heating of the fault surface as it slides.

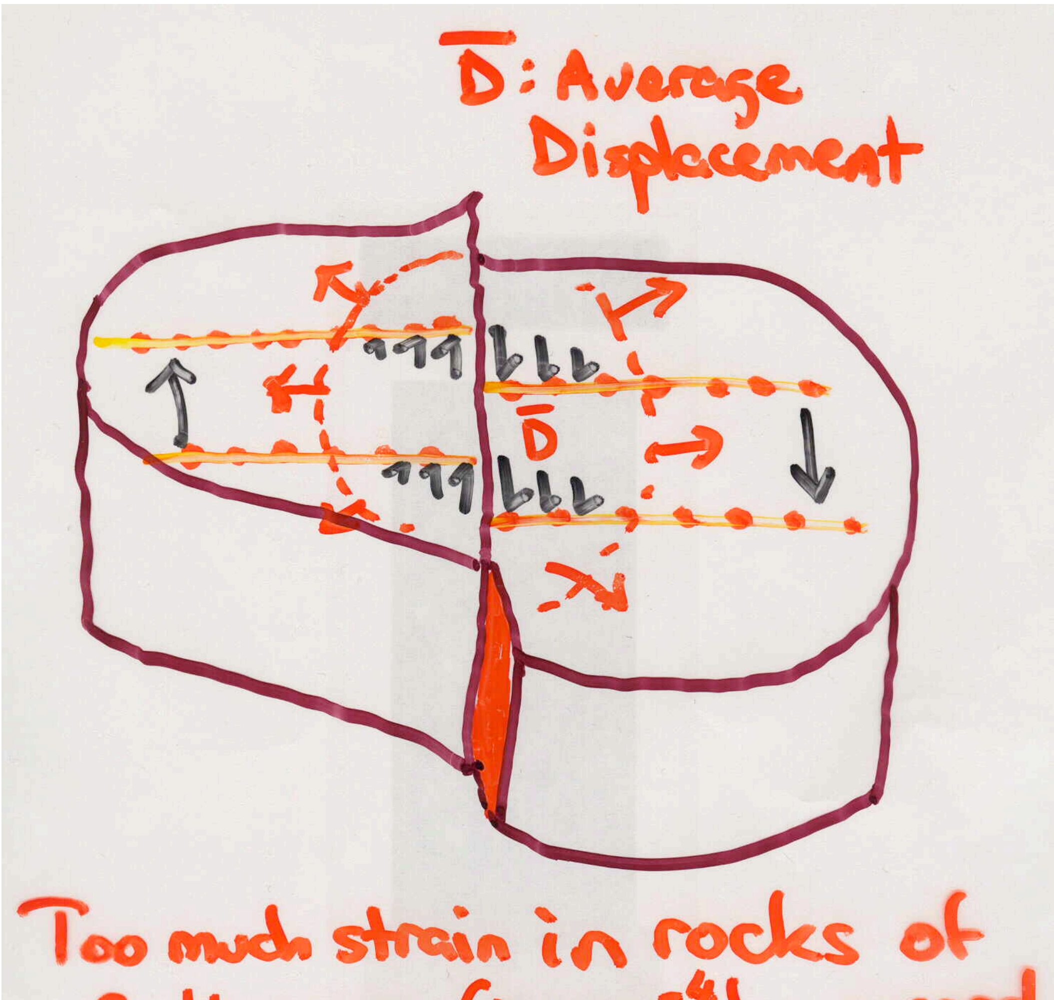

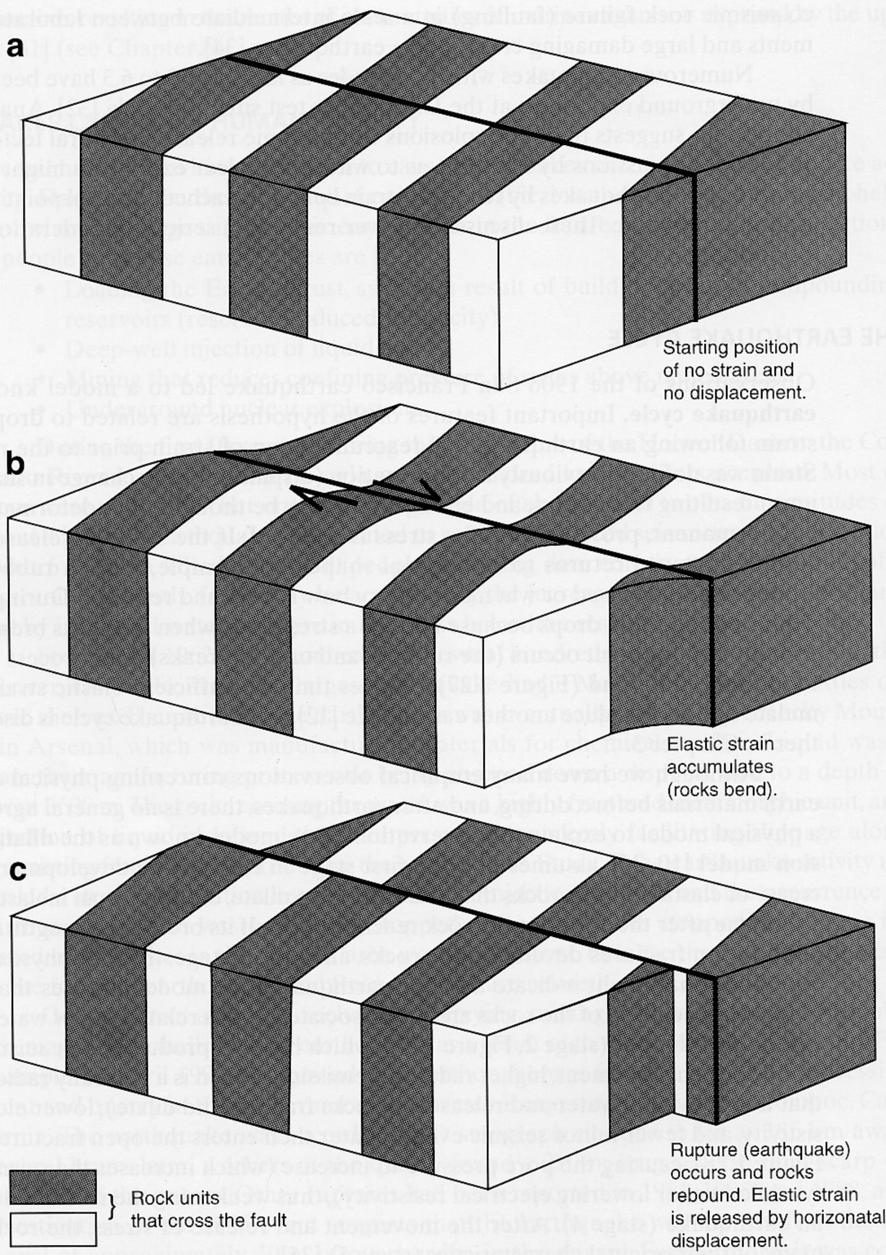

Figure 1.27 Idealized block diagrams illustrating the earthquake cycle and elastic rebound. (a) Beginning position with no strain or displacement. (b) After accumulation of elastic strain. (c) Following earthquake and rupture. (Courtesy of F. Duennebier.)

From Keller & Pinter

Deformation measured prior to an earthquake by GPS stations crossing San Andreas fault

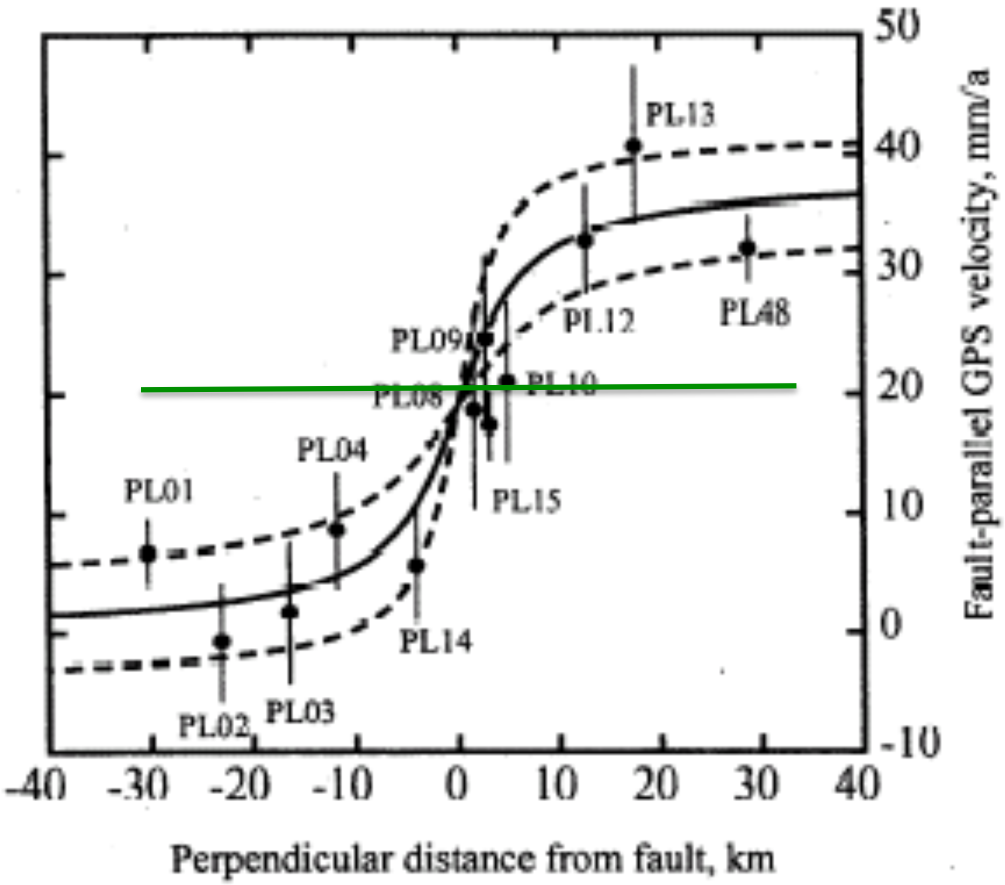

When the earthquake happens, the actual change in position of the ground along the green line on the left will have a pattern like this:

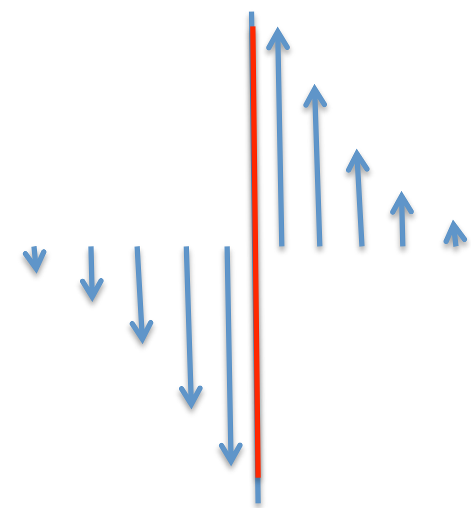

The slip on the fault at the green line intersection will equal D, the displacement there indicated by the length of the red line.

The Fault Does Not Slip all at Once

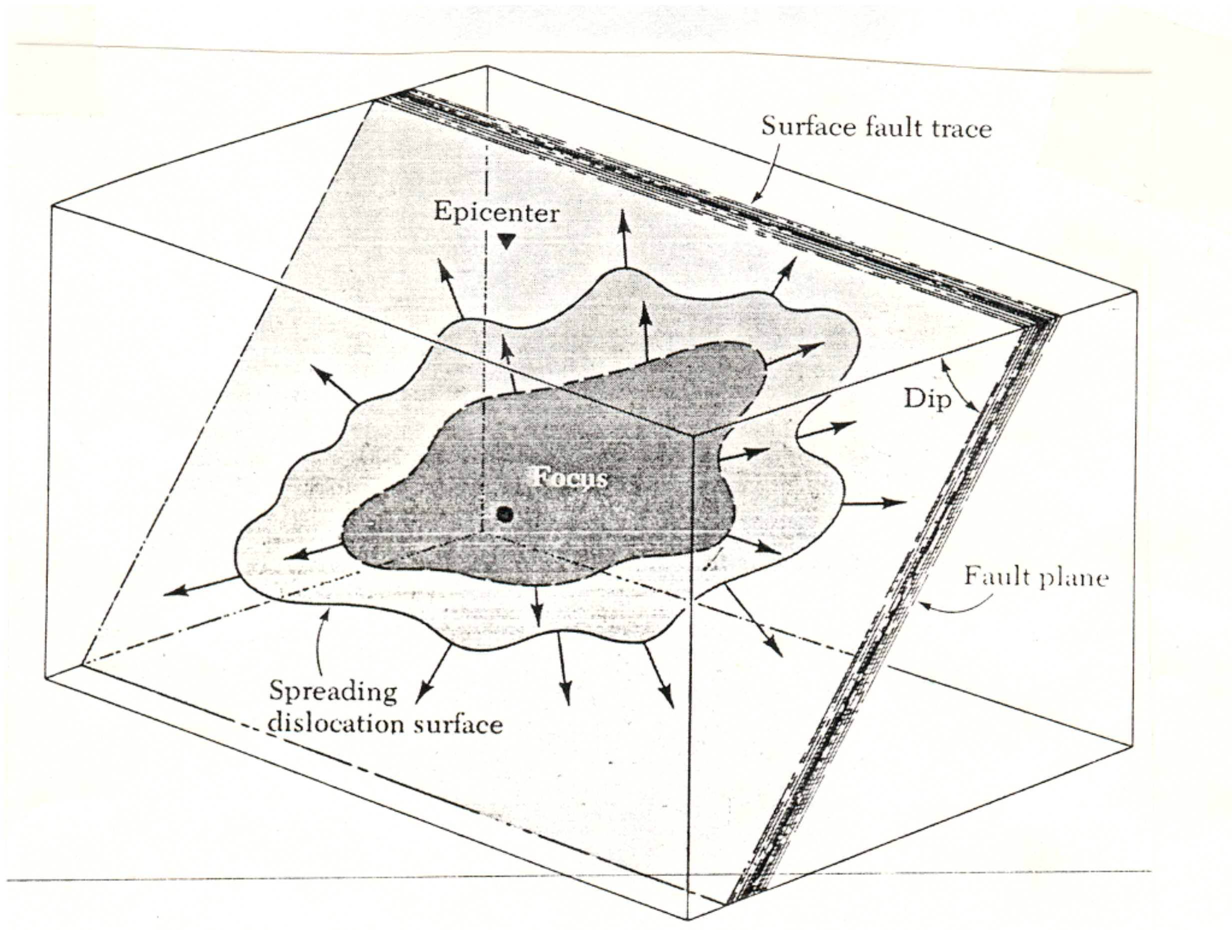

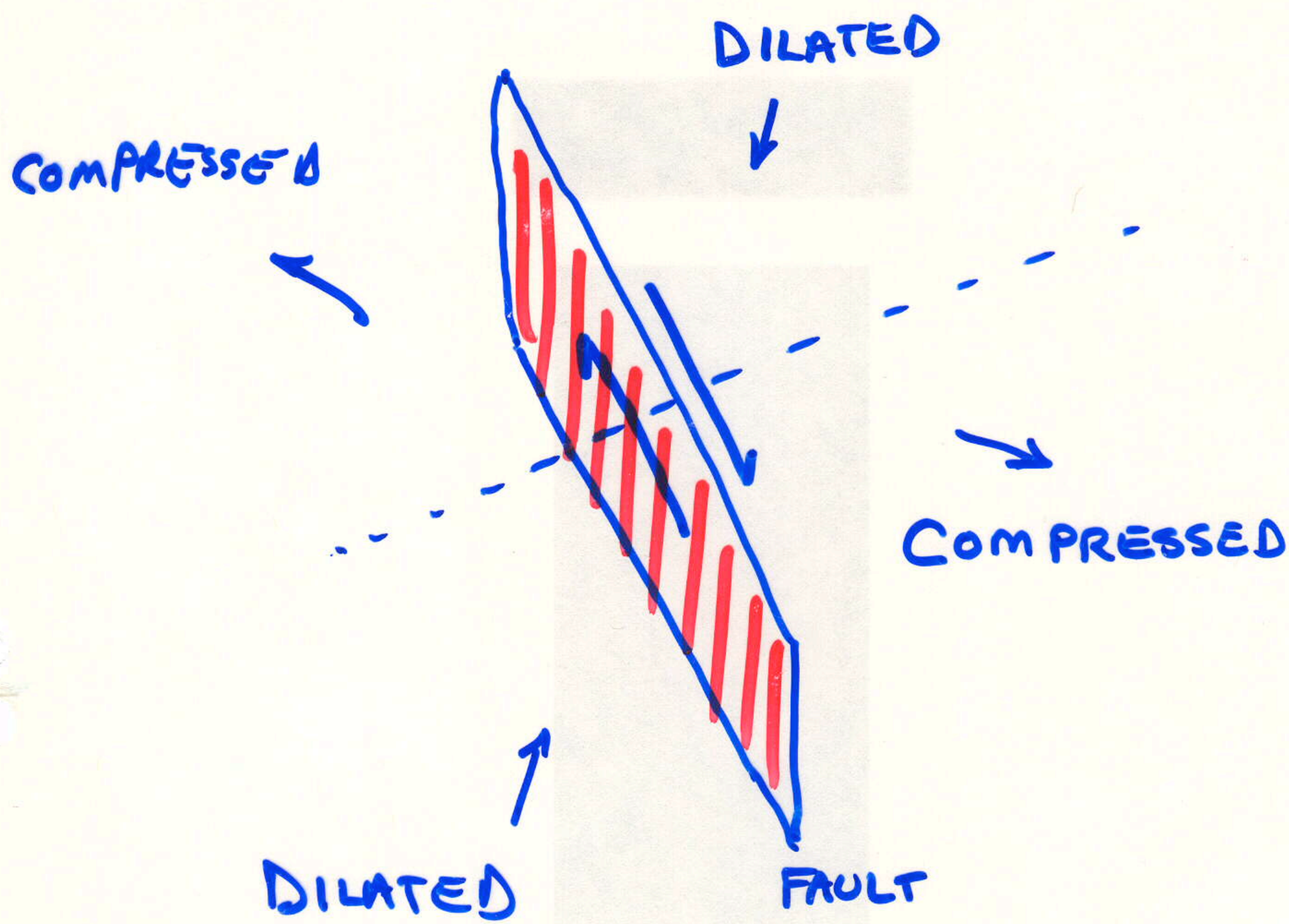
DILATED
COMPRESSED
COMPRESSED
DILATED
FAULT

STUDY EARTHQUAKE USING SEISMIC WAVES IT GENERATES

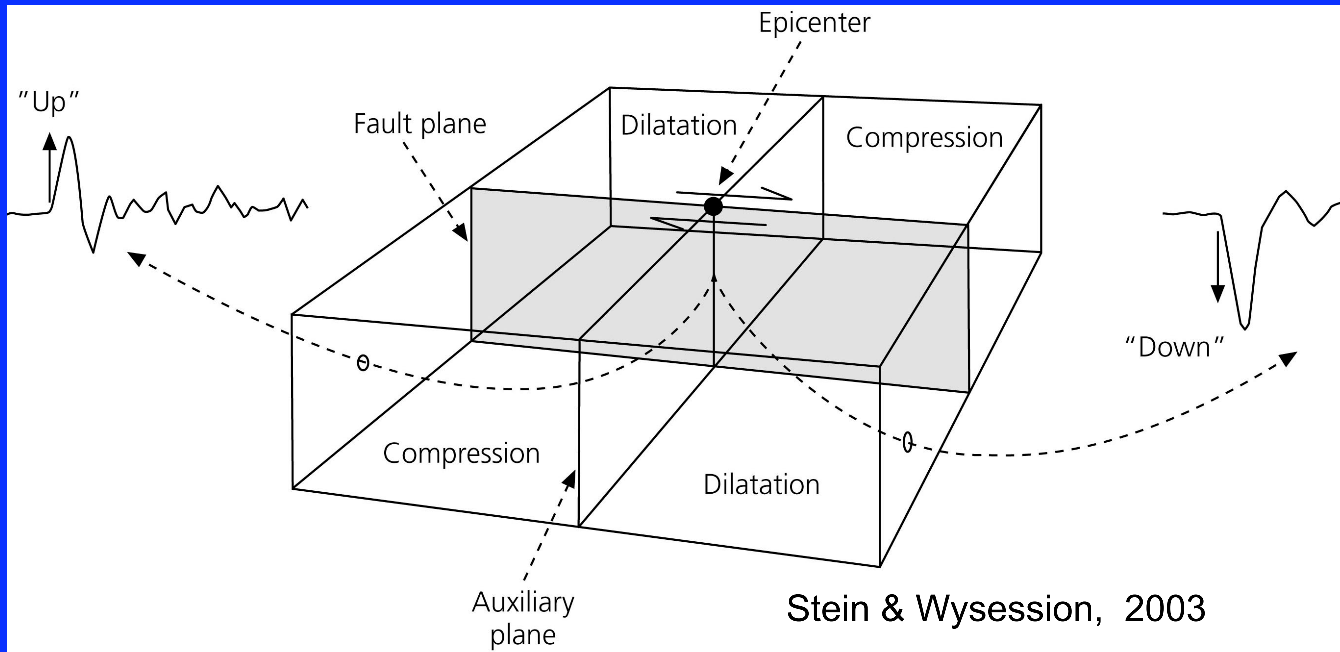

Polarity of first P-wave arrival varies between seismic stations in different directions, depending on fault geometry.

First motion is compression for stations located such that material near the fault moves ``toward'' the station, or dilatation, where motion is ``away from'' the station.

When a P wave arrives at a seismometer from below, a vertical component seismogram records up or down first motion, corresponding to either compression or dilatation.

Method requires understanding effect of earth structure on seismic waves

P WAVE

FIRST MOTIONS

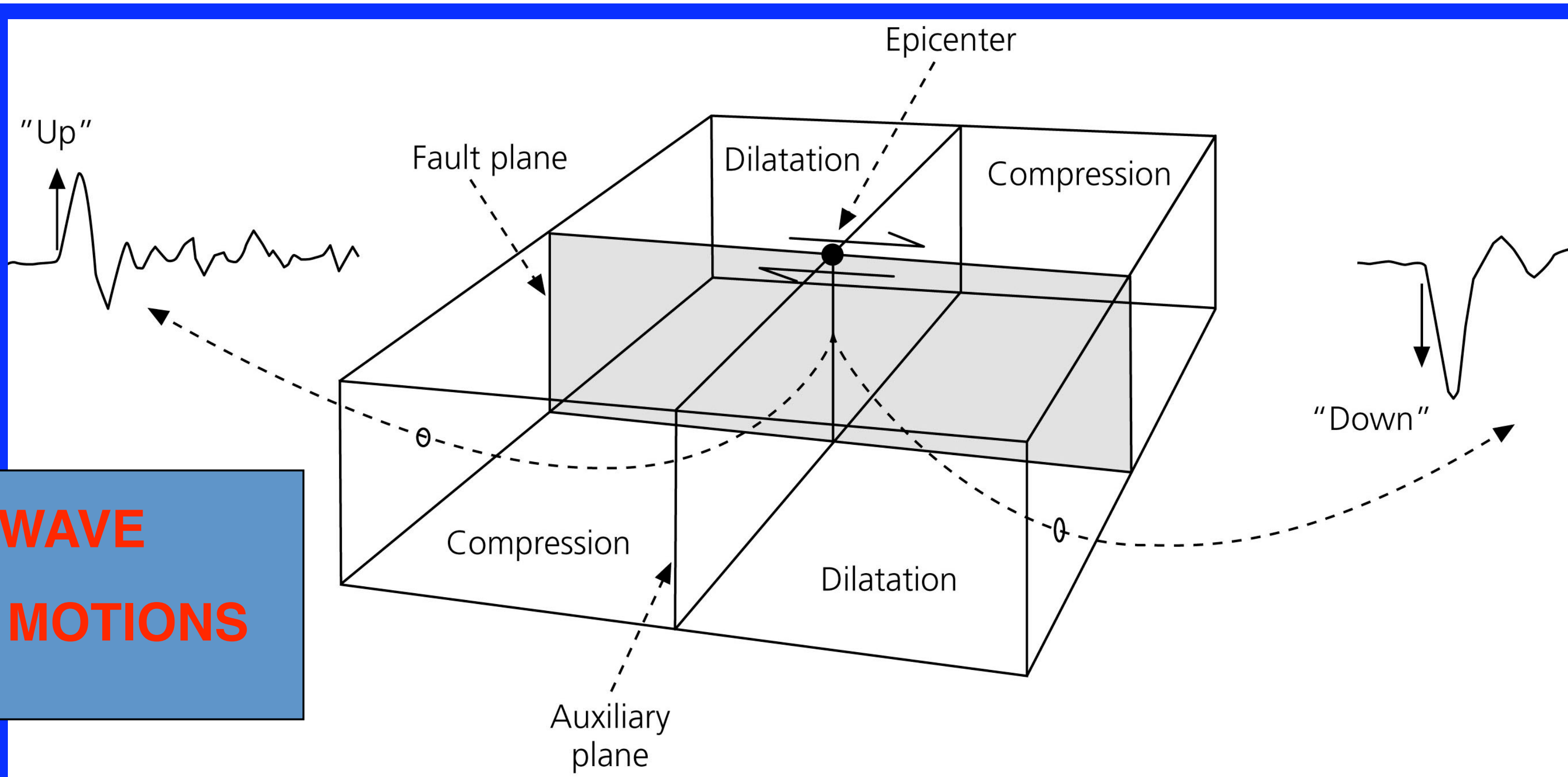

First motions define four quadrants; two compressional and two dilatational.

Quadrants separated by nodal planes: the fault plane and auxiliary plane perpendicular to it.

From the nodal planes fault geometry is known.

Because motions from slip on the actual fault plane and from slip on the auxiliary plane would be the same, first motions alone cannot resolve which is the actual fault plane.

The four-quadrant pattern of motions toward or away from the source is imparted to the P wavefront. That expands through the Earth as a ‘wave’ disturbance, without change (other than by predictable interactions with the Earth layering). Thus, remote observations sample the pattern of motions at the source, which are controlled by the specific fault orientation and sense of slip.

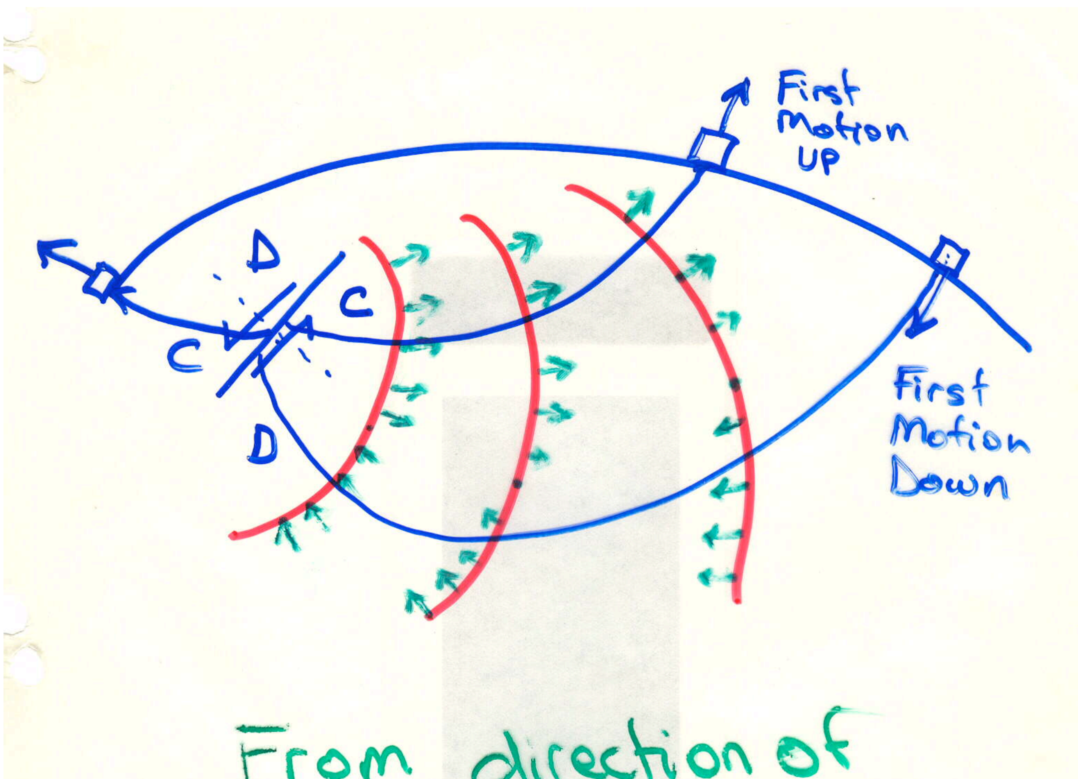

EARTHQUAKE FOCAL MECHANISM STUDY

Seismograms recorded at various distances and azimuths used to study geometry of faulting during an earthquake, known as the focal mechanism.

Use fact that the pattern of radiated seismic waves depends on fault geometry.

Simplest method relies on the first motion, or polarity, of body waves.

More sophisticated techniques use waveforms of body and surface waves.

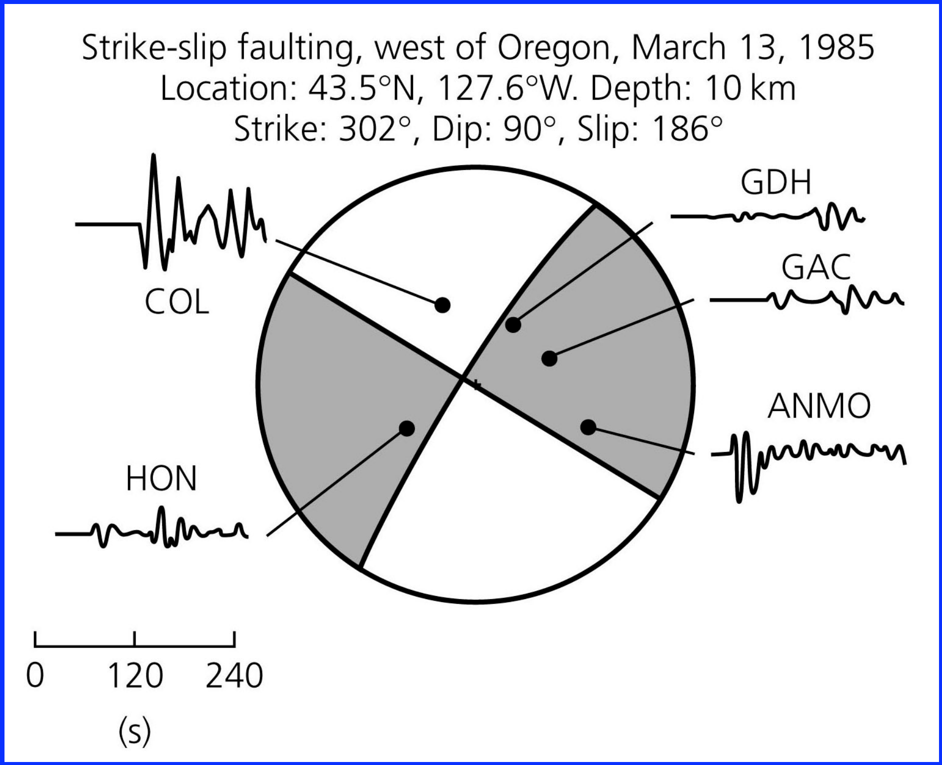

Figure A.7-4: Definition of the azimuth and back-azimuth for a great circle path.

$$\Delta = 86^\circ$$

$$\zeta = 35^\circ$$

$$\zeta' = 245^\circ$$

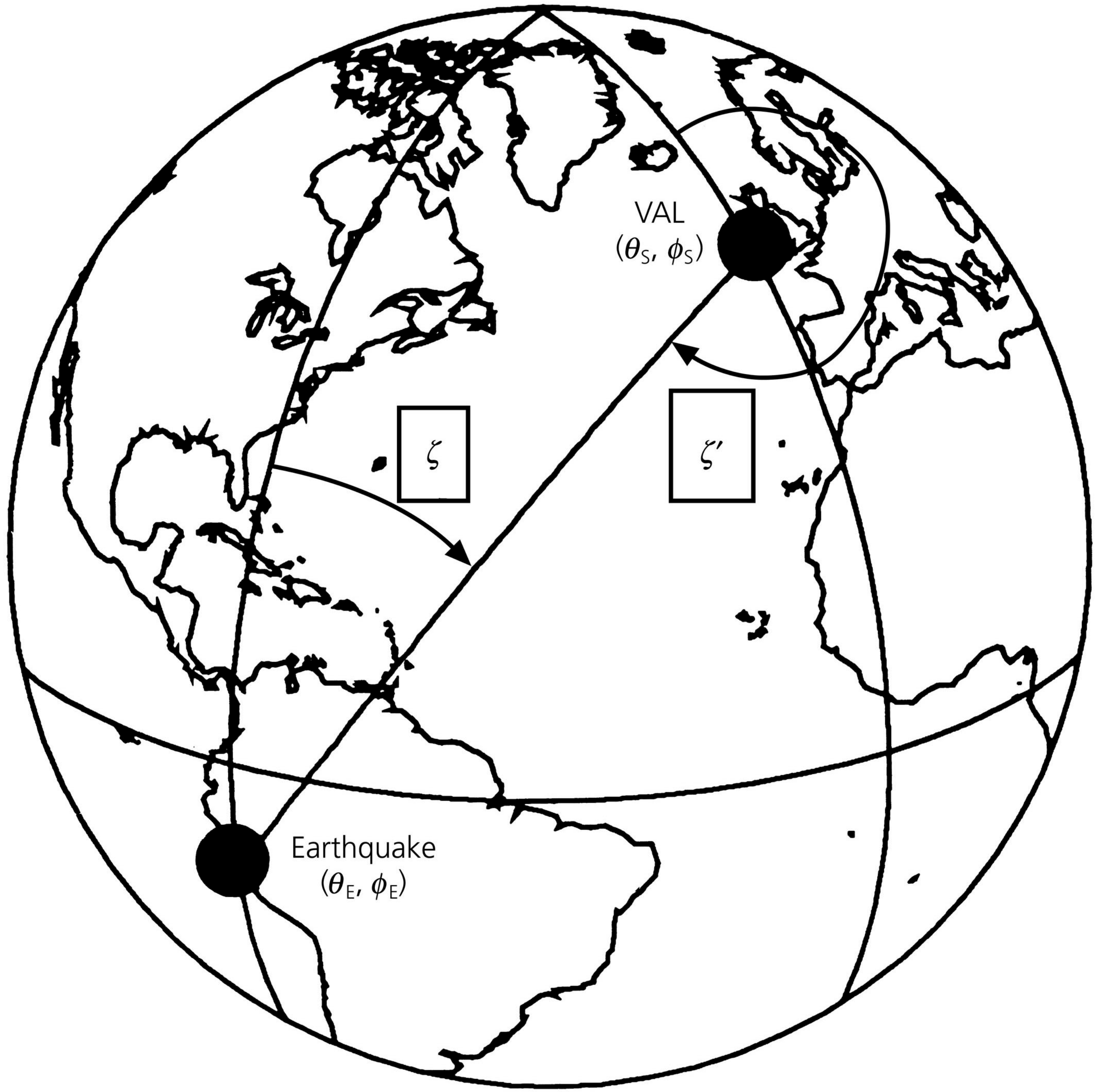

SEISMIC RAYS BEND DUE TO VELOCITY INCREASING WITH DEPTH

Snell's law for ray path in sphere places arrivals recorded at distant stations where they would be on hemisphere just below earthquake

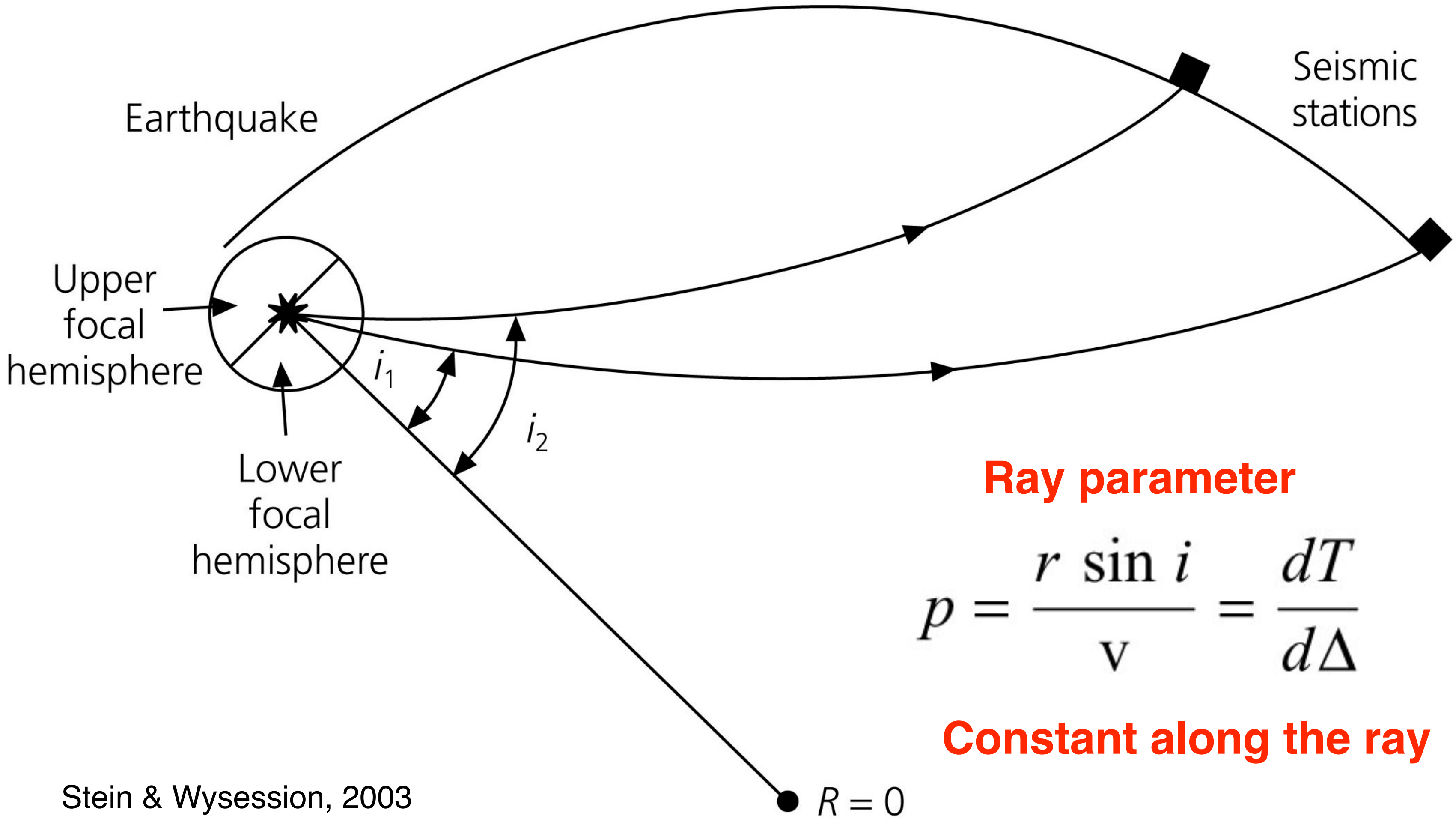

Stein & Wysession, 2003

Ray parameter

$$p = \frac{r \sin i}{v} = \frac{dT}{d\Delta}$$

Constant along the ray

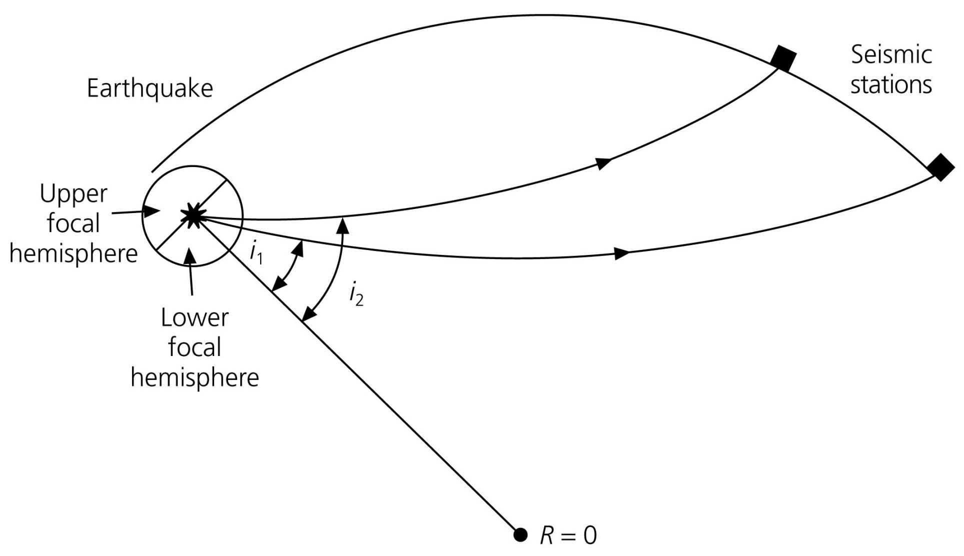

Table 4.2-1 *P*-wave take-off angles for a surface-focus earthquake.

Distance (°)	Take-off angle (°)	Distance (°)	Take-off angle (°)	Distance (°)	Take-off angle (°)
21	36	47	25	73	19
23	32	49	24	75	18
25	30	51	24	77	18
27	29	53	23	79	17
29	29	55	23	81	17
31	29	57	23	83	16
33	28	59	22	85	16
35	28	61	22	87	15
37	27	63	21	89	15
39	27	65	21	91	15
41	26	67	20	93	14
43	26	69	20	95	14
45	25	71	19	97	14

Source: After Pho and Behe (1972).

Top of focal sphere

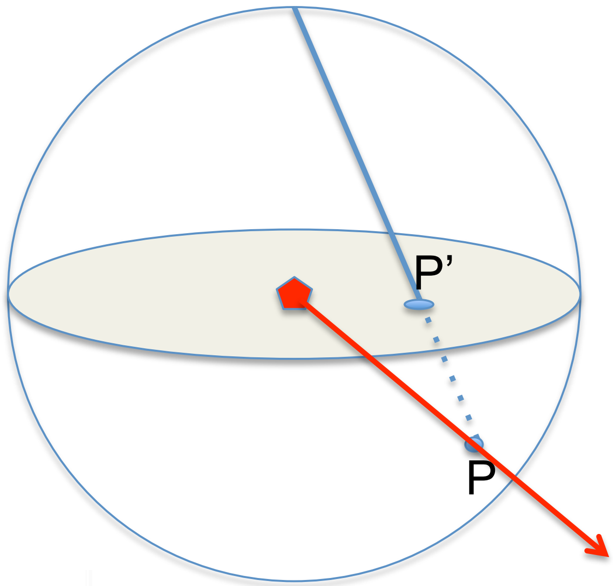

Stereographic Projection. Every point P on lower hemisphere of a focal sphere projects to a unique position P' on the equatorial plane defined by a line from the top of the focal sphere to the point on the focal sphere.

A planar surface intersection with the focal sphere maps to a curve on the equatorial plane.

Can map the 3D fault geometry to a 2D display: this is stereographic projection. Can conserve angles or area in projection.

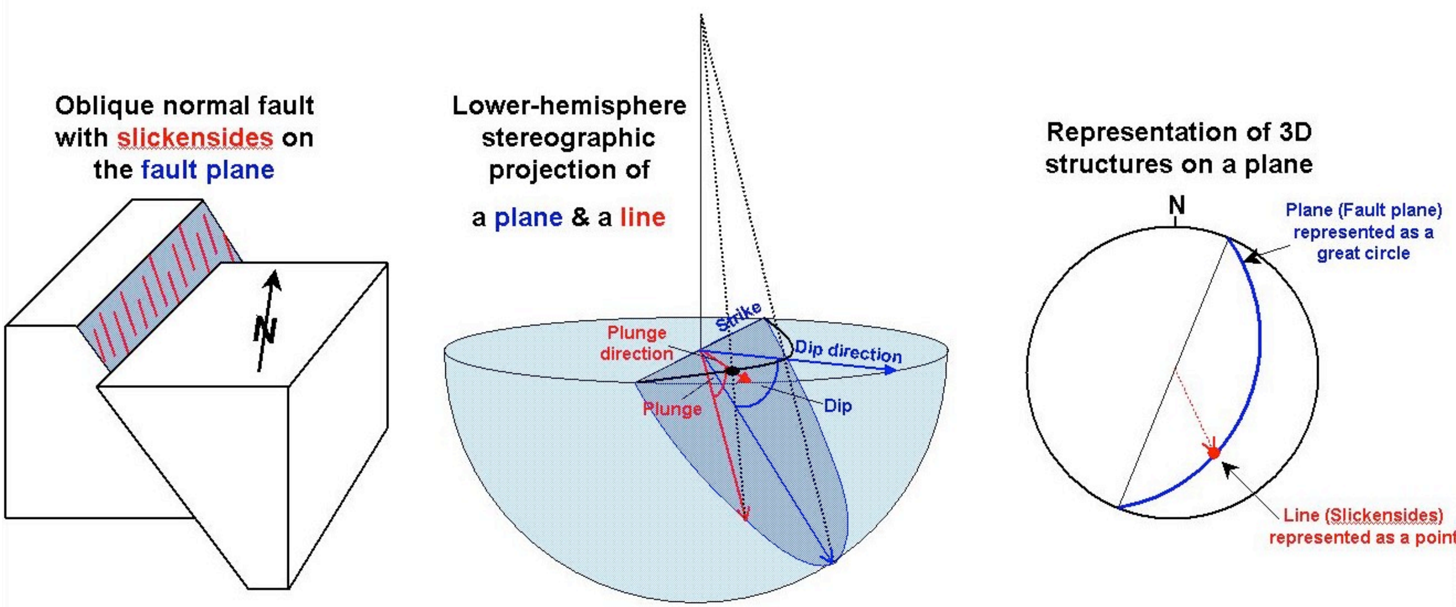

PLOT LOWER FOCAL HEMISPHERE USING STEREONET

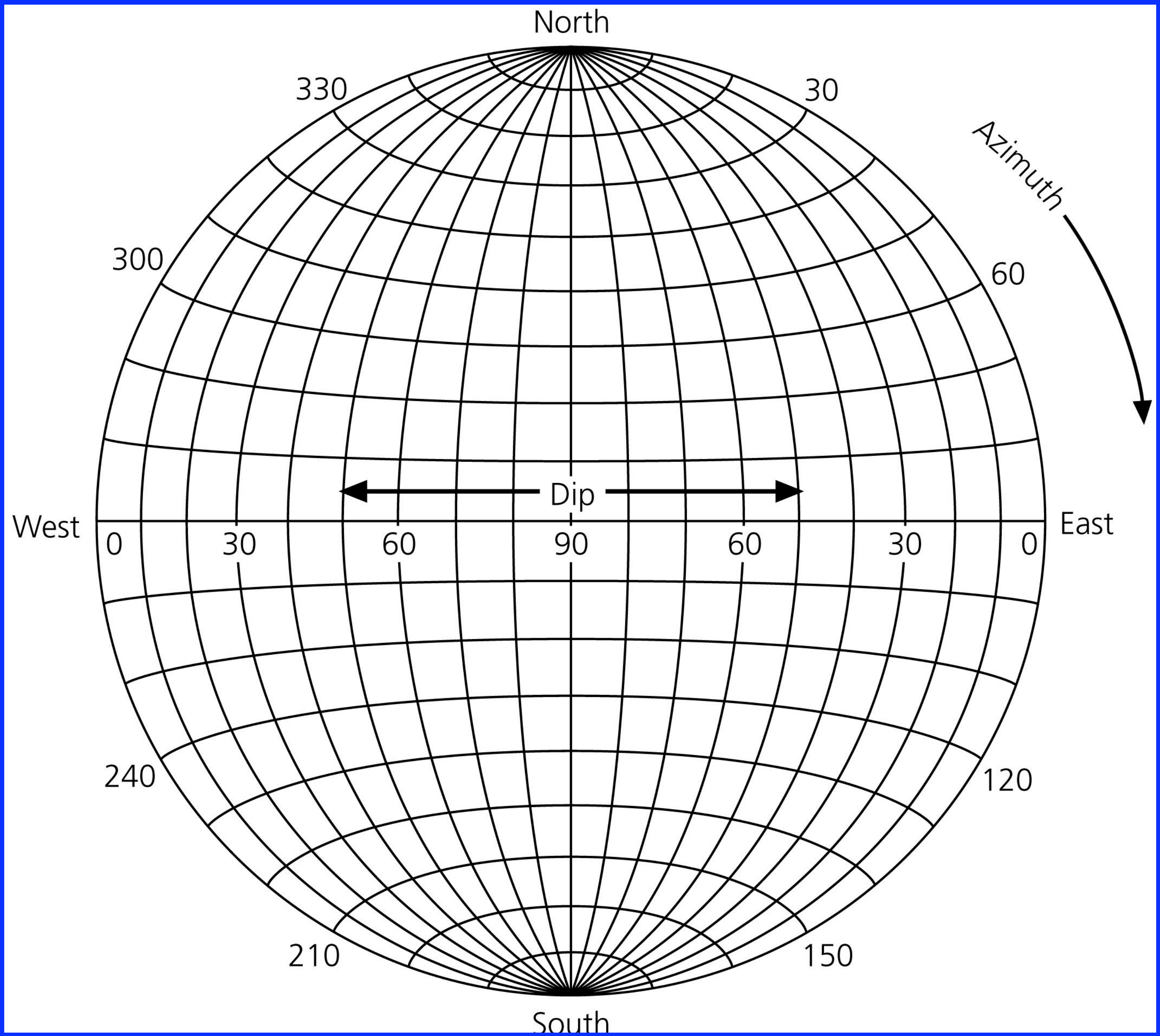

PLOT FIRST MOTIONS

Find polarities of the first arrivals at seismic stations.

Station corresponds to a point on the focal sphere with the same azimuth and an incidence angle corresponding to the ray that emerged there. Az 40°, i_h 60°.

Plot stations on the stereonet, and mark whether the first motion is dilatation or compression

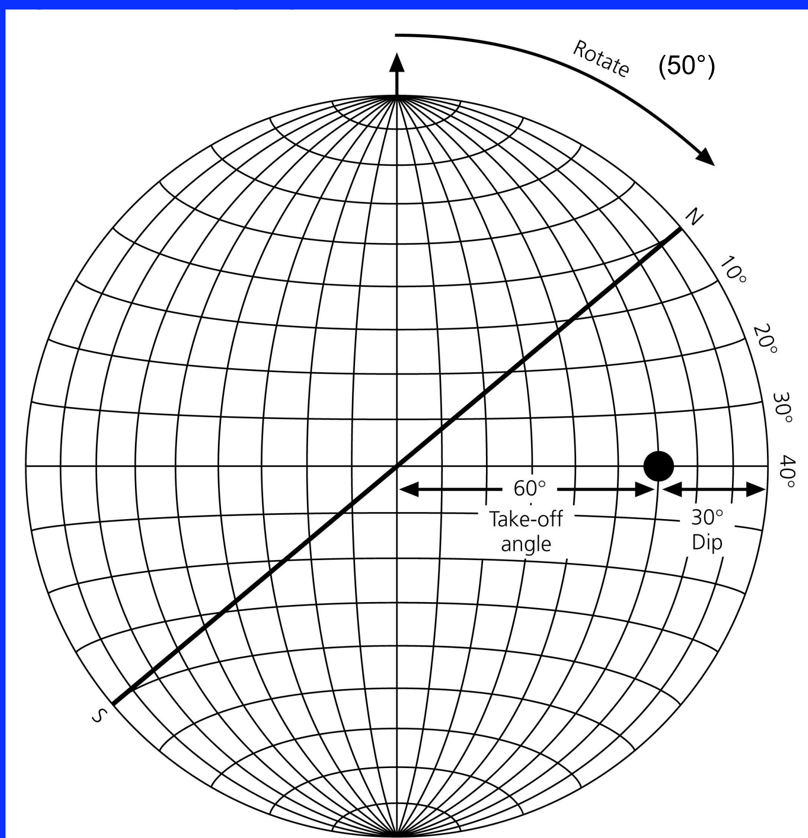

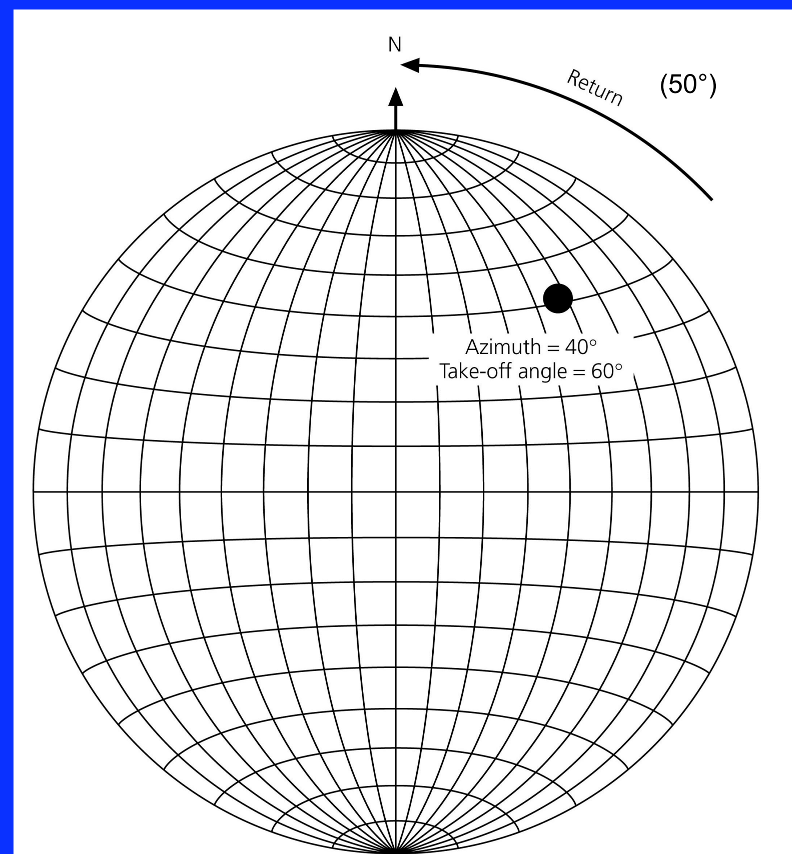

PLOT NODAL PLANES

Find nodal planes that separate compressions from the dilatations.

Ensure the two planes are orthogonal, with each one passing through the pole to the other.

If distribution of stations on the focal sphere is adequate, we can find the nodal planes, which are the fault plane and the auxiliary plane.

Figure 4.2-10: Example of three planes on a stereonet.

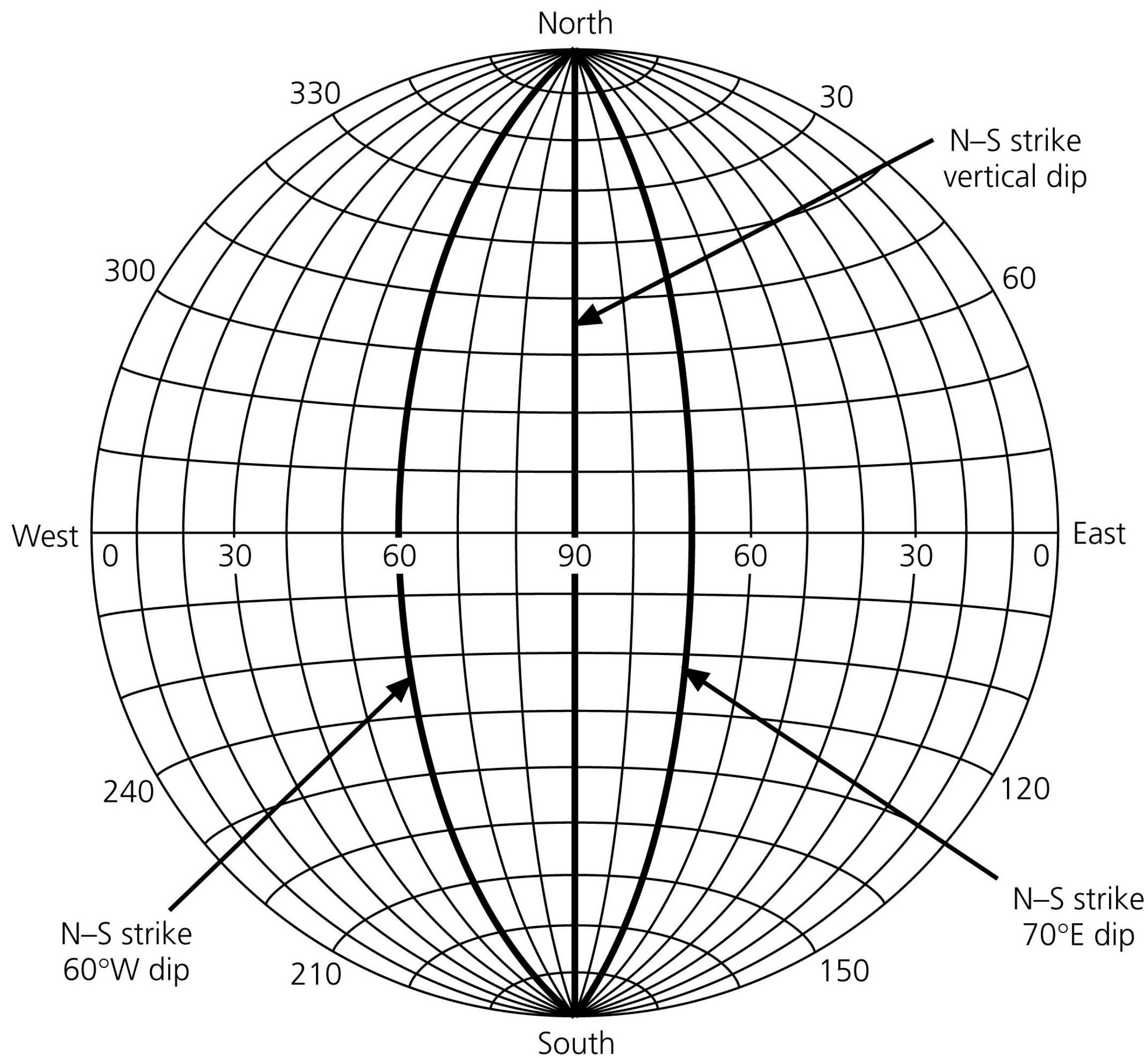

Stein & Wysession, 2003

Strike 45°, dip 60°

Figure 4.2-11: Example of plotting a plane on a stereonet.

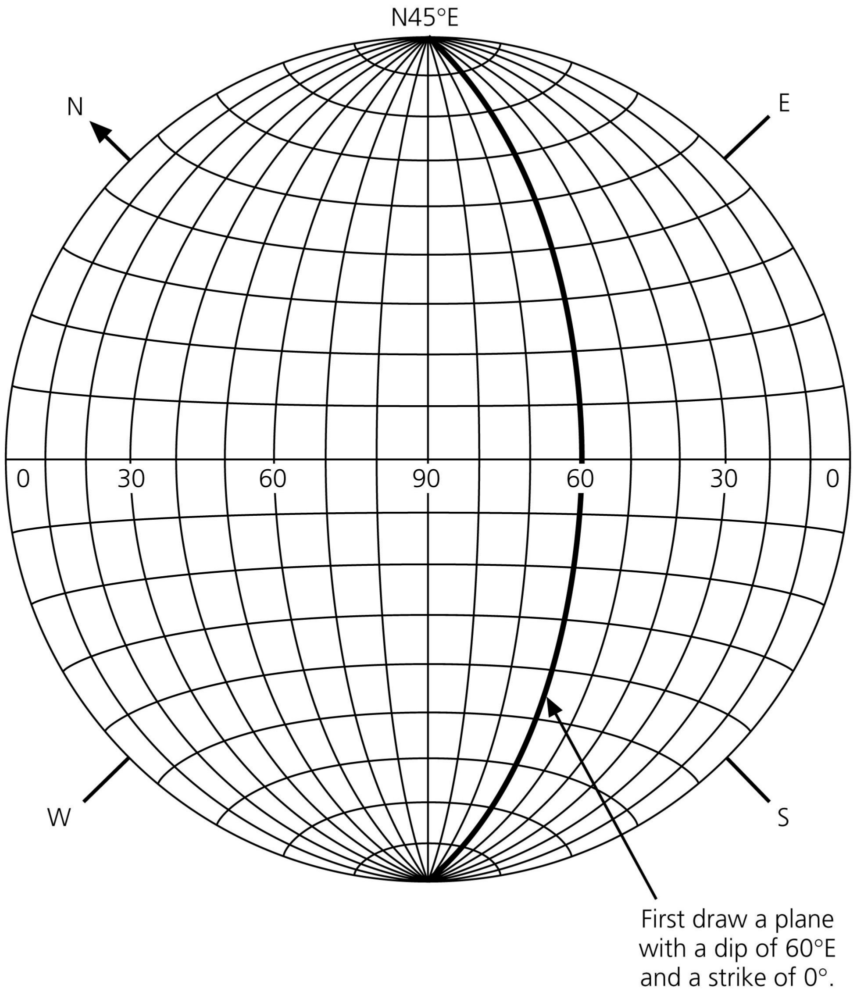

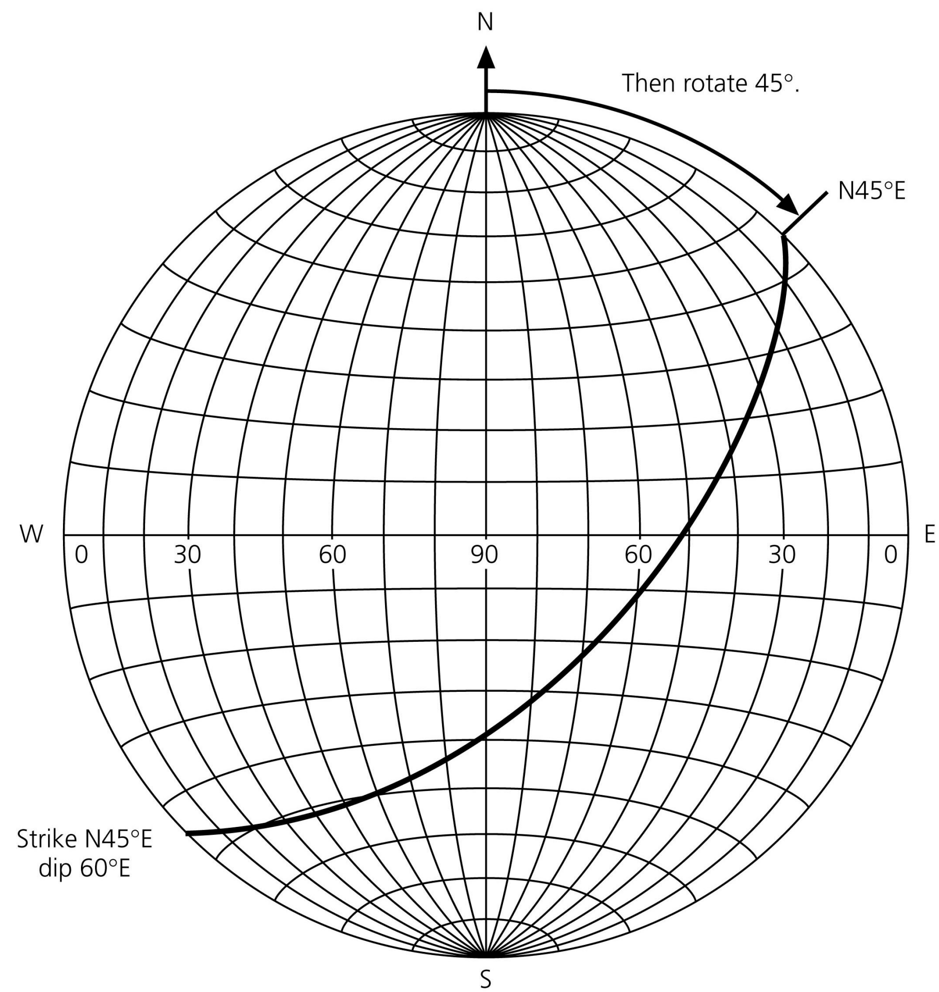

Stein & Wysession, 2003

Figure 4.2-12: Example of plotting perpendicular planes on a stereonet.

Perpendicular planes will go through the pole of the plane they are perpendicular to. The pole is the point corresponding to the normal to a plane.

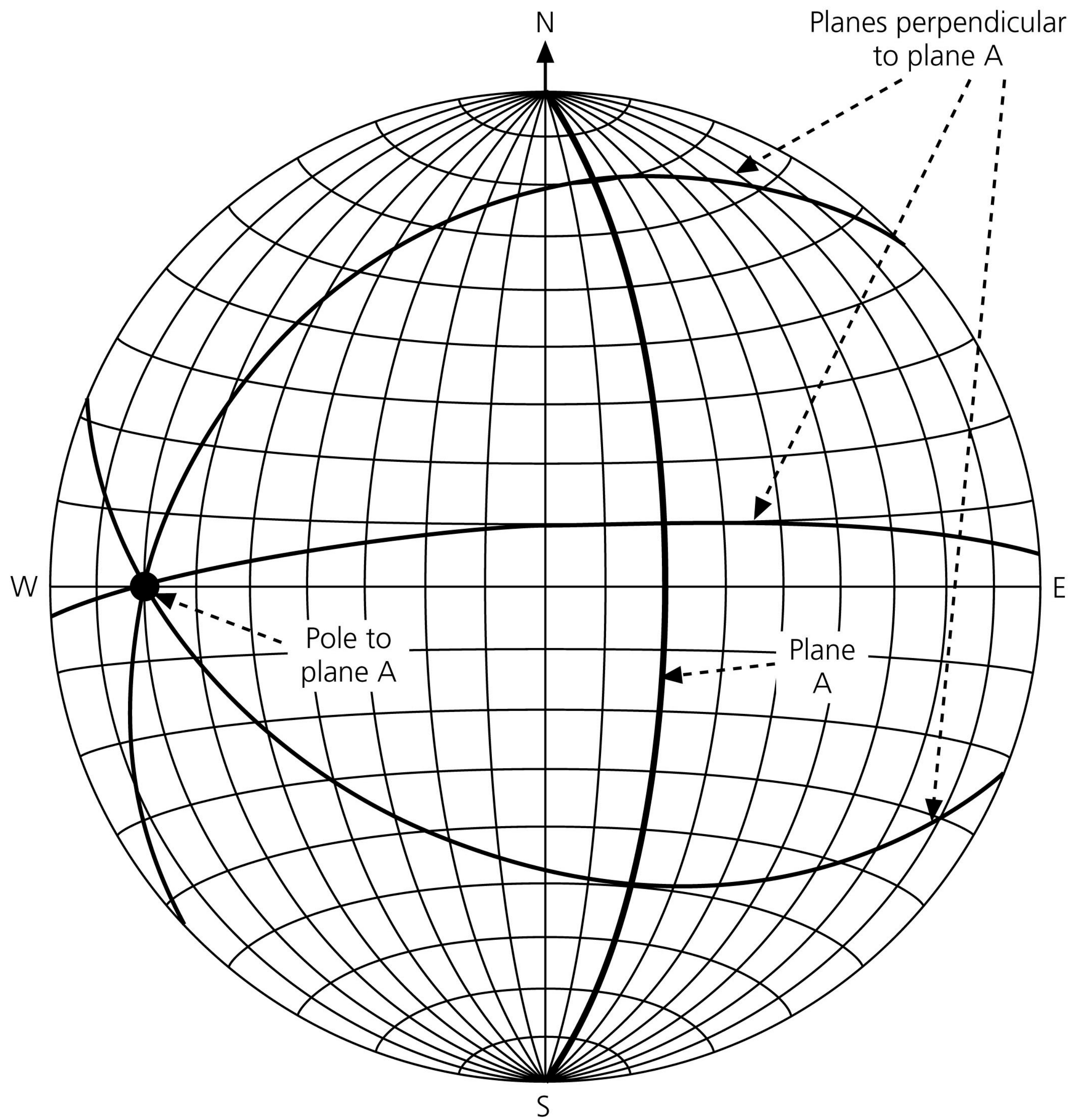

Although the focal mechanisms look different, they **reflect the same four-lobed P-wave radiation pattern**

However, because the fault plane and slip direction are oriented differently relative to the earth's surface, the projections of the radiation pattern lobes on the lower focal hemisphere differ

To see this, mark the P wave quadrants on a ball and rotate it.

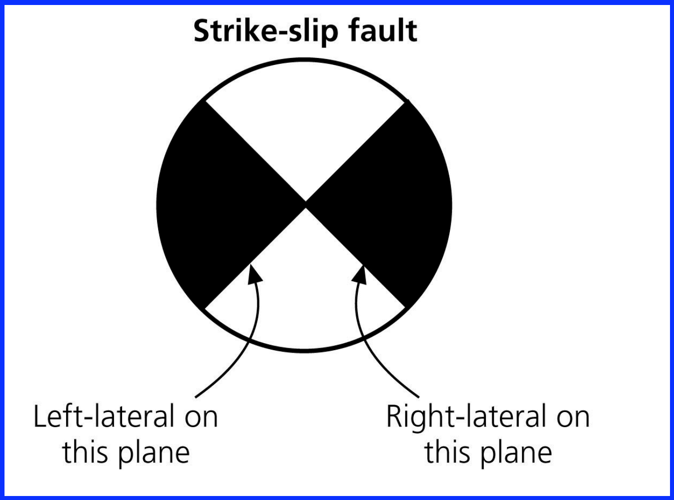

FOCAL MECHANISMS FOR BASIC FAULTS

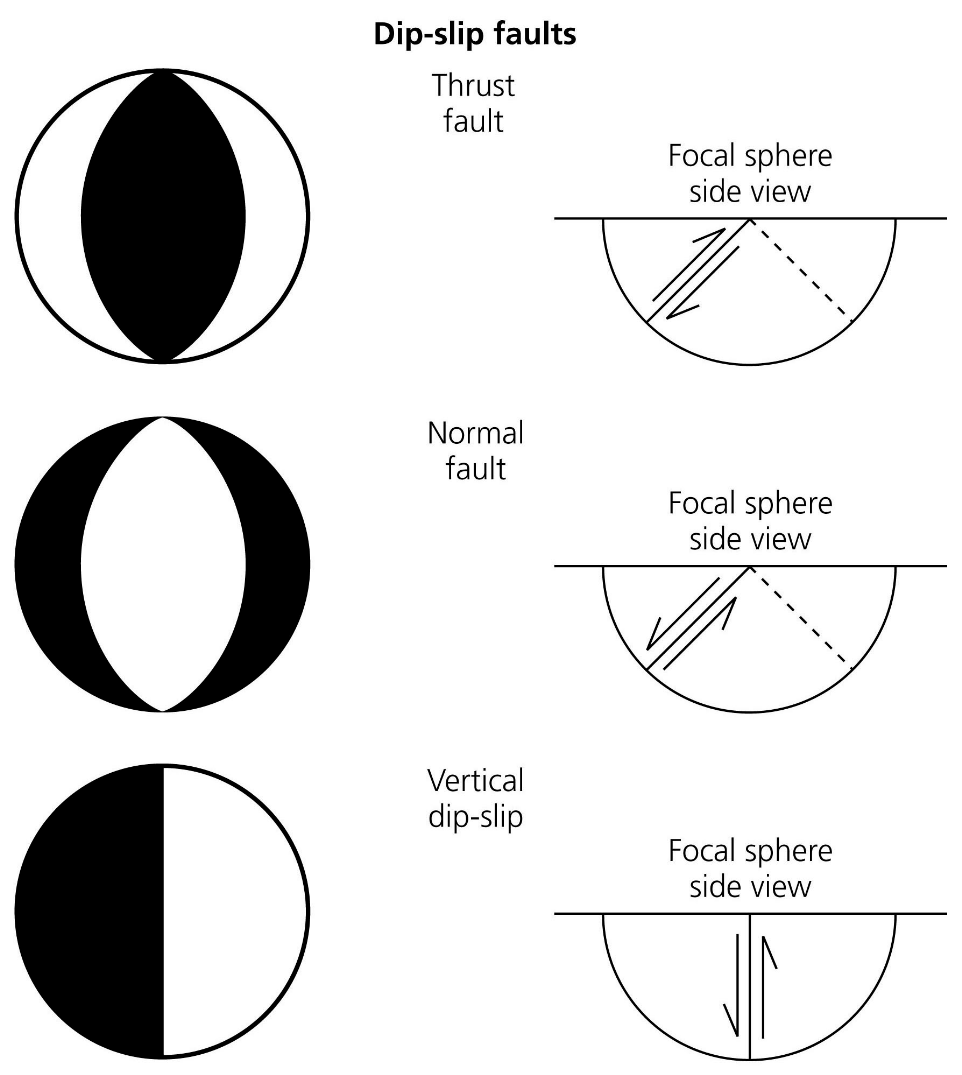

Stein & Wysession, 2003

FOCAL MECHANISMS FOR DIFFERENT FAULTS

All have same N-S striking plane, but with slip angles varying from pure thrust, to pure strike-slip, to pure normal

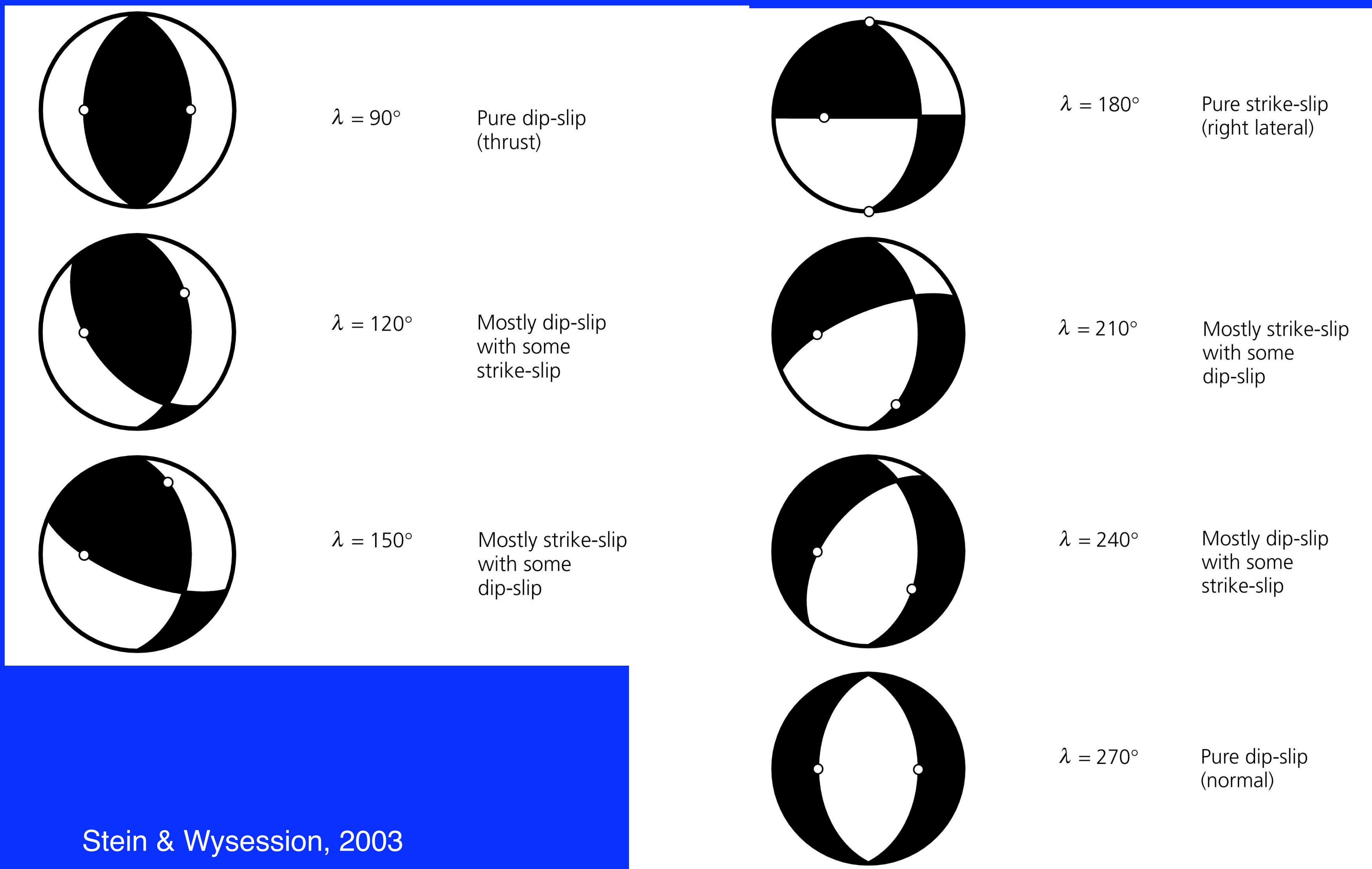

Stein & Wysession, 2003

Figure 4.2-17: Examples of focal mechanisms and first motions.

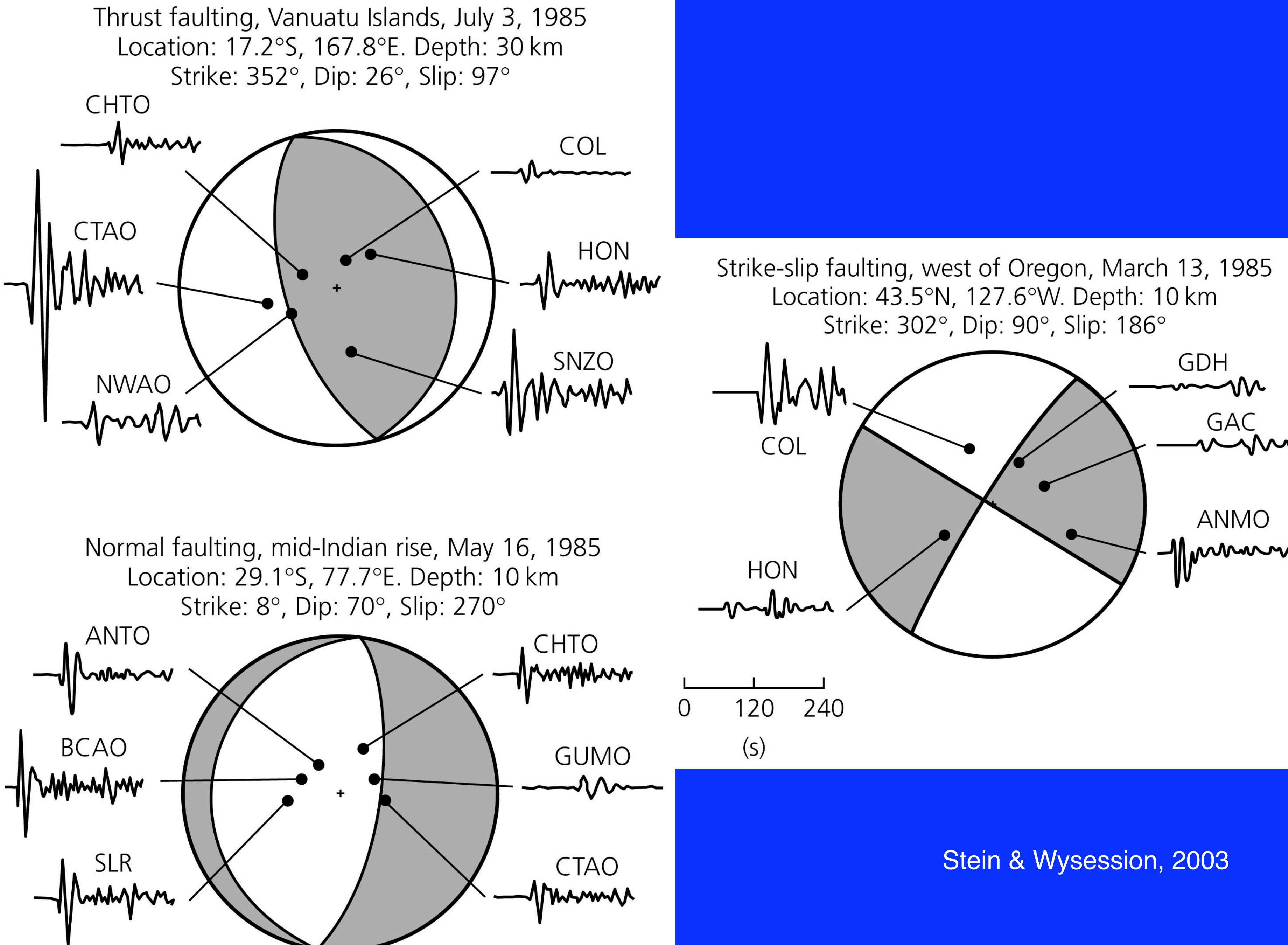

Stein & Wysession, 2003

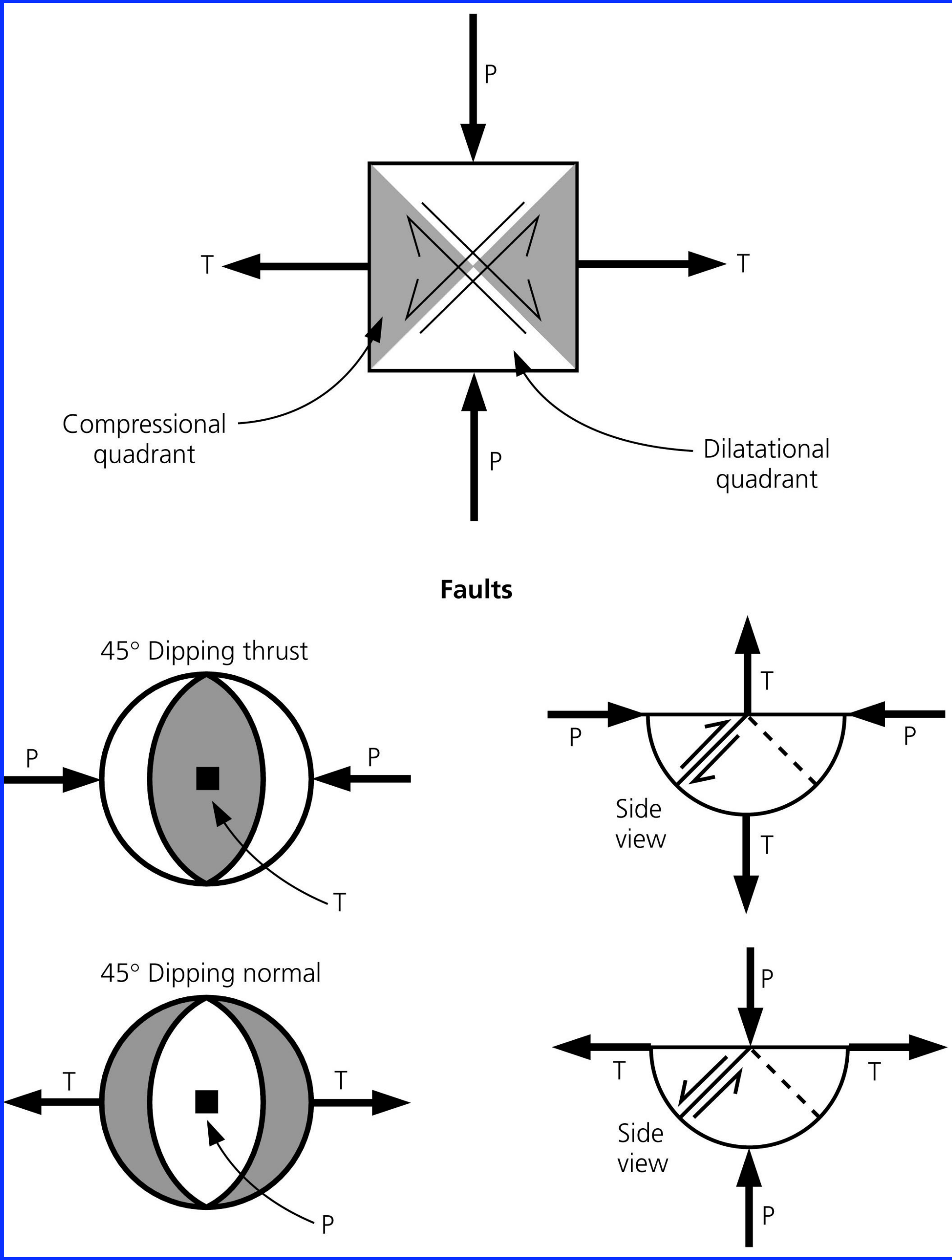

INFER STRESS ORIENTATIONS FROM FOCAL MECHANISMS

Simple model predicts faulting on planes 45° from maximum and minimum compressive stresses

These stress directions are halfway between nodal planes

Most compressive (P) and least compressive stress (T) axes can be found by bisecting the dilatational and compressional quadrants

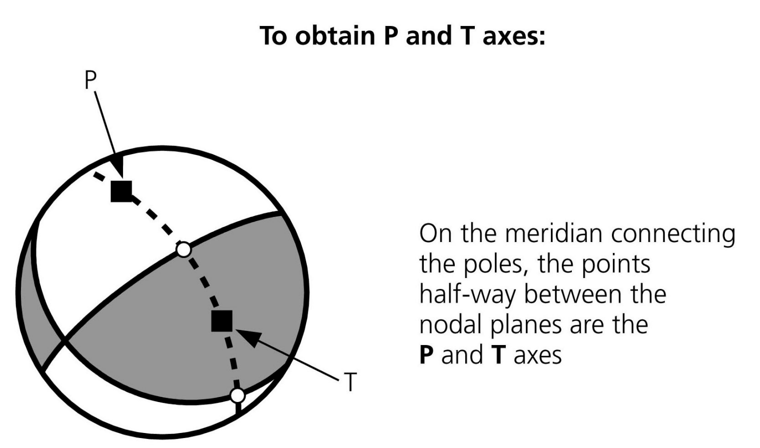

Stein & Wysession, 2003

Confused?

We will do a lab:

Determining a Focal Mechanisms

Additional Reading

A draft primer on focal mechanism solutions for geologists by Vince Cronin

http://serc.carleton.edu/files/NAGTWorkshops/structure04/Focal_mechanism_primer.pdf

Supplementary Info on Spherical Geometry

Figure A.7-2: Geometry of the latitude and longitude system.

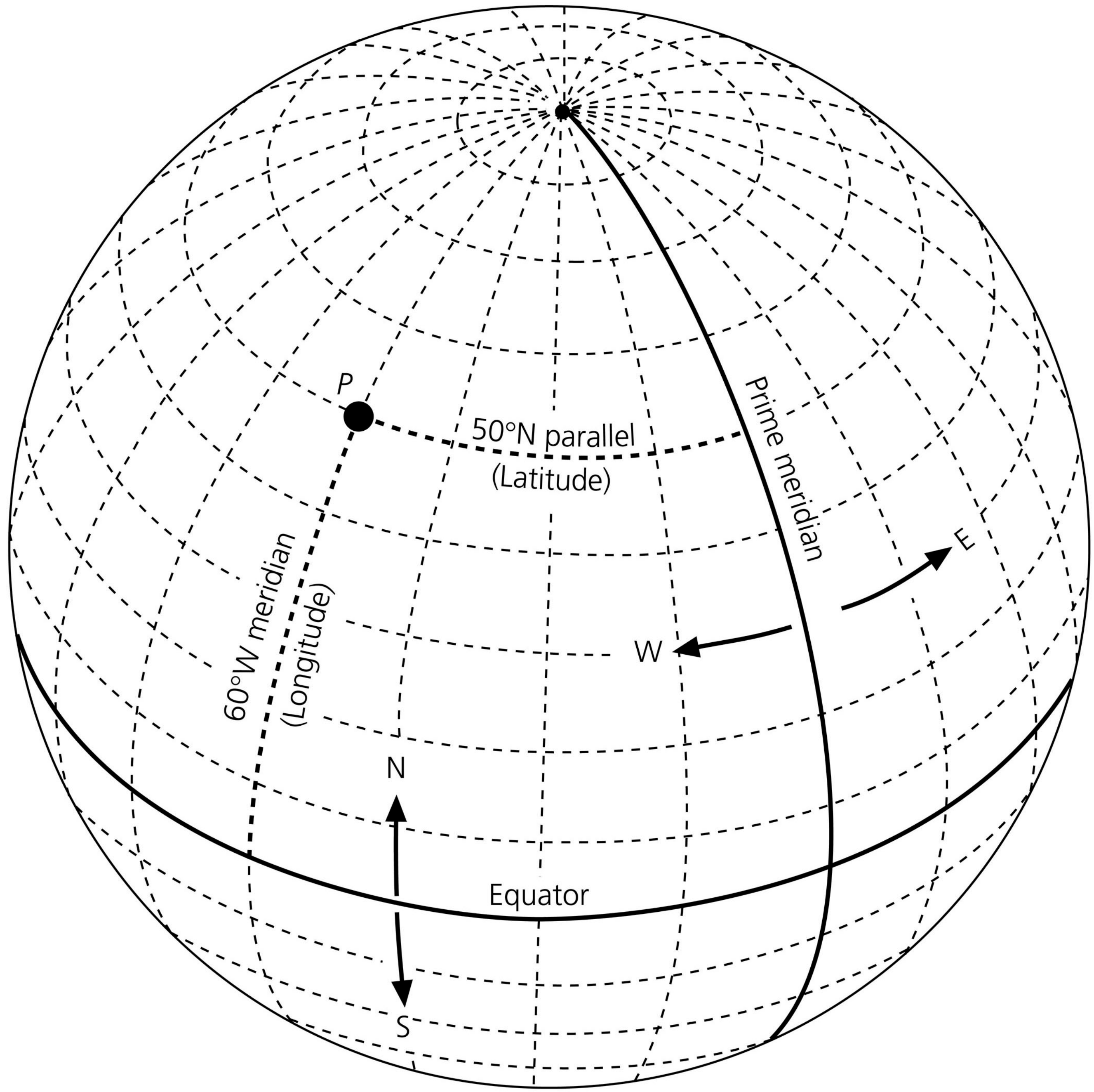

Figure A.7-1: Relations between spherical and Cartesian coordinates.

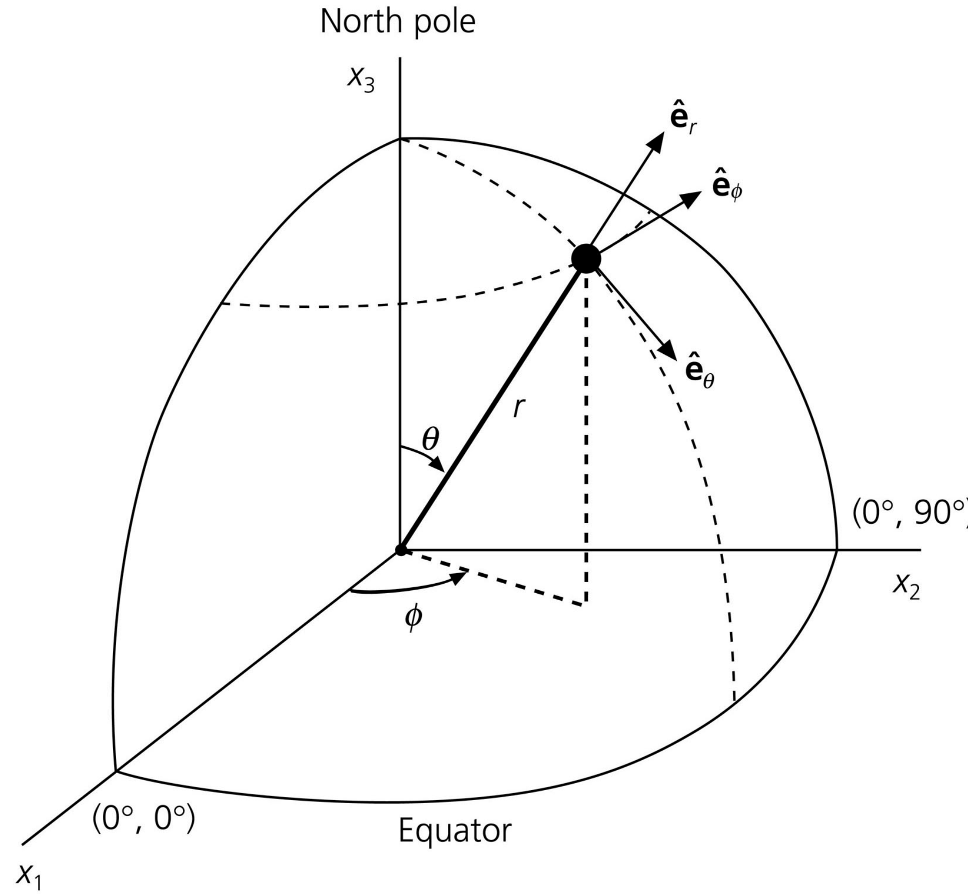

$$\mathbf{x} = x_1\hat{\mathbf{e}}_1 + x_2\hat{\mathbf{e}}_2 + x_3\hat{\mathbf{e}}_3$$

$$\mathbf{x} = \begin{pmatrix} x_1 \\ x_2 \\ x_3 \end{pmatrix} = \begin{pmatrix} r\sin\theta\cos\phi \\ r\sin\theta\sin\phi \\ r\cos\theta \end{pmatrix}$$

$$r = (x_1^2 + x_2^2 + x_3^2)^{1/2} \qquad \theta = \cos^{-1}(x_3/r) \qquad \phi = \tan^{-1}(x_2/x_1)$$

$$\hat{\mathbf{e}}_\phi = \begin{pmatrix} -\sin\phi \\ \cos\phi \\ 0 \end{pmatrix} \qquad \hat{\mathbf{e}}_\theta = \begin{pmatrix} \cos\theta\cos\phi \\ \cos\theta\sin\phi \\ -\sin\theta \end{pmatrix} \qquad \hat{\mathbf{e}}_r = \begin{pmatrix} \sin\theta\cos\phi \\ \sin\theta\sin\phi \\ \cos\theta \end{pmatrix}$$

Figure A.7-3: Geometry of the great circle path between earthquake and station.

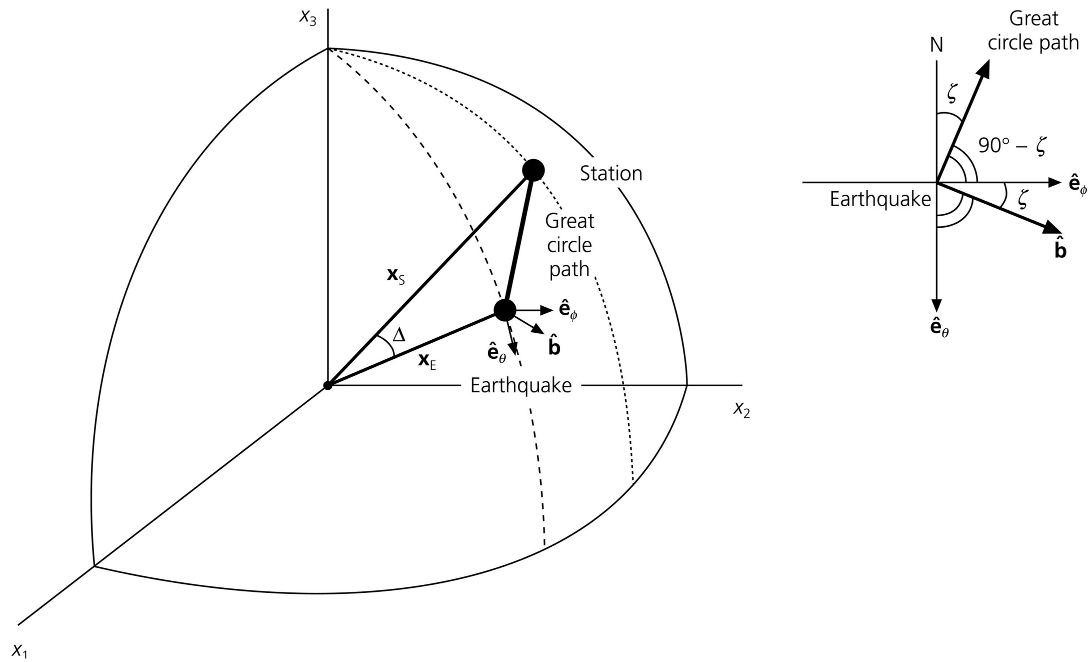

To find the distance between two locations:

$$\mathbf{x}_E = \begin{pmatrix} R \sin\theta_E \cos\phi_E \\ R \sin\theta_E \sin\phi_E \\ R \cos\theta_E \end{pmatrix} \qquad \mathbf{x}_S = \begin{pmatrix} R \sin\theta_S \cos\phi_S \\ R \sin\theta_S \sin\phi_S \\ R \cos\theta_S \end{pmatrix}$$

The distance Δ, the angle between $\mathbf{x}_S$ and $\mathbf{x}_E$, is given by the scalar product:

$$\mathbf{x}_S \cdot \mathbf{x}_E = R^2 \cos\Delta$$

$$\Delta = \cos^{-1}[\cos\theta_E \cos\theta_S + \sin\theta_E \sin\theta_S \cos(\phi_S - \phi_E)]$$

Figure A.7-3: Geometry of the great circle path between earthquake and station.

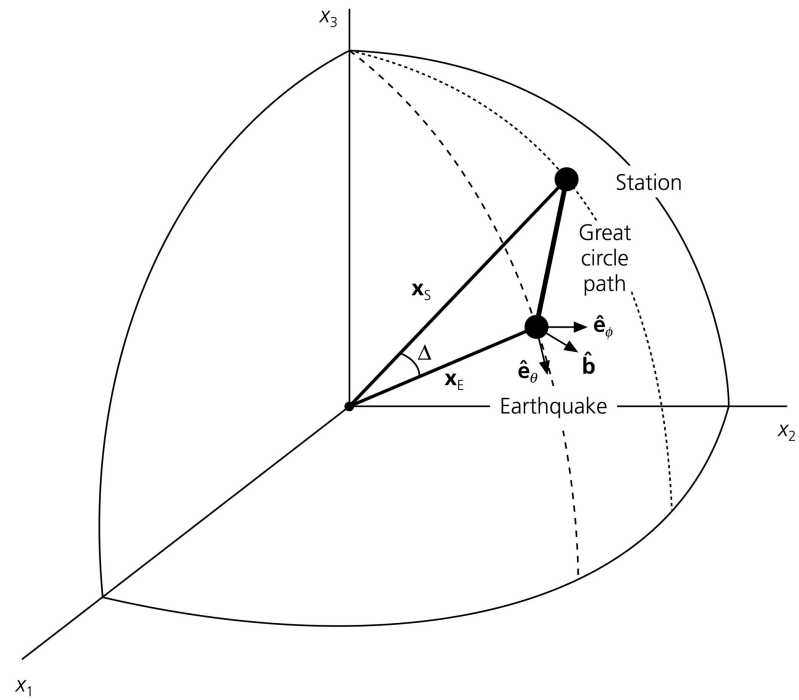

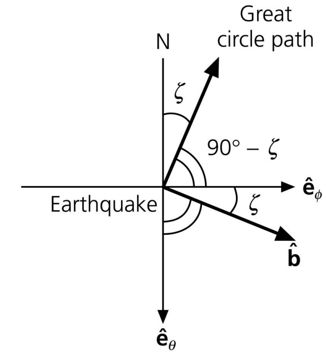

To find the azimuth:

$$\mathbf{x}_S \times \mathbf{x}_E = \hat{\mathbf{b}}\ R^2\ \sin\Delta$$

$$\hat{\mathbf{b}} = \frac{1}{\sin\Delta}\begin{pmatrix} \sin\theta_S\ \cos\theta_E\ \sin\phi_S - \sin\theta_E\ \cos\theta_S\ \sin\phi_E \\ \cos\theta_S\ \sin\theta_E\ \cos\phi_E - \cos\theta_E\ \sin\theta_S\ \cos\phi_S \\ \sin\theta_S\ \sin\theta_E\ \sin(\phi_E - \phi_S) \end{pmatrix}$$

$$\cos\zeta = \hat{\mathbf{b}}\cdot\hat{\mathbf{e}}_\phi = \frac{1}{\sin\Delta}\ (\cos\theta_S\ \sin\theta_E - \sin\theta_S\ \cos\theta_E\ \cos(\phi_S - \phi_E))$$

$$\sin\zeta = \hat{\mathbf{b}}\cdot\hat{\mathbf{e}}_\theta = \frac{1}{\sin\Delta}\ \sin\theta_S\ \sin(\phi_S - \phi_E)$$

Also
Called

Schmidt

Equal
Area
Stereonet

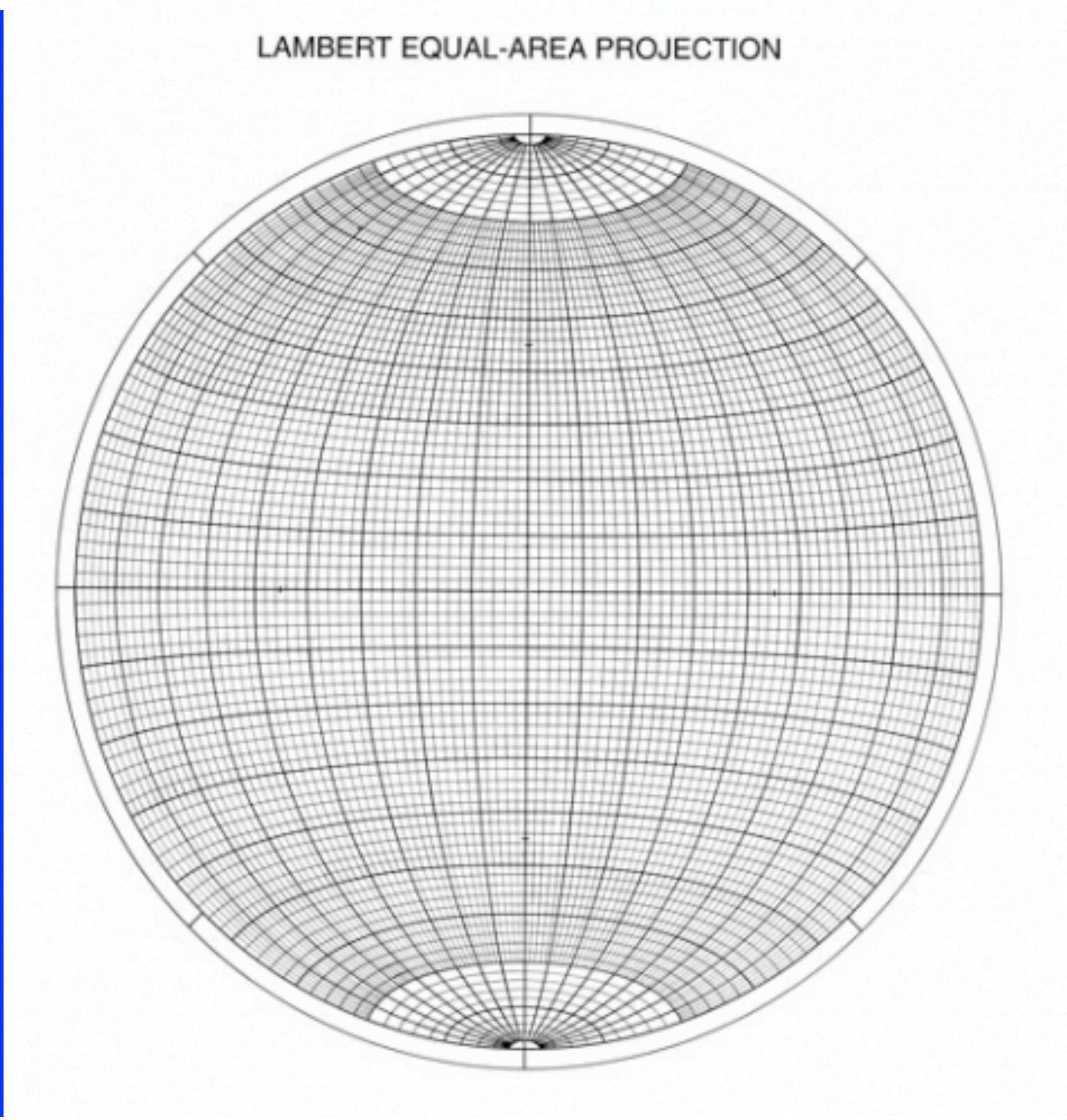

Wulff

Equal
Angle
Stereonet

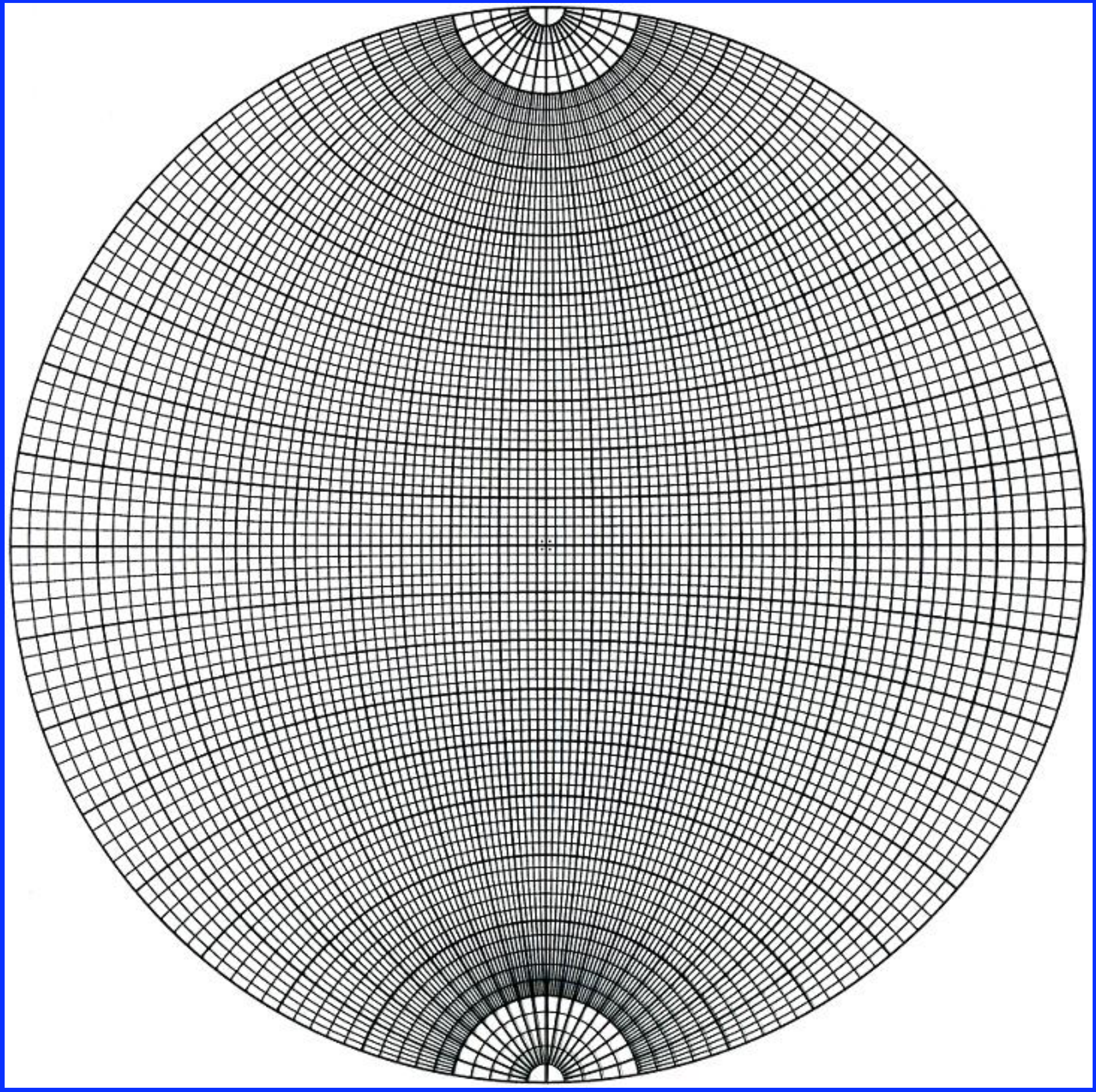

Wulff Steronet with 2° grid

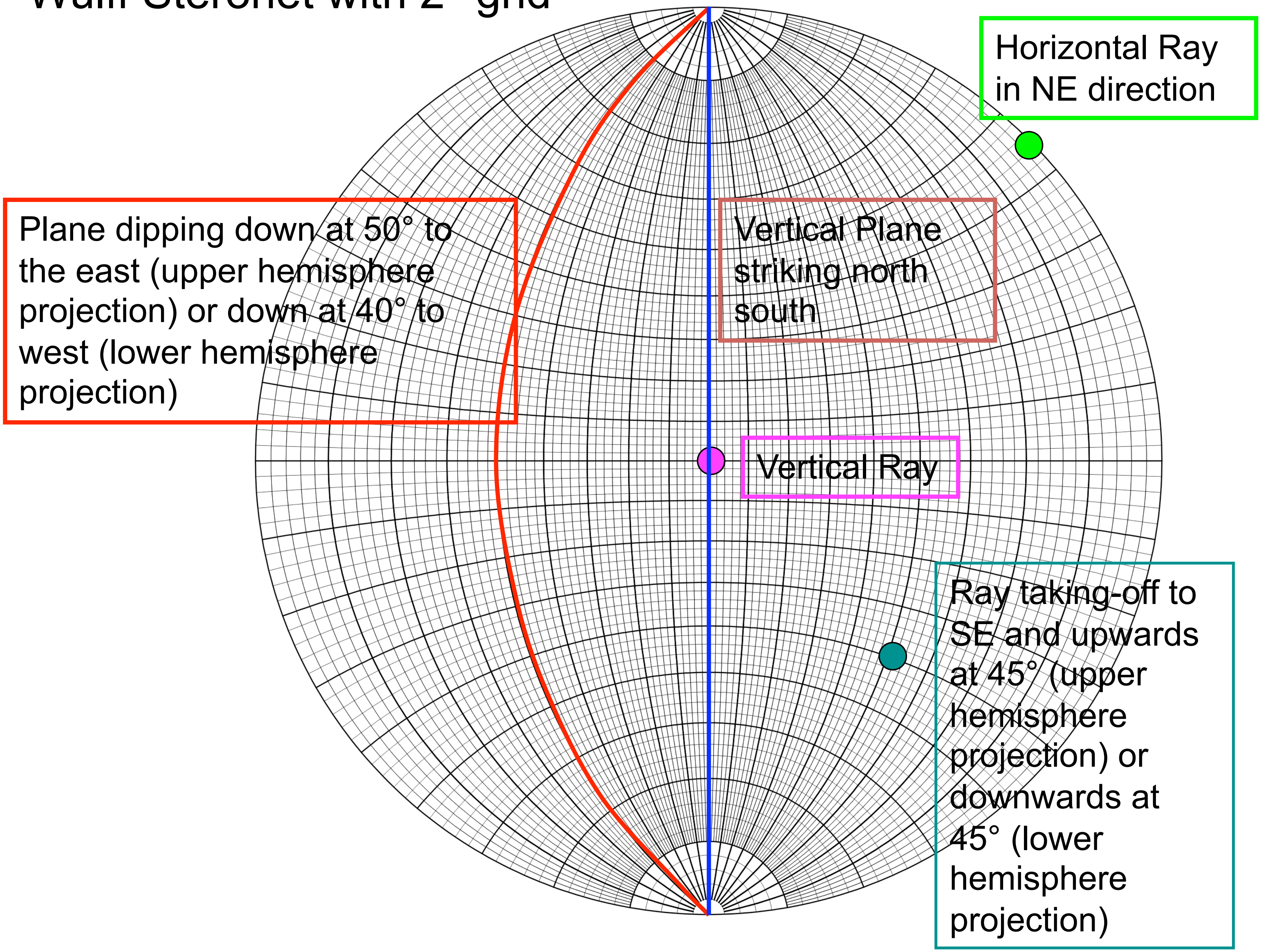

Normal Faulting

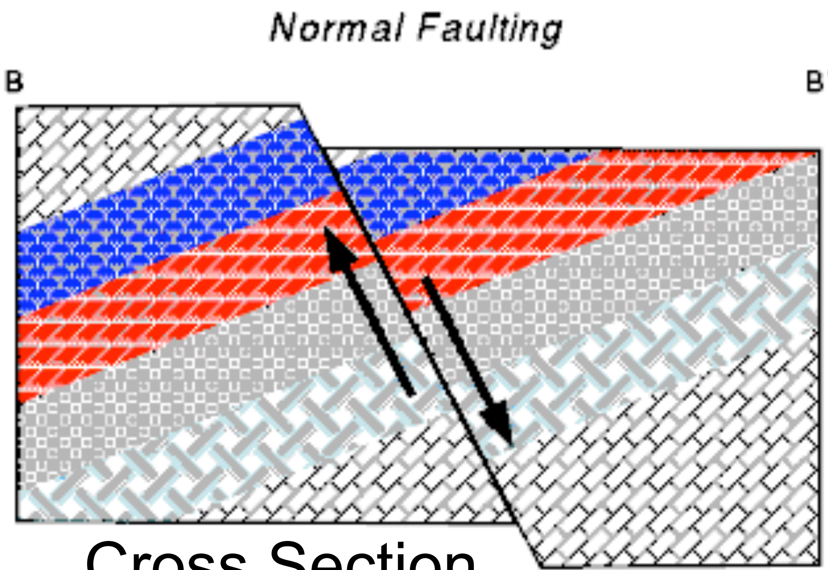

Cross Section

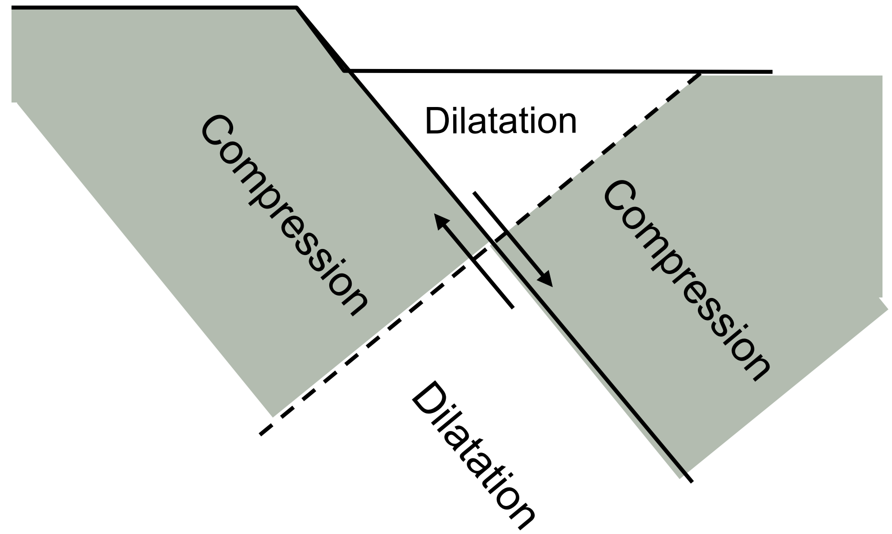

Cross Section

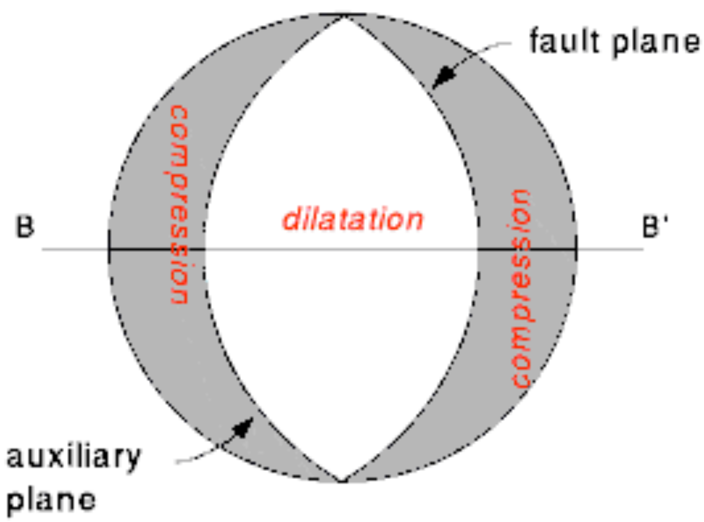

Thrust (Reverse) Fault

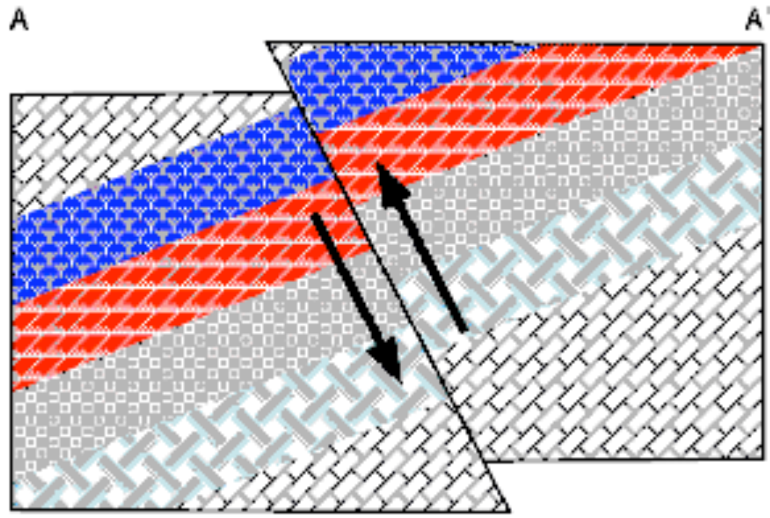

Cross Section

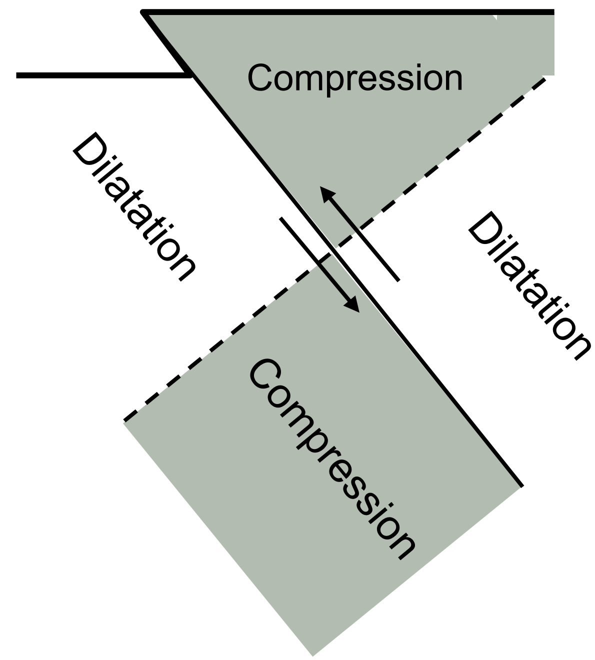

Cross Section

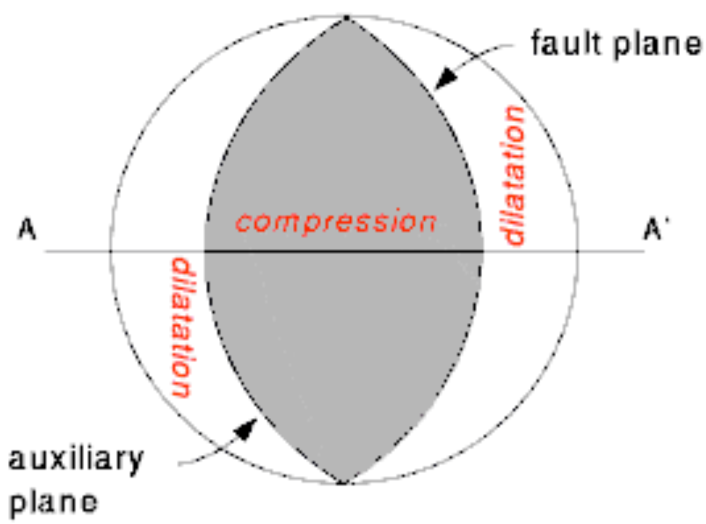

Supplementary Information on the ω-squared model.

For the two time scales of the earthquake process, T_R and T_D, one can think of seismic wave radiation turning on during the corresponding intervals, essentially radiating for a 'boxcar' interval of time. Each position on the fault reached by the rupture front experiences a boxcar duration of sliding and radiation. The overall interaction of the two boxcar intervals is given mathematically by a convolution. Convolution of two boxcars of different width gives a trapezoid source time interval of radiation. The area under the trapezoid is the seismic moment.

The spectrum of a trapezoid in the Fourier transform domain has the shape of the ω-squared source model.

Figure 4.3-3: Derivation of a trapezoidal source time function.

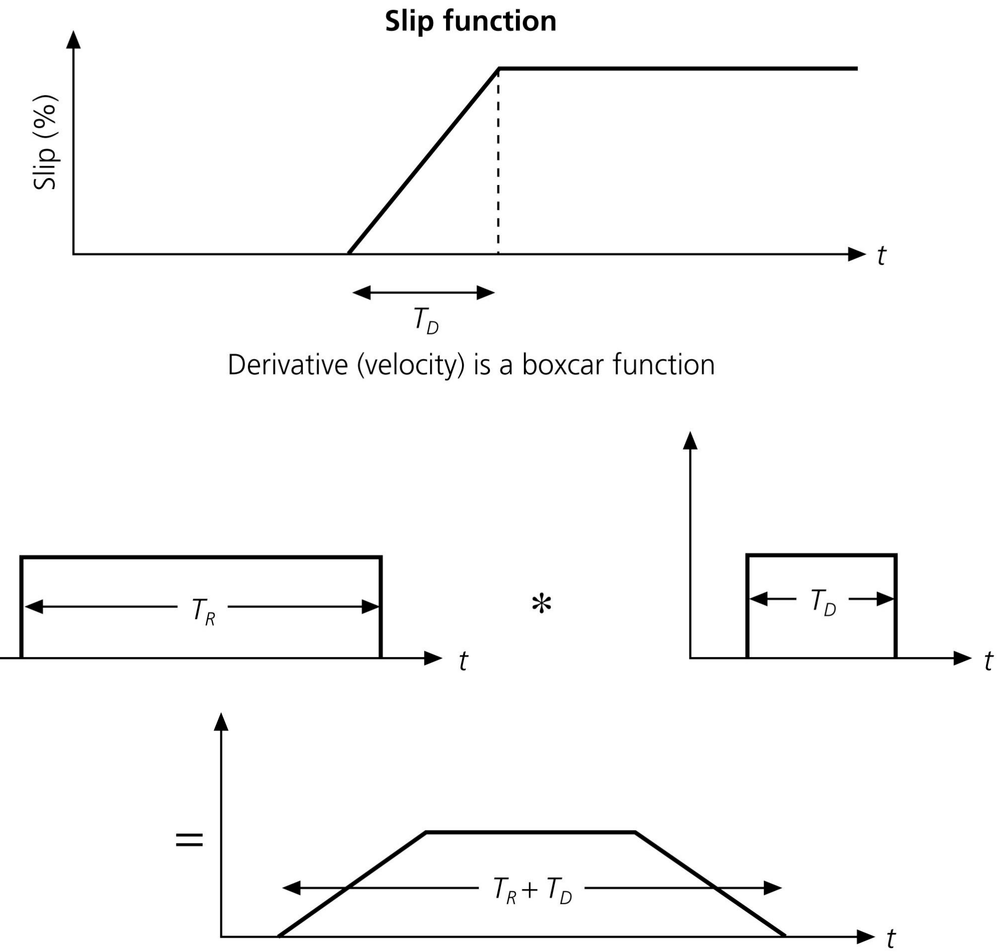

What would this source time function look like in the frequency domain?

Write the fault area in terms of a shape factor f and the square of a dimension L:

$M_0 = \mu \bar{D} S = \mu \bar{D} f L^2$

For large earthquakes, faults are often approximated as rectangles, so L is the length and f is the ratio of width to length.

For circular faults, L is the radius and $f = \pi$.

The rupture time can be approximated as $T_R = L / V_R = L/(0.7\beta)$

The rise time can be approximated as $T_D = \mu \bar{D} \,/\, (\beta\, \Delta\sigma) = 16 L f^{1/2} / (7 \beta \pi^{1.5})$

($\Delta\sigma$ is the stress drop during the earthquake)

Assuming a shear velocity of 4 km/s gives $T_R = 0.35\ L$ $T_D = 0.1\ L f^{1/2}$

Because stress drops are approximately independent of seismic moment, slip is roughly proportional to fault length, allowing for theoretical scaling laws.

The transform of a boxcar of height $1/T$ and length T is

$$F(\omega) = \int_{-T/2}^{T/2} \frac{1}{T} e^{i\omega t} dt = \frac{1}{Ti\omega}\left(e^{i\omega T/2} - e^{-i\omega T/2}\right) = \frac{\sin(\omega T/2)}{\omega T/2}$$

(has the form of a "sinc" function: sinc $x = (\sin x)/x$)

The spectral amplitude of the source signal is the product of the seismic moment and two sinc terms

$$|A(\omega)| = M_0 \left| \frac{\sin(\omega T_R/2)}{\omega T_R/2} \right| \left| \frac{\sin(\omega T_D/2)}{\omega T_D/2} \right|$$

T_R and T_D are the rupture and rise times.

$$\log A(\omega) = \log M_0 + \log\left[\mathrm{sinc}(\omega T_R/2)\right] + \log\left[\mathrm{sinc}(\omega T_D/2)\right]$$

Approximation of the amplitude spectrum of a trapezoidal box car function:

$\log|A(\omega)| =$

$$= \begin{cases} \log M_0 & \omega < 2/T_R \\ \log M_0 - \log(T_R/2) - \log\omega & 2/T_R < \omega < 2/T_D \\ \log M_0 - \log(T_R T_D/4) - 2\log\omega & 2/T_D < \omega \end{cases}$$

The spectrum os often defined in terms of the "corner frequencies"

Figure 4.6-4: Approximation of the (sin *x*)/*x* function, and derivation of corner frequencies.

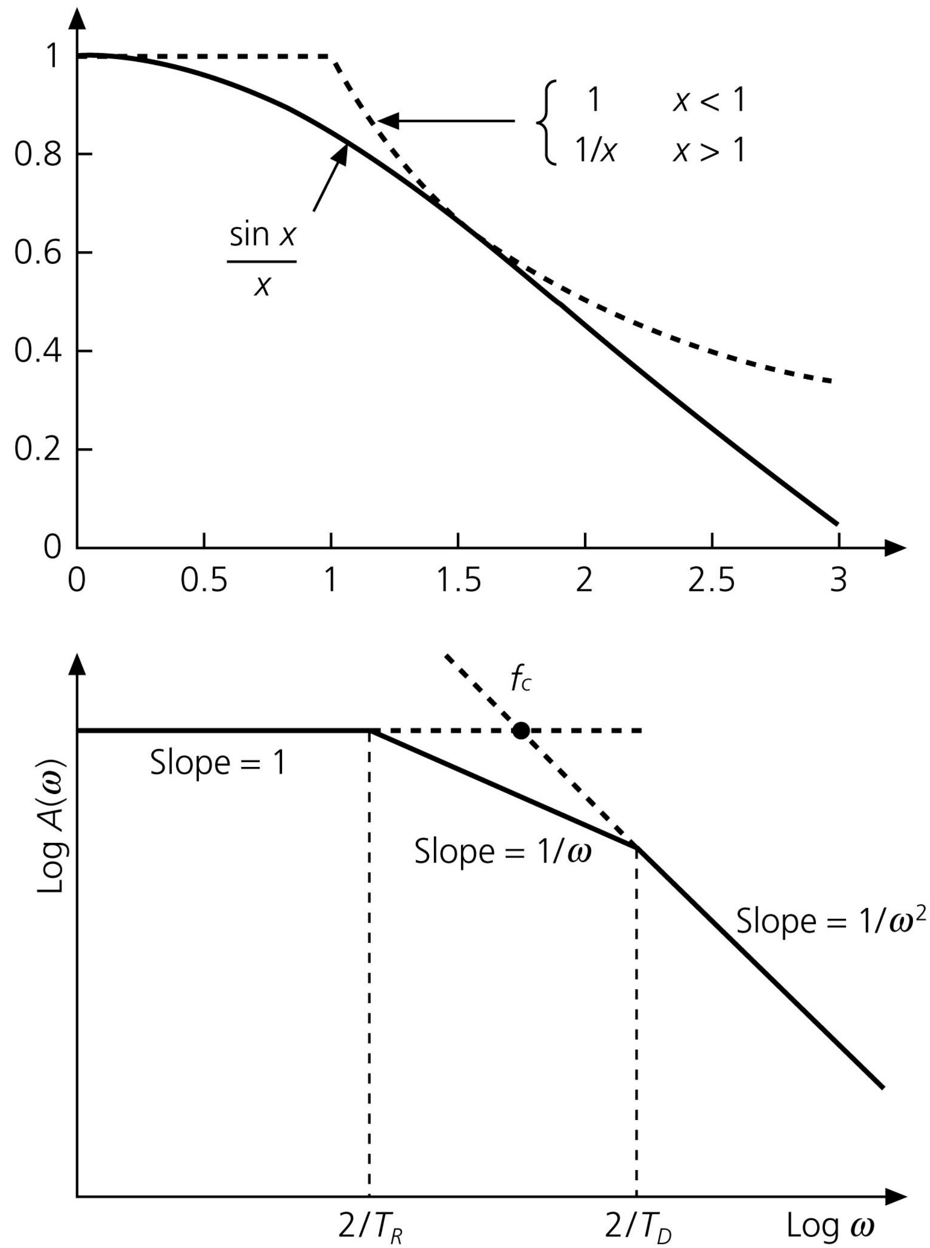

Fourier transform: $F(\omega) = \int_{-\infty}^{\infty} f(t)e^{-i\omega t}\,dt$

Inverse Fourier transform: $f(t) = \frac{1}{2\pi}\int_{-\infty}^{\infty} F(\omega)e^{i\omega t}\,d\omega$

$F(\omega) = A(\omega)e^{i\phi(\omega)}$

with a magnitude, $A(\omega) = |\,F(\omega)\,|$, and phase, $\phi(\omega)$.

So the Fourier transform represents a time series by two real functions of angular frequency: the *amplitude spectrum,* $A(\omega)$, and the *phase spectrum,* $\phi(\omega)$.

The displacements are: $u(x, t) = \frac{1}{2\pi}\int_{-\infty}^{\infty} A(\omega)\exp i[\omega t - k(\omega)x + \phi_i(\omega)]d\omega$

The phase has two parts (propagation and initial phase): $\Phi(\omega) = \omega t - k(\omega)x + \phi_i(\omega)$

The phase velocity $c(\omega) = \omega/k(\omega)$ describes wave surfaces of constant phase (individual peaks).